DEVELOPMENT AND VALIDATION OF A LC-MS/MS METHOD FOR THE PHARMACOKINETIC STUDY OF THIAMET-G AND ITS ANALOGUES IN RAT

by

Sze Mun Shirley Ko
B.Sc., The University of British Columbia, 2005

THESIS SUBMITTED IN PARTIAL FULFILLMENT OF
THE REQUIREMENTS FOR THE DEGREE OF

MASTER OF SCIENCE

In the
Department of Chemistry

SIMON FRASER UNIVERSITY

Fall 2010

APPROVAL

Name: Sze Mun Shirley Ko

Degree: Master of Science

Title of Thesis: Development and Validation of a LC-MS/MS Method for the Pharmacokinetic Study of Thiamet-G and Its Analogues in Rat

Examining Committee:

Chair:

Dr. Erika Plettner
Graduate Chair, Chemistry
Associate Professor, Department of Chemistry

_____

Dr. David Vocadlo
Senior Supervisor
Associate Professor, Department of Chemistry

_____

Dr. George Agnes
Supervisor
Professor, Department of Chemistry

_____

Dr. Andrew Bennet
Supervisor
Professor, Department of Chemistry

_____

Dr. Luis Sojo
Internal Examiner
Adjunct Professor, Department of Chemistry

Date Defended/Approved: December 9th, 2010

ABSTRACT

Thiamet-G inhibits the activity of *N*-acetyl-β-glucosaminidase, a glycoside hydrolase known as OGA. A validated bioanalytical method has been developed to enable pharmacokinetic studies of Thiamet-G and its related analogues. The bioanalysis was carried out using high performance liquid chromatography (HPLC) coupled to a tandem mass spectrometer (MS/MS). In the MS/MS, multiple reaction monitoring (MRM) was used to monitor the transition of analyte parent ions to diagnostic daughter ions. The validated method utilized the Hypercarb SPE cartridge as the cleanup tool and the ZIC-HILIC column as the suitable stationary phase. The method was validated for linearity, specificity, accuracy, precision, recovery, matrix effect, stability, and sensitivity. Pharmacokinetic samples obtained from rats treated by oral gavage with Thiamet-G were subjected to analysis using the validated method. Thiamet-G was found to be absorbed with a C_{max} of 370 ± 20 ng / mL and showed a t_{max} of 2 h.

Keywords: Thiamet-G; MRM; pharmacokinetics; N-acetyl-β-glucosaminidase; OGA; bioanalytical method validation

Subject Terms: LC-MS/MS, bioanalytical validation

DEDICATION

Dedicated to my parents, Betty and Joseph, and Matthew Lam…

ACKNOWLEDGEMENTS

I sincerely thank my senior supervisor, Dr. David J. Vocadlo, for his full support and guidance throughout the years. I am very fortunate to work on a project related to Thiamet-G, which is a lead compound with therapeutic usage for slowing down the disease state of Alzheimer's. David is a professor with a brilliant idea, and he has given me an opportunity to work on a stand-alone project through which I have built up research skills and the ability to work independently. I honestly thank Dr. Luis Sojo, who has many years of experience in developing bioanalytical assays, for assisting me with the project. He showed genuine kindness by teaching me the skills necessary for validating a method from scratch. I would like to acknowledge a number of people at SFU. Our departmental MS technician, Hongwen Chen, has helped me a lot with his expertise in MS and analytical chemistry. The machine shop custom made a vacuum manifold for me that really improved the method developmental state of the project. The animal facility looked after the animals and collected rat plasma for our laboratory. Dr. Renee Mosi has many years of experience in editing scholarly journals. She provided me exceptional help in compiling the whole thesis. Dr. Tracey Gloster, our postdoctorate fellow, also contributed her biological knowledge in proofreading my thesis. Lastly, I was grateful for the friendship from the members of the Vocadlo lab who indirectly helped me to grow from an inexperienced person into a more experienced research scientist.

TABLE OF CONTENTS

LIST OF FIGURES

LIST OF TABLES

ABBREVIATIONS

Accy	Accuracy
ACN	Acetonitrile
Asp	Aspartic acid
ADP	Adenosine diphosphate
ATP	Adenosine triphosphate
AUC	Area under the curve
AUC_{IV}	Area under the curve for intravenous route
$AUC_{other\ route}$	Area under the curve for administration via routes other than the intravenous route
*Bt*GH84	*Bacteroides thetaiotaomicron* β-*N*-acetylglucosaminidase from CAZy GH family 84
CAZy	carbohydrate active enzymes
CE	Collision energy
Cer	ceramide
CID	Collisionally induced dissociation
CL	Clearance
Cm	Concentration at the detection limit
Cp	Drug concentration in plasma
Cp^{SS}	Drug concentration at steady state
Cp(0)	Initial plasma concentration
CSS	Control standard solution
CSSs	Calibration standard solutions
CUR	Curtain gas
CV	Coefficient of variation
CV_{empty}	Column volume of an empty column
Dalton	Da
DC	Direct current
DCM	Dichloromethane

DET	Detector
DF	Deflector
DP	Declustering potential
ESI	Electrospray ionisation
ESI-MS	Electrospray ionisation mass spectrometry
EP	Entrance potential
ER	Endoplasmic reticulum
EXB	Exit lens for linear ion trap mode
F	Bioavailability
FA	Formic acid
FP	Focusing potential
FT	Freeze-thaw
GalNAc	*N*-acetylgalactosamine
GH	Glycoside Hydrolase
GS1	Nebulizer gas
GS2	turbo ion spray gas
GlcNAc	*N*-acetyl glucosamine
GM2	GalNAc(β1-4)[NeuAc(α2-3)]Gal(β1-4)Glcp(β1-1)Cer
h	hour(s)
HexA	β-hexosaminidase A
HexB	β-hexosaminidase B
HILIC	Hydrophilic interaction
HPLC	High performance liquid chromatography
k	Variation of blank due to random errors
k′	Retention factors
k_1	Elimination rate constant
I	Current
IS	Internal standard (Thiambu-G)
ISP	Ionspray voltage
IQ1	Q1 entrance lens
IQ2	Collision cell entrance lens
IQ3	Q3 entrance lens
LADME	Liberation, absorption, distribution, metabolism, elimination

LC	Liquid chromatography
LC-MS	Liquid chromatography with mass spectrometry
LC-MS/MS	Liquid chromatography with tandem mass spectrometry
LD	Loading dose
LLE	Liquid-liquid extraction
LLOQ	Lower limit of quantification
LOD	Limit of detection
LOQ	Limit of quantification
MAPT	Microtubule-associated protein tau
MeOH	Methanol
m	Slope of the calibration curve
min	minute
MRM	Multiple-reaction monitoring
MS	Mass spectrometer
MS/MS	Tandem mass spectrometry
m/z	mass-to-charge
NAG-thiazoline	1,2-dideoxy-2′-methyl-α-D-glucopyranoso-[2,1-*d*]-Δ2′-thiazoline
NButGT	1,2-dideoxy-2′-propyl-α-D-glucopyranoso-[2,1-*d*]-Δ2′-thiazoline
N_t	The number of theoretical plates
O-GlcNAc	β-*O*-linked *N*-acetylglucosamine
OGA	β-*N*-acetylglucosaminidase
OGT	Uridine diphospho-*N*-acetylglucosamine:polypeptide β-*N*-acetylglucosaminyltransferase
PA	Peak area
PGC	Porous graphite carbon
PK	Pharmacokinetics
PUGNAc	*O*-(2-Acetamido-2-deoxy-D-glucopyranosylidene)-amino-*N*-phenylcarbamate
Q0	First quadrupole, RF only
Q1	Second quadrupole
q2	Third quadrupole, RF only (called the collision chamber)
Q3	Fourth quadrupole
QC	Quality control

RF	Radio frequency
RSD	Relative standard deviation
RT	Retention times
S	Salt factor
S / B	Signal-to-background
$_{sbl}$	Standard deviation of the background levels
$\bar{S}_{bl}$	Background level measured from the blank mass spectra
S / N	Signal-to-noise
Sm	Minimum distinguishable analytical signal
SPE	Solid phase extraction
SS	System suitability
ST	Short-term stability
$Stock_{IS}$	Stock solution containing internal standard
$Stock_{mixed}$	Stock solution containing Thiamet-G, Thiampro-G, and Thiamme-G
STZ	Streptozotocin
T	Dosing interval
t	Time
TEM	Temperature
T_o	Void time
$T_{recommended}$	The time recommended for eluting the least retained analogue
	Dosing interval
$t_{1/2}$	Half life
TDC	Total droplet current
Thiambu-G	1,2-dideoxy-2′-aminobutyl-α-D-glucopyranoso-[2,1-*d*]-Δ2′-thiazoline
Thiamet-G	1,2-dideoxy-2′-aminoethyl-α-D-glucopyranoso-[2,1-*d*]-Δ2′-thiazoline
Thiampro-G	1,2-dideoxy-2′-aminopropyl-α-D-glucopyranoso-[2,1-*d*]-Δ2′-thiazoline
TIC	Total ion chromatogram
U	DC potential
UDP	Uridine diphosphate
UDP-GlcNAc	Uridine diphosphate *N*-acetyl glucosamine
ULOQ	Upper limit of quantification
V	Amplitude of the applied RF voltage
V_d	Volume of distribution

V_0	Void volume
ω	Angular frequency
WCSS	Working calibration standard solution
X	Amount of compound
XIC	Extracted ion chromatogram

CHAPTER 1: INTRODUCTION

1.1 Carbohydrates and the O-GlcNAc Modification

The central dogma of molecular biology was a theory originally established in 1958. It describes the transcription process, in which genetic information encoded in the chains of DNA are converted into messenger RNA. Following transcription, the messenger RNA is translated into protein. The resulting proteins are either used for various functions inside the cell or secreted out of the cell. Many proteins interact with each other to enable functioning of a cell, which is the smallest dividing unit of all living things[1].

In addition to proteins and lipids, carbohydrates are important biomolecules that act as signalling molecules and structural components[1-3]. Carbohydrates also play a role as crucial intermediates in generating energy within cells[1]. Carbohydrates often exist on the surface of proteins as glycans, which are covalently linked sugar chains of varying structures and sizes[4]. These glycoproteins act to enable cells and their surroundings to interact and therefore enable construction of complex muticellular organs and organisms[1].

The exact functions of glycans *in vivo* are difficult to define, but they have been found to be important for the development, growth, functioning, and survival of the organism that synthesizes them[1]. The biological roles of glycans can be separated into three main categories. First, glycans function in the maintenance of cellular structure and

to modulate cell-cell interactions[2]. Second, glycans regulate the proper folding of the newly synthesized polypeptides in the endoplasmic reticulum (ER) and Golgi apparatus. Proper glycosylation within the secretory pathway helps to maintain protein stability and conformation. If proteins are not properly glycosylated and / or they fail to fold properly, they are removed from the ER and subjected to proteolysis [2]. The other key biological function of glycans is their role as targets for recognition by other molecules[2], which can influence the localization of the glycans and glycoproteins.

1.1.1 Monosaccharides, the Basic Components for all Carbohydrates

The basic component for all carbohydrates is monosaccharides. Monosaccharides contain multiple hydroxyl groups and exist predominantly as either a six- or five-membered ring. There are two classes of monosaccharides, aldoses and ketoses (Figure 1.1). An aldose has an aldehyde function whereas a ketose contains a ketone group[5]. Many aldoses and ketoses exist in either an open chain form and a cyclic form[5]. The cyclic form of many 6-carbon and 5-carbon sugars is formed by the nucleophilic attack of the hydroxyl group, typically the stereogenic centre furthest from the carbonyl group, on the open chain sugar[5]. A pyranose, a 6-membered ring, or a furanose, a 5-membered ring are the most common cyclic species formed in carbohydrates[5].

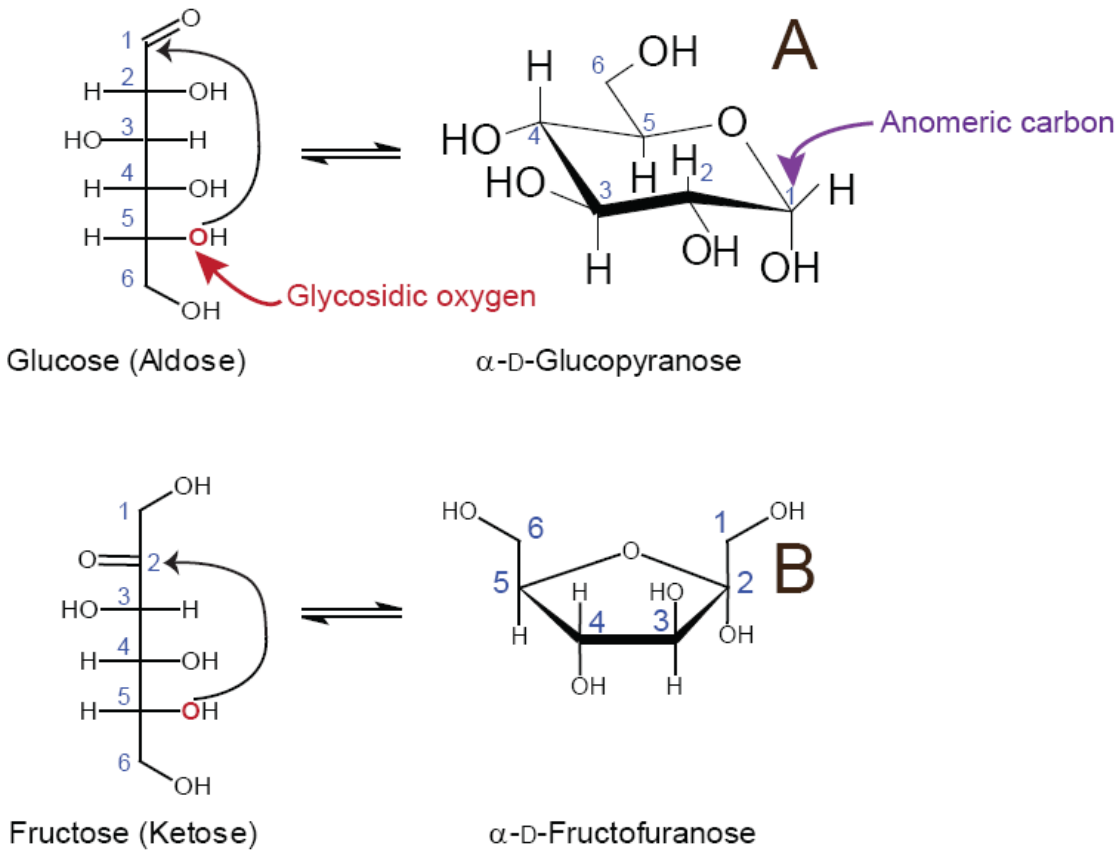

Figure 1.1. Examples of an Aldose, Glucose (A), and a Ketose, Fructose (B). The structures on the left hand side are the open chain forms of the sugars shown in Fisher projection while the structures on the right hand side are in the ring forms illustrated in modern projection.

One of the two anomers, α and β, can be generated during formation of the ring. The open chain forms of glucose and fructose are shown in the middle of Figure 1.2 (A) and (B) respectively. Anomers for D-glucopyranose and D-fructofuranose are illustrated in Fischer projection on the left hand side (α-anomer) and the right hand side (β-anomer) of the figure. In an α-anomer, the hydroxyl group attached to the anomeric carbon is on the same side of the carbon backbone, as drawn in Fischer projection, as is the oxygen atom attached to the highest numbered stereogenic centre. On the other hand, when the two substituents are on opposite sides of the carbon background in the Fischer projection, the configuration is β[5].

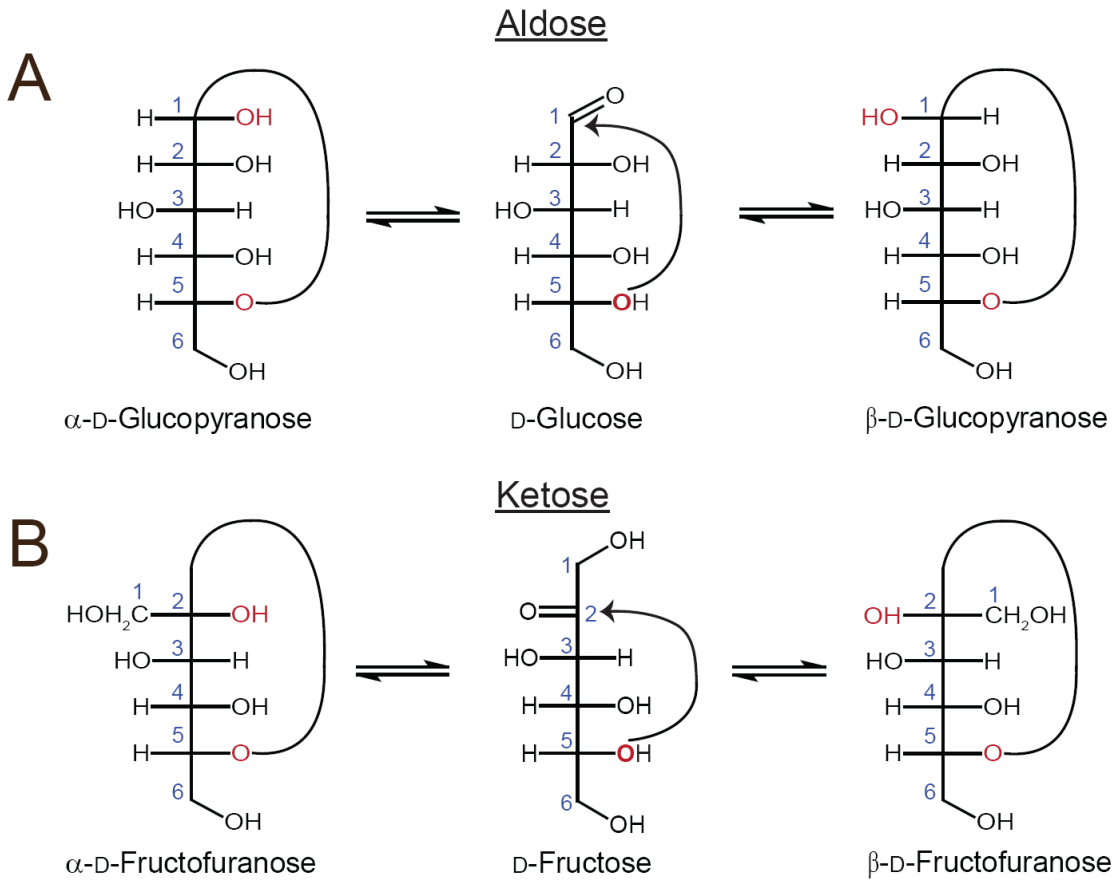

Figure 1.2. Formation of Two Different Anomers Resulting from the Cyclisation of Carbohydrates.
(A) Glucose and (B) ketose are shown in the figure as examples of an aldose and ketose respectively. All structures are illustrated in Fischer projection format. The order of the structures from left to right in the figure are the **α-anomer (left), the open chain forms (middle), and the β-anomer (right). After the formation of the ring, when the nucleophilic oxygen is on the same side as the hydroxyl group attached to the anomeric carbon, the configuration is α When the substituents are on the opposite side, the configuration is β.**

There are several forms of monosaccharides, some of the most commonly found forms in nature are hexoses and hexosamines. A hexose is composed of six carbons and an example is glucose. A hexosamine has the same structure as hexose, except that an amino group replaces a particular hydroxyl group substituent. *N*-acetylglucosamine (GlcNAc) and *N*-acetylgalactosamine (GalNAc) are examples of hexosamines (Figure 1.3) [1, 5].

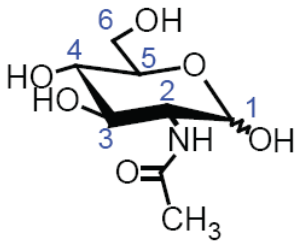

Figure 1.3. *N*-acetylglucosamine (GlcNAc) is Example of a Hexosamine with a 2-Acetamido Group Replacing the 2-Hydroxyl Group of Glucose.

In eukaryotic cells, proteins and lipids are commonly modified by glycosylation. In order for chains of monosaccharides to become covalently linked or to become linked to another molecule (whether it be another saccharide, protein, or lipid), they need to be attached via glycosidic linkages, which are usually formed through the hydroxyl group of the anomeric centre. The formation of a glycosidic bond is initiated by the nucleophilic attack of the oxygen of a hydroxyl group to the anomeric carbon. In Figure 1.4, the nucleophilic oxygen is part of the hydroxyl group of R′OH while the anomeric carbon is carbon 1 of D-glucopyranose. Each monosaccharide can form an α- or a β-glycosidic linkage when attached to another molecule[5]. Due to the fact that there are numerous possible positions on a monosaccharide which can attach to another molecule to form a glycosidic linkage, the study of glycobiology can be very challenging. Luckily, the possible combinations of glycosidic linkages that exist in natural biological macromolecules are limited. However, the diversity of different glycan structures in nature is still large because the hydroxyl groups can also be modified by phosphorylation, sulfation, methylation, *O*-acetylation, or fatty acid acylation[1, 5]. This thesis involves a particular type of *O*-linked glycosylation on proteins, the *O*-GlcNAc modification, which is the focus of further discussion.

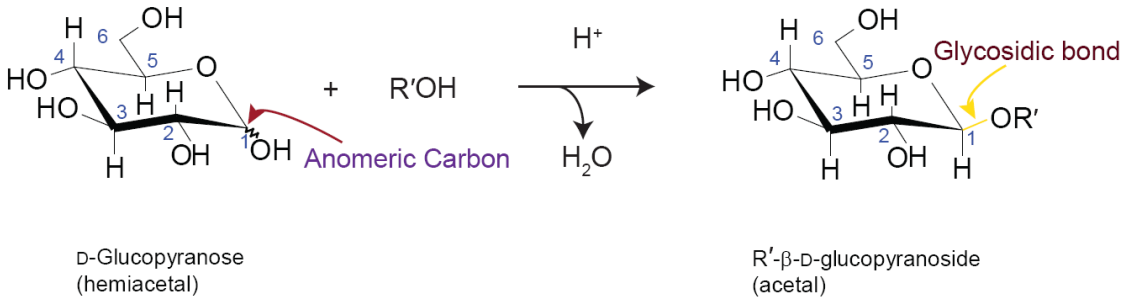

Figure 1.4 The Reaction Mechanism for Acid Catalyzed Glycosidic Bond Formation. A hemiacetal has reacted with R′OH to yield an acetal group with a β-configured glycosidic bond.

1.1.2 The *O*-GlcNAc Modification

β-*O*-linked *N*-acetylglucosamine, abbreviated as *O*-GlcNAc, is produced by an enzymatic transfer of the monosaccharide *N*-acetyl glucosamine (GlcNAc) to the hydroxyl group of certain serine and threonine residues of eukaryotic proteins. Different from other characterised glycosylations, this type of glycosylation happens in the nucleus and cytoplasm and consists of the addition of just a single GlcNAc unit[6]. The *O*-GlcNAc modification was discovered more than two decades ago[7]. During studies of the *O*-GlcNAc modification in rat hepatocytes, it was found to dominantly occupy the nuclear envelope and the chromatin, especially at the nuclear pore complex[8]. Researchers also discovered *O*-GlcNAc on many cytoplasmic proteins, including cytoskeletal proteins[9]. The *O*-GlcNAc modification is one of the most common post-translational modifications found on proteins[10-12]. Approximately 500 proteins have been classified as *O*-GlcNAc modified proteins to date, and these proteins are involved in a number of roles[10, 12], including stress responses[13, 14], transcription[15-18], translation[19], and cellular signalling[20]. A number of *O*-GlcNAc modified proteins are part of the cytoskeleton, and regulate the assembly of microtubules and the bridging of actins[21-24]. Research has suggested that this modification of proteins is involved in

type II diabetes[25, 26], Alzheimer's disease[25, 26], and cancer[17]; however, their exact roles are unclear and are contentious[27, 28].

The cycling of *O*-GlcNAc relies on two enzymes (Figure 1.5). Uridine diphospho-*N*-acetylglucosamine:polypeptide β-*N*-acetylglucosaminyltransferase (OGT), a glycosyltransferase, transfers the sugar moiety from the donor sugar substrate, uridine diphosphate (UDP)-GlcNAc, onto target proteins[29, 30]. In the reverse process, β-*N*-acetylglucosaminidase (OGA) removes the *O*-GlcNAc moiety from proteins[26, 31]. As a result, *O*-GlcNAc is a dynamic process in which the addition and removal of the moiety can happen numerous times during the lifespan of a protein[12].

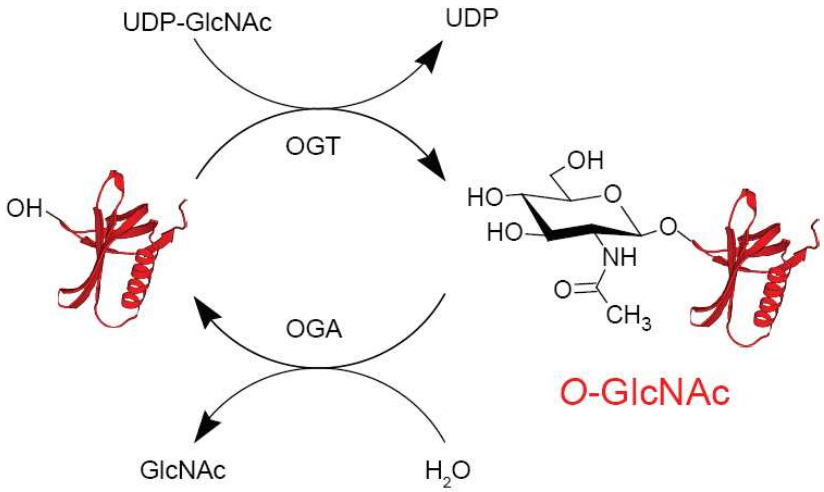

Figure 1.5. The Cycling of the O-GlcNAc Modification.
OGT, a Glycosyltransferase, Transfers the Sugar Moiety from the Donor Sugar Substrate, UDP-GlcNAc, onto Target Proteins. In the Reverse Process, OGA Removes the *O*-GlcNAc Moiety from Proteins.

Researchers have found that disruption of the gene encoding for the OGT is lethal at the single cell level and is essential for mouse embryogenesis[32]. Furthermore, when the genes encoding for either the *O*-GlcNAc transferase or the hydrolase, OGA, were knocked out in *Caenorhabditis elegans*, defects were detected in dauer larvae formation

and in the regulation of macronutrient storage[33, 34]. To date, gene deletion of OGA has not been done in mammals, although evidence suggests that *O*-GlcNAc cycling is important for development[33, 34].

Analogous to phosphorylation, the *O*-GlcNAc modification appears to play a key role in regulating the activity of target proteins[35]. The *O*-GlcNAc modification has some analogies to phosphorylation (Figure 1.6). For the *O*-GlcNAc modification, a transferase, and for a phosphorylation, a kinase, is responsible for putting the moiety onto the hydroxyl group of certain serine and threonine residues of eukaryotic proteins[36]. Similarly, for phosphorylation, a phosphatase, and for the *O*-GlcNAc modification, a hydrolase, removes the moiety from the modification site[37].

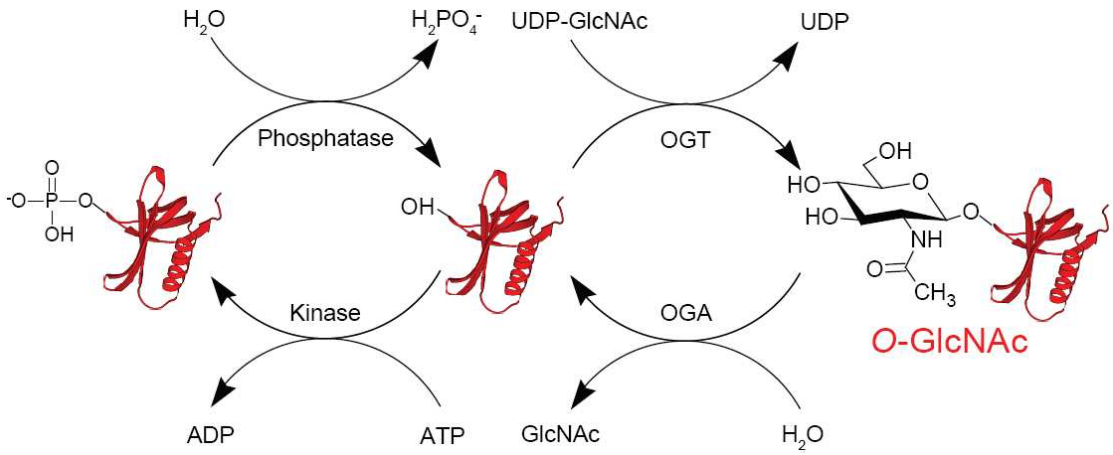

Figure 1.6. Cycling of *O*-GlcNAc and *O*-phosphate on the Same Amino Acid Residue of a Protein Molecule.

As illustrated in Figure 1.6, *O*-phosphate and *O*-GlcNAc can occur on the same or nearby residues[38, 39]. In the case of the C-terminal domain of RNA polymerase II, competitive cycling was observed for the *O*-GlcNAc modification and phosphorylation[40]. Studies of oestrogen receptor-β suggested that two types of modification at the same site might function in regulating the activity and the turn over of

the receptor[41]. There are some cases where the *O*-GlcNAc modification modulates a nearby phosphorylation site[35, 42]. Historical evidence suggests that the *O*-GlcNAc modification alters phosphorylation and protein expression in crucial signalling pathways[43].

1.1.3 Methods to Modulate Levels of *O*-GlcNAc

Altering *O*-GlcNAc levels in cells either *in vivo* or *in vitro* helps to provide a better understanding of the functions of the post-translational modifications on proteins. Researchers have tried various techniques to modulate the levels of *O*-GlcNAc. Upregulation can be done by elevating the concentrations of UDP-GlcNAc[44, 45] and increasing the expression of OGT[46].

One can elevate the concentration of UDP-GlcNAc by increasing the concentration of glucose or glucosamine, which are metabolic precursors[47]. However, when introducing glucosamine, various other effects at the cellular level are observed, which complicates the study of the upregulation of UDP-GlcNAc[48-50]. Aside from OGT, other enzymes also transfer UDP-GlcNAc to proteins or other molecules during other types of glycosylation processes[51, 52]. Thus, methods to elevate levels of UDP-GlcNAc for purposes of defining the role of *O*-GlcNAc by feeding metabolic precursors to increase the levels of the modification is ambiguous because these other glycosylation pathways are also affected[53].

Another common approach is to overexpress OGT in cultured cells[30] or in animals[54]. Consistent with OGT being a large multidomain macromolecule, it has been found to interact with many other proteins. Slawson *et al.* found that

overexpression of OGT actually disturbs the progression of the cell cycle[55]. Although the non-catalytic roles of OGT have not been defined, these data suggest that OGT may have functions other than just cycling *O*-GlcNAc. Overexpression of OGT can induce other unavoidable effects due to the non-catalytic activities or interactions of OGT with other proteins[56-58]. Furthermore, OGT overexpression usually only results in small increases in *O*-GlcNAc levels.

Another method for increasing the levels of *O*-GlcNAc modified proteins is to use inhibitors to block the activity of the enzyme responsible for removing *O*-GlcNAc from target proteins. Haltiwanger *et al.* first showed that the inhibition of OGA can significantly increase the levels of *O*-GlcNAc in cells[59]. In order to understand the background about inhibitors currently used for OGA, some general information regarding OGA will first be discussed in the following section.

1.1.4 OGA

Many glycosyltransferases and glycoside hydrolases found in nature are responsible for the post-translational modification of proteins with sugar units. Enzymes that have been identified from gene sequencing are classified in the CAZy database[60] according to their amino acid sequence and structural information where available[61]. OGA is a member of family 84 of glycoside hydrolases (GH84).

Aside from OGA, there are other enzymes found in the lysosome that are also capable of cleaving terminal *N*-acetylglucosamine residues off from glycoconjugates[62]. They are called β-hexosaminidase A (HexA) and B (HexB). These enzymes are members of family 20 of glycoside hydrolases (GH20)[62]. The substrates of these

enzymes are mainly gangliosides such as ganglioside GM2 which is directed to the lysosome for degradation[63]. These enzymes share no apparent sequence similarity to OGA[62]. A good inhibitor for use in cells or *in vivo* should be highly specific for OGA over the functionally related HexA and HexB so as to avoid concomitant inhibition of all three enzymes.

Human OGA is composed of two domains, a C-terminal domain, which was proposed to have an acetyltransferase[64] and an N-terminal domain which has the glycoside hydrolase activity[64]. Some bacterial enzymes share high sequence similarity to the N-terminal domain of eukaryotic OGAs, and have been grouped into GH84[65]. A close homolog of human OGAs from *Bacteroides thetaiotaomicron* (*Bt*GH84) is able to cleave *O*-GlcNAc from proteins and uses the same catalytic mechanism[66]. The crystal structure of human OGA has never been solved but that of *Bt*GH84 is known[66] as is the structure of two other bacterial homologues[67, 68]. These structures have provided a good model of the human OGA to enable studies of inhibitors of OGA[69].

The substrate-assisted catalytic mechanism used by human OGA is shown in Figure 1.7. In this double replacement retaining mechanism, the 2-acetamido group of the substrate acts a nucleophile[62]. The catalytic residues, two aspartate residues, in the active site of the human OGAs are involved in catalysis. One residue polarises the 2-acetamido group, which increases its nucleophilicity and assists its attack at the anomeric centre. It most likely acts as a general base in the first step of the reaction. The second residue acts as a general acid during the first step of the reaction, aiding the departure of the leaving group and leading to formation of an oxazoline intermediate. During the

second step, the first residue acts as a general acid and the second residue now acts as a general base, aiding the attack of a molecule of water at the anomeric centre.

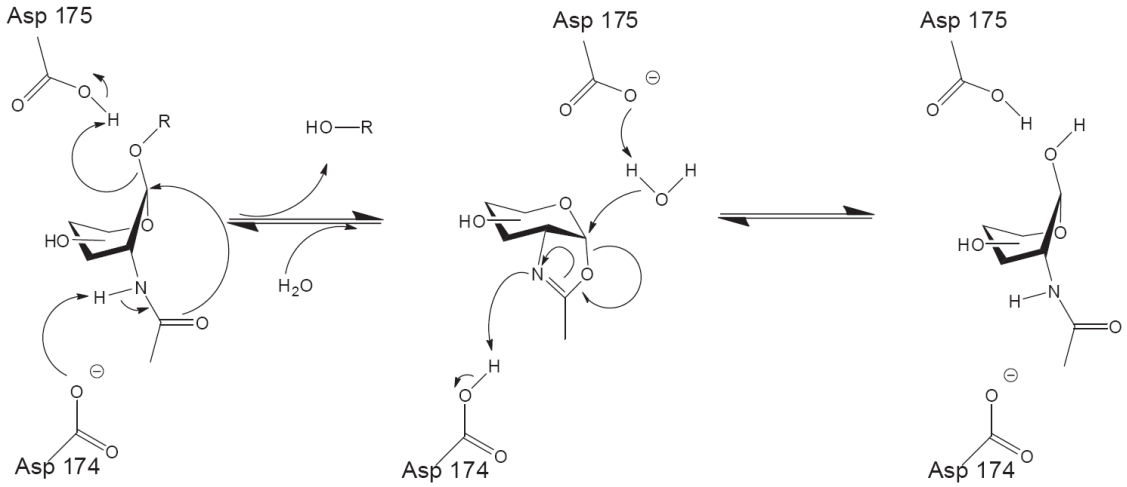

Figure 1.7. The Retaining Mechanism for OGA.
Amino Acid Residues are Labelled Based on the Numbering of the Human OGA[62].

1.1.5 Small Molecule Inhibitors

Small molecule inhibitors are crucial for understanding the functional roles of many enzymes. Using a cell permeable small molecule inhibitor to increase the *O*-GlcNAc levels in cells through inhibition of OGA is in many ways more advantageous than genetic methods or altering the nutrient flux[70]. Given that not all the cells are capable of undergoing transfection employing a cell permeable small molecule inhibitor is more convenient[71]. The level of dosing can be easily adjusted and if necessary, the inhibitor can be removed to observe the effect on the cells[70]. Furthermore, the levels of the proteins themselves are not directly perturbed. Hence, inhibition of OGA is often performed in cultured cells[20, 27], and tissues both *in vitro*[72, 73] and *in vivo*[74, 75] for studying the effects of increasing levels of *O*-GlcNAc. One drawback of using inhibitors is that they are not all able to penetrate into all tissues types, and some

inhibitors are not selective for OGA, which can lead to some unanticipated results[62]. Several inhibitors for OGA are known and these are summarised briefly below.

PUGNAc and Streptozotocin

O-(2-Acetamido-2-deoxy-D-glucopyranosylidene)-amino-*N*-phenylcarbamate (PUGNAc) is both an inhibitor of mammalian OGA (K_I = 52 nM) and the functionally related lysosomal β-hexosaminidase (K_I = 52 nM)[76]. By treating cells with PUGNAc, some off-target effects were observed that resulted from inadvertant inhibition or alteration of enzymes or processes, other than OGA[28, 50, 77, 78]. Since PUGNAc inhibits the function of the lysosomal β-hexosaminidases, which are important for recycling glycosphingolipids, levels of the ganglioside GM2 in cultured neuron cells increase after PUGNAc treatment[77]. PUGNAc treatment, which causes an increase in *O*-GlcNAc levels, has been shown to cause insulin resistance. But this effect could be due to an off-target activity and not solely by inhibition of OGA[28, 78]. An additional important factor which makes PUGNAc a poor candidate inhibitor is that it is not able to cross the blood brain barrier[75]. The structure of PUGNAc is shown in Figure 1.8 Structure A.

Streptozotocin (STZ) has poor potency towards OGAs (K_I = 2 mM)[79, 80]. Many disastrous effects, such as the death of β-cells that ultimately leads to an insulin-dependent diabetic phenotype in rodents, were observed following treatment with STZ[81-83]. Two studies support that these complications do not arise from the inhibition of OGA by STZ, but instead from off-target effects[84, 85]. These complications indicate that both PUGNAc and STZ (Figure 1.8 Structure B) are poor tools for investigating the functional role of *O*-GlcNAc.

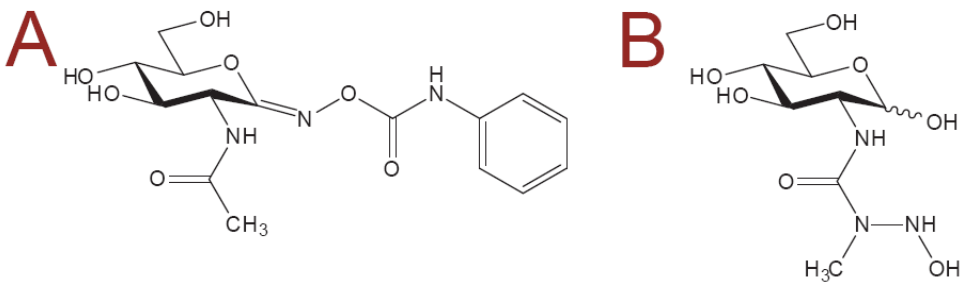

Figure 1.8. Structures of (A) PUGNAc and (B) Streptozotocin.

NAG-thiazoline, NButGT and Thiamet-G

1,2-Dideoxy-2′-methyl-α-D-glucopyranoso-[2,1-*d*]-Δ 2′-thiazoline (NAG-thiazoline) was first synthesized by Knapp *et al*[86]. This compound has since been shown to be a good inhibitor of both OGA (K_I = 0.07 µM) and lysosomal β-hexosaminidases (K_I = 0.07 µM) but shows no selectivity[62]. Figure 1.9 shows the structures of NAG-thiazoline (A) and its derivative that possesses a butyl chain, NButGT (B).

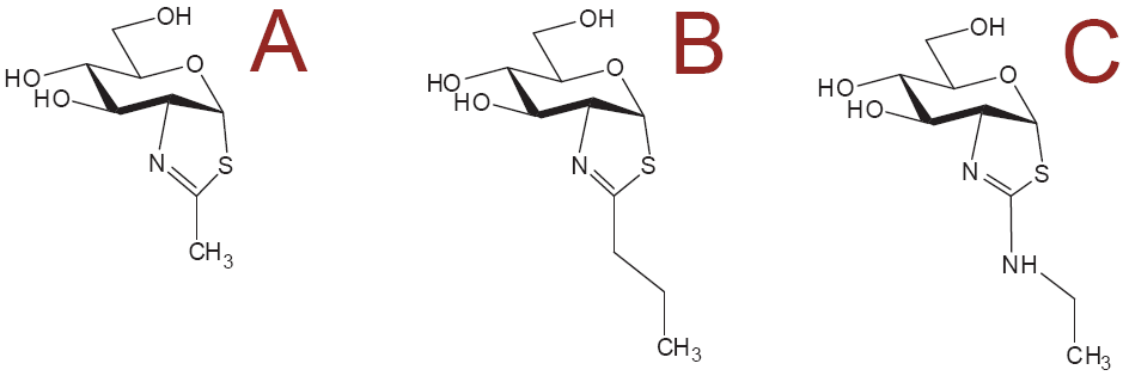

Figure 1.9. Structures of (A) NAG-thiazoline, (B) NButGT and (C) Thiamet-G.

The active site on the structure of OGA (or a bacterial homologue) was not known when the structure of lysosomal HexB was crystallized[71]. The active site of HexB, an enzyme known to be similar in function to OGA, has been shown to bind the 2-acetamido

group of inhibitors[87]. However, since the pocket surrounding this group is very small, lengthening the 2-acetamido group by adding larger substituents should weaken the binding of the inhibitor towards HexB. A series of NAG-thiazoline derivatives with extending chains at the 2-acetamido group were therefore synthesized[62]. One of the derivatives, NButGT, was identified to be highly selective (700-fold) for OGA (K_I = 0.230 μM) over HexB (K_I = 340 μM) with good potency[62]. The crystal structure of NButGT which possesses a butyl chain, in complex with *Bt*GH84 supported the proposal that there is indeed a deep pocket able to accommodate substituents where the 2-acetamido group of substrates are bound to OGA and its homologues[69].

Research studies have shown that Asp^{174} (Asp^{242} in *Bt*GH84) located in the active site of OGA is a crucial catalytic residue having a pK_a of 5.2[88, 89], making it deprotonated and anionic at physiological pH. It has been found that the protonated form of NButGT has a pK_a of 3.4[74]. These findings suggest that the majority of NButGT in solution would not be protonated at a physiological pH of 7.4 and, therefore, a favourable ionic pair interaction with Asp^{174} cannot be formed[71].

In the crystal structure of *Bt*GH84 in complex with NAG-thiazoline[66] or NButGT[69] (Figure 1.10), the endocyclic nitrogen of the thiazoline is within hydrogen bonding distance of the side chain of Asp^{174}. In order to generate a favourable ionic pair with Asp^{174}, a new series of compounds, Thiamet-G (Figure 1.8 Structure C) and its analogues, were made by increasing the basicity of the endocyclic nitrogen of the thiazoline ring of NButGT[74]. The first methylene unit of the alkyl chain was replaced with an amine[74]. This change makes Thiamet-G much more basic (pK_a = 8). As a result it shows selectivity for OGA over HexB (37,000-fold) and the binding potency to

OGA is increased by 30-fold (K_I = 21 nM at pH 7.4)[74]. Thiamet-G was also shown to be able to increase the *O*-GlcNAc levels in both cultured cells and *in vivo* in the rat brain[74].

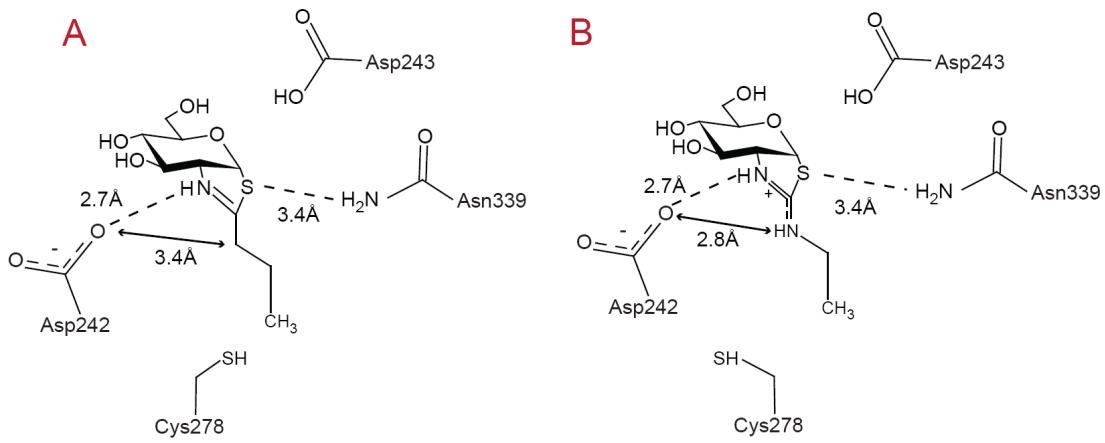

Figure 1.10. The Crystal Structures of *Bt*GH84 Glycoside Hydrolase Active Centre in Complex with either, (A) NButGT or (B) Thiamet-G.
Adapted from [74].

1.2 Pharmacokinetics

Pharmacokinetics (PK) is the study of the relationship between doses of administered drugs and the measurable drug concentration in the blood in a quantitative fashion[90]. PK investigates how a drug behaves in the body after administration whereas pharmacodynamics investigates the relationship between the concentration of a drug at the site of receptors and the corresponding efficacy of the drug[91]. The focus of this thesis will be on PK.

The LADME (Liberation, Absorption, Distribution, Metabolism, Excretion) processes are illustrated in Figure 1.11. The abbreviation L stands for liberation of the drug from its dosage form while A stands for absorption of the drug from the site of dosage into the blood circulation. The letter D represents distribution of the drug by

diffusion or active transporters transferring from the intravascular space into the body tissues while M represents metabolism of the drug transforming into metabolite. Finally, E symbolizes excretion of the unchanged drug and / or metabolites from the body[92].

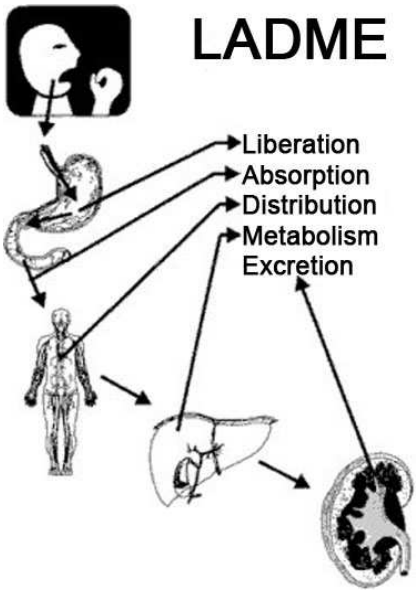

Figure 1.11. LADME Processes that Take Place after Drug Administration
Adapted from [93].

PK is the study of LADME processes of a drug by determining the drug concentration during a time course in body fluids[91]. LADME or pharmacokinetic processes rely on the physical and chemical properties as well as the amount of drug administered into the body[92]. The LADME processes are generally considered to happen simultaneously. For example, the liberation process does not need to be completed in order to initiate the absorption process.

One important factor to consider while administering drugs into a body is the process which occurs to transfer drugs across cell membranes. Cellular membranes are composed of phospholipid bilayers with apolar hydrocarbon chains facing inward and the polar head groups facing outward[94]. Proteins are located in between the membranes

and form small gaps or pores[95], which permit flow of polar substances or drugs into cells[94]. Non-polar drugs usually enter the cells by diffusion through the hydrocarbon barriers located between the phospholipid bilayers[96]. Many factors influence the transport of a drug across cell membranes including the size, shape, solubility, and the degree of ionisation of the drug[94]. Some drugs might strongly bind to plasma or tissues in the body[94]. Consequently, only the free form of the drug is able to pass through the membranes[94]. At the steady state, the concentration of the unbound drugs is the same on both sides of the membrane[94]. pH differences across membranes also play a role in drug transfer only if the compounds are ionisable under physiological conditions[94]. For ionisable drugs, their transfer relies upon the pKa of the drug and the pH gradient[94].

1.2.1 Basic Understandings of the LADME System

Liberation of the drug is important for all drug products administrated via routes other than the intravenous route[92]. The main reasons for formulating drugs inside tablets are to protect the perishable drugs from decomposition, to minimize odour, and to smoothen the progress of swallowing[97]. The drug is released from its formulation during liberation and this process determines the rates of absorption and the bioavailability of the drug, and it is governed by the properties of the drug within the tablet[97].

By definition, absorption is the act of taking the drug from the site of administration into the bloodstream of the body. The absorption site depends on the route of administration and the most common forms are oral and intravenous. Other factors that affect the rate of absorption are the physical state of the drug, concentration

of the drug, the circulation at the absorption site, and the area of the absorbing surface. Among the various routes of administration, intravenous administration inputs the drug directly into the venous bloodstream, thereby eliminating the process of absorption[94].

After the drug is in the circulation system, the process of distribution takes place from the bloodstream into the body tissues, to the site of action. The rate of the process is dependent on the blood flow and the diffusion of the drug across cell membranes of a variety of tissues and organs in the body. Only the unbound fraction of the drug is available for transfer and the distribution of this fraction of drug is governed by the binding to proteins or uptaken by cells in the body. When drugs tend to bind to protein in the plasma, the amount of drug reaching into tissues is limited. Hence, the distribution of the drug depends on the physicochemical properties of the drug and several physiological factors[94].

Metabolism, sometimes referred to as biotransformation, is the bio-chemical alteration of a drug in the body prior to elimination. To avoid the build up of foreign substances, the body uses enzymes to chemically convert lipophilic compounds into more water-soluble metabolites. The processes of biotransformation are divided into Phase I and Phase II reactions. In the Phase I reaction, a polar group is added to the drug to increase its water solubility. These reactions are generally either oxidative or hydrolytic. Phase II reactions involve formation of a covalent bond(s) with endogenous substances. The liver is known as the primary location of metabolism. Processes of metabolism generally modify the drug into a substance which is inactive or less active than the parent compound[94].

After the drug has undergone metabolism, it is ready to be eliminated from the body. Among the various excretory organs, the most important organ is the kidney as the majority of drugs are excreted in the urine[92]. Substances in the feces are typically either unabsorbed drugs or compounds removed into the bile[94]. A portion of both non-ionised and ionised drugs may be passively reabsorbed by the kidney[94].

The efficacy of a given drug is largely governed by the concentration of the drug in the body. To measure efficacy, the ideal location for measuring the concentration of the drug is at the receptor, which is the site of action of the drug. Practically, however, drug concentrations are usually measured in whole blood or other body fluids, such as plasma, saliva, urine, or cerebrospinal fluid. The drug content in these fluids is believed to be in steady-state with the amount of drug at the receptor. The measured drug concentration in these fluids is often referred to as the drug level, which is the free fraction of drug in equilibrium within the body[91].

1.2.2 Compartmental Modelling

For purposes of PK, a body consists of more than one compartment. The input and output of drug from the body, and the transfer of the drug content between the compartments of the body are represented by rate constants. PK models are often used to describe how a drug behaves in a biological system after administration. The models that have been well classified are the one-compartment, two-compartment, and multicompartment models[98].

In a one-compartment model, all the tissues of the body are considered to be homogenous. The drug is assumed to distribute instantly throughout the body upon

administration and hence the drug is instantaneously at steady state. However, the drug concentration in plasma is not equal to the drug concentration in tissues. In this model, the changes in the plasma concentration are proportional to the changes in the tissues. As a result, a monophasic response or a monoexponential curve is observed when the drug concentration in plasma is plotted against time (Figure 1.12 A). The plot of the log of concentration of drug in plasma versus time graph will show a linear relationship (Figure 1.11 B) [98].

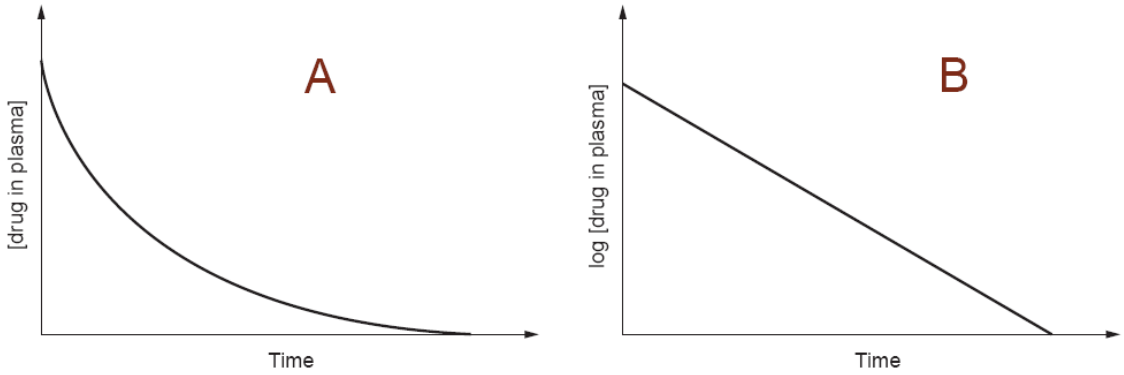

Figure 1.12. Plots that Exhibit a One-compartment Model.
(A) Concentration of drug in plasma versus time plot, (B) the log of concentration of drug in plasma versus time plot. In both plots, the data is for intravenous administration.

In a two-compartment model, the tissues of the body are not simply a homogenous unit. In this model, the body is composed of a central compartment and a peripheral compartment. The central compartment is considered to be the organs including the heart, lungs, kidneys, liver, and brain. The peripheral compartment is mainly the muscle, fat, and skin of the body. It is assumed that the central compartment has tissues that are highly perfused whereas the peripheral compartment is less perfused. In this model, when drug is administered into the central compartment, equilibration is not achieved instantly between the two compartments due to the differences in the rate of

drug distribution. A biphasic response is demonstrated when the concentration of drug in plasma is plotted against time (Figure 1.13 A). When one takes the log of the concentration of drug in plasma and plots it against time, a plot consisting of two distinct lines is obtained (Figure 1.13 B) [98].

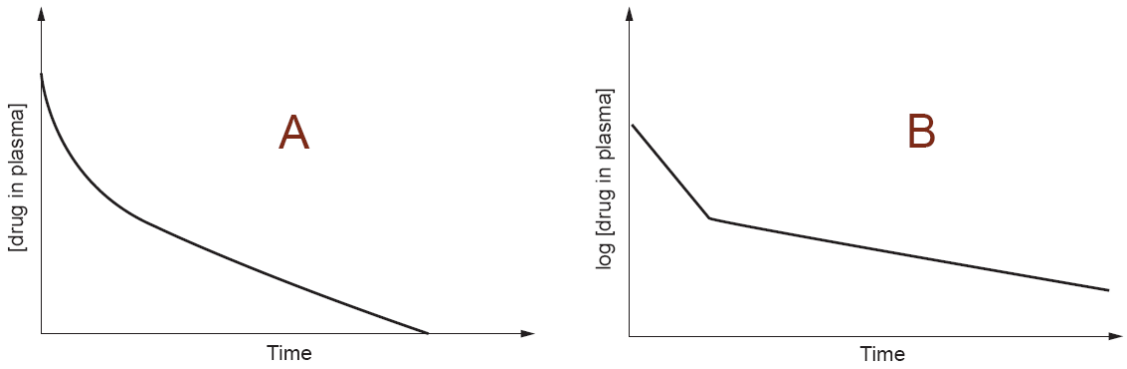

Figure 1.13. Plots that Exhibit a Two-compartment Model.
(A) Concentration of drug in plasma versus time plot, (B) the log of concentration of drug in plasma versus time plot. In both plots, the data is for intravenous administration.

The last model is called the multicompartment model. As the name suggests, the model takes into account the presence of an additional compartment in the body system into which the drug will distribute. In a plot of the concentration of drug in the plasma versus time, one would expect more than a single exponential decay. Differences are also expected in the log of concentration of drug in the plasma versus time curve[98]. Consult Appendix A 1.1 for a description of the fundamental parameters for PK.

1.3 Analytical Issues in PK

1.3.1 Complexity of Biological Samples

Biological samples are highly complex due to the influence of many endogenous substances. Quantitation of administered drugs in biological fluids can also be a

challenge because of the low quantity of the target analytes. In blood fluids, such as serum and plasma, there are often proteins and phospholipids present along with the target analytes. Plasma is about 55 % of the total blood volume. Roughly, 90 % of the plasma is water. The other 10 % is comprised of many dissolved substances, such as fibrinogen, proteins, nutrients, hormones, and inorganic mineral salts. Plasma serves an important role as a storage and transport medium for blood clotting factors[99].

The ideal analytical method to monitor the concentration of a compound in plasma would enable isolation of the analytes from the matrix in a fast, simple, inexpensive, and reproducible way, while yielding high recoveries and avoiding degradation of the analytes[100].

1.3.2 Sample Preparation Processes

1.3.2.1 Deproteinisation before LC-MS/MS Analysis

After the collection of plasma from a body, the samples have to undergo some extraction and clean up processes before the instrumental analysis by LC-MS. This step is essential to ensure that the mass spectrometer is not contaminated and that it remains operational. One of the common processes is deproteinisation by protein precipitation. Sometimes protein precipitation is followed by some form of solid phase extraction to further clean up the extracts[101, 102]. In the protein precipitation method, the plasma extract is treated with a common organic solvent or low pH aqueous solution to denature the proteins. After centrifugation, the analyte remains in the supernatant while the proteins present in the plasma will aggregate and be concentrated in the pellet[102]. Another method uses ultrafilters to trap proteins present in the plasma extracts followed by HPLC using a configuration in which an ion exchange column is placed in front of the

analytical column enabling further online purification of the target analytes[103]. In 2001, Chou and Cheng described a method involving deproteinisation with acetonitrile followed by extraction of the polar analytes from the supernatant using dichloromethane and water[104]. This procedure is a liquid-liquid extraction (LLE) that can remove various contaminants present in the supernatant after organic deproteinisation.

1.3.2.2 Further Cleanup of Plasma Extracts before LC-MS/MS Analysis

Plasma extracts contain abundant salts, lipids, proteins, and surfactants[105]. All of these compounds can be a cause of ion suppression during ESI–MS/MS bioanalysis, but it is generally thought that phospholipids are the major cause of ion suppression[105]. Lipids can also build up on the analytical column over time and lead to analytical complications[105].

Using protein precipitation alone in the sample preparation process will lead to a significant amount of ion suppression and therefore the removal of lipids is also an important step for achieving reliable drug quantification. Accordingly, further treatment of samples after deproteinisation enables the depletion of many of the remaining matrix ions, contributing to improved reproducibility of peak shapes in the chromatograms[105].

1.3.2.3 Common Sample Cleanup Techniques

Among the various cleanup processes, solid phase extraction (SPE) is a common technique adopted for isolating analytes of interest from a wide variety of matrices including urine and blood[106]. SPE can be useful for removing matrix interference but it does require considerable method development and optimization. Many different commercially available stationary phases can trap analytes and remove contaminants

from the matrices or vice versa. Other than SPE, usage of an online trap column before the actual stationary phase can also help to remove matrix interference[107].

1.3.3 HPLC Chromatography for Separation of Polar Compounds

1.3.3.1 Column Separation Challenges Encountered for the Thiamet-G analogues

As commented by Li X. et al., "The physicochemical characteristics of a monosaccharide, such as low molecular weight and high hydrophilicity pose a significant analytical challenge[108]." Due to the sugar-like structure of the compounds of interest, the analogues are very polar and highly soluble in water. As a result of these hydrophilic properties, they cannot easily be retained using typical reverse stationary phases, including those which are silica-based and organic polymer-based[109]. The compounds are also hard to analyse due to their poor volatility and the fact that they have low UV absorption[110]. Although ion exchange chromatography is generally used for separation of polar compounds, it is also not a good choice when carrying out LC-MS/MS bioanalysis since the use of high salt containing mobile phases is not compatible to the ion sources of mass spectrometers. A normal phase column is more suitable for hydrophilic compounds, however, the solvents for normal phase, such as dichloromethane, hexane, toluene, and other hydrocarbons, are not suitable for ESI-MS[111]. This incompatibility arises because ESI requires the use of a polar mobile phase for ionisation[111]. None of the traditional chromatography methods therefore are ideal for separating highly polar compounds.

1.3.3.2 Alternative Phases for HPLC Chromatography: HILIC Stationary Phase

There are some techniques reported that can enable online separation of polar compounds coupled with ESI-MS. In 1990, Alpert explained the mechanism of hydrophilic interaction liquid chromatography (HILIC), a variant form of normal-phase chromatography using aqueous solvent[112]. HILIC is compatible with polar organic mobile phase solvents despite the hydrophilic stationary phase[113]. The addition of small amounts of water in the mobile phase creates an aqueous layer on the surface of the stationary phase and this essentially leads to the generation within the column of a liquid-liquid extraction system[113]. The analyte of interest then partitions between the mobile phase and the aqueous layer present on the stationary phase[113]. The polar functional groups of the analytes form hydrogen bonds with the polar groups of the stationary phase[113]. Lastly, the elution of analytes is governed by the polarity of the eluent as well as the solubility of the sample in the mobile phase[113].

1.3.3.3 Alternative Phases for HPLC Chromatography: PGC Phase

Another attractive alternative for the analysis of carbohydrate-like molecules involves the use of a porous graphite carbon (PGC) column that can be coupled online to ESI-MS[114]. PGC columns enable the retention of very polar compounds using standard reversed phase chromatography eluents[114]. The retention of polar solutes onto this chemically stable and super-hydrophobic stationary phase is believed to be driven by hydrophobic interactions and the polarisability of the surface[114]. The PGC column is made up of flat sheets of hexagonally arranged carbon atoms, graphite[114]. In 2002, Jackson and Carr were able to show that the presence of any functional group inducing polarization of a benzene ring, such as an electron-donor or electron-acceptor,

will lead to greater retention of the molecule[115]. The binding of the analyte is due to interactions between the hybridized orbitals of the carbon surface and analyte. The result suggests that there are dipole-type and electron lone pair donor-acceptor interactions, and that graphite can donate as well as accept electrons[116]. Compared to other packing materials, a porous graphite column often offers better retention and selectivity of polar compounds[116]. The material can in some cases discriminate between compounds that differ only by a single methylene unit[116]. Möckel *et al.*[117] and Tanaka *et al.*[118] have both shown that graphite offers better separation of various analogues than either C_{18}-silica or pyrenylethyl-silica.

1.3.3.4 Mobile Phase Optimization

There are a great variety of columns available for use, so selection and optimization of a column for separating analogues of interest is the crucial step for development of an appropriate HPLC method. Other than column choice, the next most important factor is the optimization of the mobile phase which is important because both the polar sample and the solvent molecules may interact strongly with the column surface[119]. As commented by Strege, the use of buffered mobile phases is important for maintaining repeatability in the separation of charged species between chromatography runs because the electrostatic interactions between the analyte and the stationary phase are strongly influenced by the buffer[120]. Strege found that increased salt concentrations in the mobile phase reduced the retaining capacity of HILIC columns[120]. However, removal of buffer from the mobile phase resulted in the pH and ionic strength of the prepared samples having a strong influence on the results[120].

Accordingly, some balance between ionic strength and buffering capacity should be aimed for.

1.4 Liquid Chromatography Coupled with Mass Spectrometry

In this thesis, liquid chromatography (LC) coupled with mass spectrometry was chosen as the platform to develop an analytical method. The mass spectrometer (MS) is a tandem quadrupole-linear ion trap MS and electrospray ionisation (ESI) is the technique used for ion production.

Analysis Using LC-MS

In general, the LC method is started by pumping mobile phase from the solvent reservoirs. Once the sample is injected into the sample loop of the autosampler, the solvent in the system pushes the sample from the injection port into the analytical column where chromatographic separation of the analyte takes place. The analytical column outlet is connected to the ionisation source, where the ions are produced and then detected using the MS[121].

The mass spectrometer is composed of five components, an ion source, vacuum system, mass analyser, detector, and computer system for acquiring the digitalised data. For this thesis, the ion source is electrospray (ESI), the mass analyser is a tandem quadrupole / linear ion trap, and the detector is an electron multiplier. Two pumps are responsible for creating the vacuum inside the mass spectrometer. They are the rotatory vane and the turbomolecular pump. In the following section, a brief introduction about the ion source, mass analyser, and the different scan modes is provided. The positive ion mode is used throughout the project.

ESI

The ionisation technique of ESI (Figure 1.13) occurs in three steps, droplet formation, shrinkage of the droplet, and formation of the gaseous ion[122]. The sample from the column outlet passes through the electrospray needle, which has a high positive voltage of 4 to 5 kV applied to it[121]. A downward electrical potential and pressure gradient is set from the electrospray needle towards the counter electrode at the entrance of the first mass analyser of the mass spectrometer[123]. The high electric field at the electrospray needle leads to partial separation of charges in the solution delivered to the end of the electrospray needle. In the positive ion-mode, the cations present in the solution gather at the tip of the electrospray needle travelling towards the counter electrode whereas the anions inside the needle move away from the tip[124]. The mutual repulsion at the end of the needle tip increases due to the accumulation of charges[125]. When the repulsion of the positive ions at the surface tension and the attraction of these ions toward the counter electrode overcomes the surface tension of the liquid, the liquid at the meniscus will deform into a cone, the Taylor cone, just outside the electrospray tip[124, 126, 127]. After the formation of the cone, a fine stream of liquid is instantaneously ejected out from the tip of the cone towards the counter electrode[124, 128]. The liquid becomes unstable and breaks down into positively charged droplets[124]. The droplets reduce in diameter through evaporation of the solvent as they are drawn toward the counter electrode[123]. During the process, the charges inside the droplets remain the same[127]. As a result, the charge density on the surface of the droplets continuously rises[127]. The droplets become unstable when the charge density reaches the Rayleigh stability limit[127, 129]. When the electrostatic repulsion has

exceeded the surface tension, which is holding the droplets in place, the droplets disintegrates into smaller droplets[127]. Droplet-jet fission[127] splits the droplets into smaller and irregularly shaped droplets[130]. During the process, the microdroplets do not explode. However, smaller microdroplets eject from the elongated end of the parent droplets[130]. Solvent evaporates continuously from the successive droplets that have been relieved from the coulombic stress through jet fission[127]. These droplets eventually reach the Rayleigh stability limit and undergo another jet fission[127].

There are two schools of thought regarding the formation of gas-phase ions from the small and highly charged droplets. The charged residue model suggests that the smallest droplets will contain an analyte with one charge remaining. When the remaining solvent is removed from the droplet by the process of evaporation, an ion is formed. On the other hand, the ion evaporation model suggests that when the radii of the droplets decreases to a particular size, an ion can be directly ejected from the droplet. In order for an ion to form, the mutual repulsive force experienced by the escaping ion has to exceed the attraction between the escaping ion and the droplet[127].

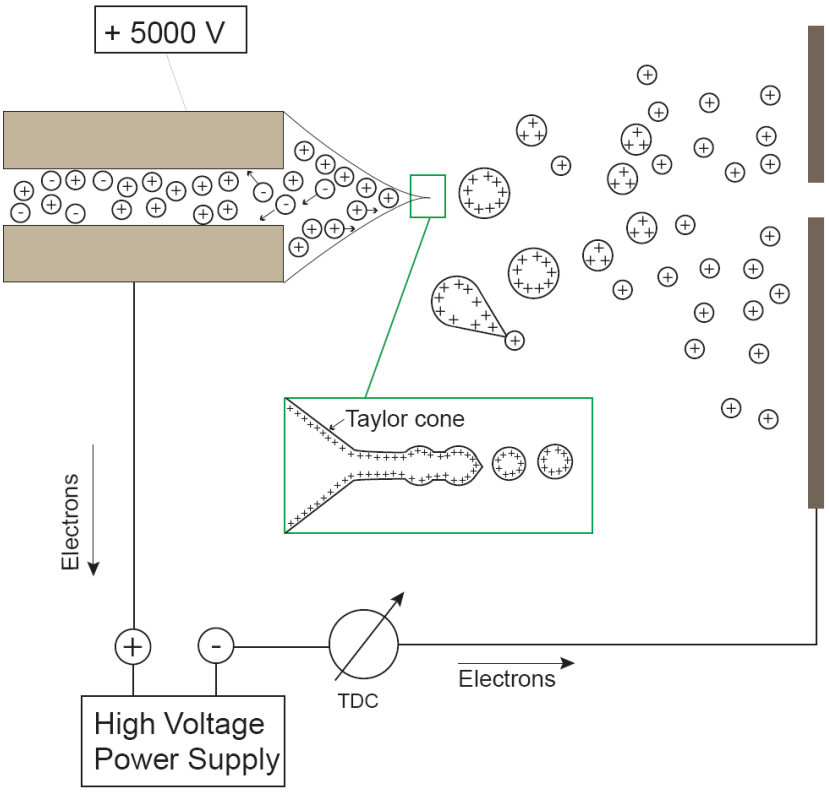

Figure 1.14. Features of the ESI Interface of the Atmospheric Pressure Region.
In the positive-ion mode, electrochemical oxidation takes place at the metal capillary while reduction occurs at the counter-electrode. The imposed electric field causes accumulation of positive ions at the tip of the electrospray needle. When the charge repulsion and electric field overcome the surface tension of the liquid at the tip, the liquid will expand into a Taylor cone. The fine jet of liquid immediately ejects out from the tip of the cone. The liquid becomes unstable and breaks down into positively charged droplets. Through solvent evaporation and the process of droplet-jet fission, the droplets shrink in size and ultimately form gaseous ions. TDC stands for total droplet current, I[124].

Once the ions are accelerated out of the ion source, they enter into the vacuum interface leading to the quadrupole mass analyser[121]. A quadrupole mass analyzer uses a stable trajectory in the oscillating electric field to separate ions according to their mass-charge-ratios[125]. It consists of four parallel rods arranged symmetrically in a square array, with opposite rods connected to each other electrically[121]. Separation of ions are achieved by applying a direct current (DC) and a time-dependent radio frequency (RF) potential on these rods[131]. Rods adjacent to each other have voltages of opposite

polarity applied to them[123]. Positive DC potential is applied to two opposite rods in the X-Z plane whereas negative DC potential is applied to the rods in the Y-Z plane[131]. The superimposed RF potential, V cos *w*t, is also applied on both pairs of rods with V, *w*, and t representing the amplitude of the applied RF voltage, angular frequency, and time respectively[123]. The magnitude of the RF potential is the same for both pairs of rods, but the polarity is opposite from each other[131]. The RF potential rapidly changes back and forth from a positive charge to negative one in a cyclic manner[123]. The trajectory of the ions is affected by the total electric field made up of the applied potentials on the rods[123]. The forces cause the ions to oscillate between the four rods[123]. If the oscillation is unstable, the ion trajectory is unstable and the ion will strike a rod and therefore fail to reach the detector[123]. The rods applied with positive DC act as a high-pass filter for the heavier ions while the rods with a negative DC act as the low-pass filter for the lighter ions[123]. Only ions with particular mass-to-charge ratios can pass through the quadrupole along the z-axis in between the four rods while other ions cannot reach the detector[123]. Consult Figure 1.15 for an expanded depiction of a quadrupole.

Tandem mass spectrometers in space

A tandem quadrupole mass spectrometer is composed of four quadrupoles. The second quadrupole (Q1) and fourth quadrupole (Q3) of the instrument are both operated with DC and RF voltages as discussed above. The first quadrupole (Q0) and the third quadrupole (q2) are RF only. Q0 is for focusing the ions before they enter Q1. For q2, collision gas is introduced so that an ion entering the quadrupole will undergo one or more collisions. Within the RF-quadrupole, when an ion collides with a neutral gas molecule, a fraction of the kinetic energy of the ion converts into internal energy[124].

This process can cause the ion to fragment in a process known as collisionally induced dissociation (CID).

The components of the tandem mass spectrometer are illustrated in Figure 1.14. As one can see, the potential energy gradually decreases from the counter electrode (1000 V) to Q3 (-33V). The electric field draws the ions across the z-axis from the entrance of the mass spectrometer towards the detector. The Decluster potential (DP) is referred to as the voltage applied to the orifice relative to ground. The orifice plate is located between the counter electrode and the skimmer. The DP energy is applied on the ions at the orifice plate in order to eliminate the solvent cluster and reduce the chemical noise in the final spectrum. The potential energy at q2 is more negative when compared to Q1. The purpose is to increase the kinetic energy of the ions significantly so that CID can take place[132].

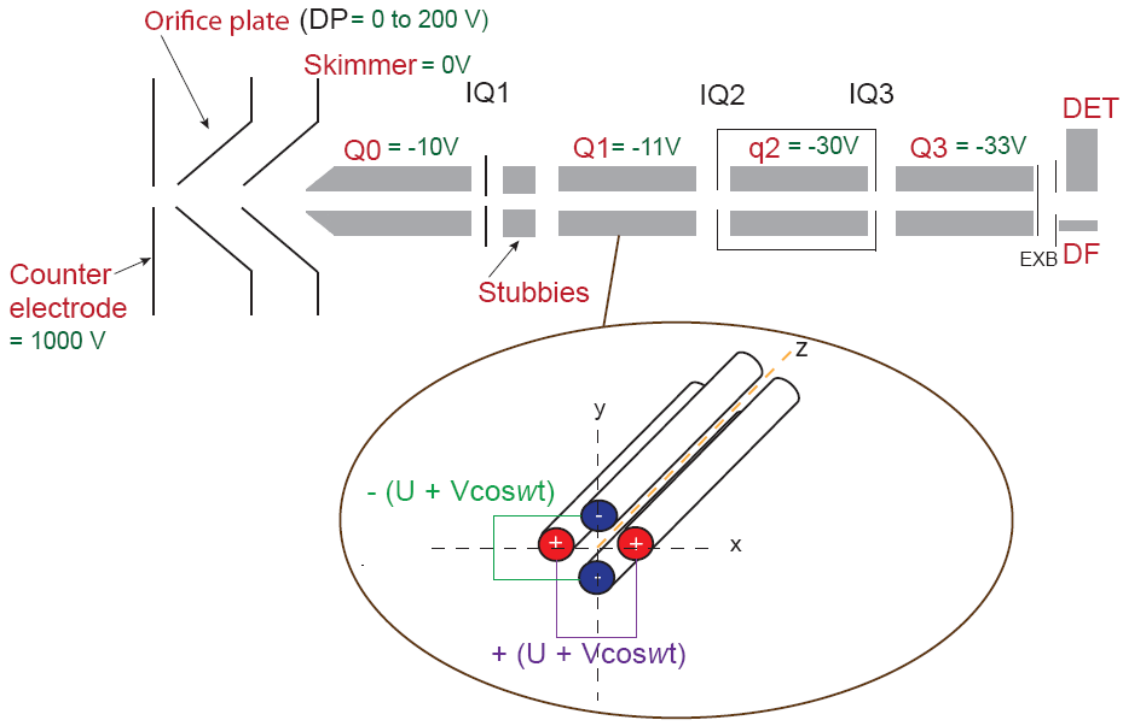

Figure 1.15. Schematic Cross-section View of the Mass Spectrometer Used for this Work. The mass spectrometer is composed of four quadrupoles (Q0, Q1, q2, and Q3) and a detector. An electric field with decreasing potential draws the ions across the z-axis towards the detector. An expanded version of the Q1 quadrupole is illustrated in the circle. (DP = declustering potential applied on the ions at the orifice plate, IQ1 = Q1 entrance lens, IQ2 = collision cell entrance lens, IQ3 = Q3 entrance lens, EXB = exit lens for linear ion trap mode, DET = detector, DF = deflector)[132].

Several scan modes that are frequently used in tandem mass spectrometry are described below (Table 1.1).

Q1 scan: The first quadrupole is set to scan simultaneously. All the ions within a preset range of m/z would pass through Q1 and be detected in the detector. This scan mode is useful for identifying a wide range of components within a mixture.

Product-ion scan: Ions with a particular mass-to-charge ratio are chosen in the first quadrupole. In the RF-only quadrupole, these ions collide with gas molecules to undergo CID fragmentation. Q3 is set to scan and analyse the entire set of fragments,

which are known as product ions The product-ion scan mode is commonly used for structure elucidation of an analyte of interest[123].

Precursor-ion scan: The third analyser is set to detect only the product ion of interest. At the same time, Q1 is scanning for a certain mass range to transmit only precursor ions that could yield the product ions of interest through CID fragmentation. Only precursor ions that generate the product ions of interest will be detected in the resulting mass spectrum. This scan mode is useful for identifying classes of compounds having similar polarities and structures within a mixture[123].

Neutral-loss scan: Both Q1 and Q3 are set to scan simultaneously and at the same rate so that all the ions pass through Q1 but only those species that fragment to give a product ion with a fixed mass offset pass through both mass analysers and are detected. Similar to the precursor-ion scan, this scan mode is useful for identifying structurally related classes of compounds in a mixture[123].

Multiple-reaction monitoring (MRM): The MRM experiment is carried out by specifying the parent mass of the compound for fragmentation in the first quadrupole and then specifically monitoring for a particular product ion in the third quadrupole. MRM is useful for quantitative measurements of analytes present in complex samples. The name also indicates that under this scan mode, more than one reaction can be monitored simultaneously[123]. Also, the duty cycle, the time allocated to monitoring the ions, is much lower when performing a MRM experiment as compared to many other experiments.

Table 1.1. The Five Common Scan Modes for Tandem MS with Quadrupole Analysers.

	Scan Mode[#]	Operation of Q_1	Operation of q_2	Operation of Q_3
1	Q_1	Scan desired range	N / A	N / A
2	Product-ion, define m_1	No scan, select m_1	CID	Scan up to m_1 to collect its fragment
3	Precursor-ion, define m_2	Scan from m_2 upwards to cover potential precursors	CID	No scan, select m_2
4	Neutral-loss, define Δm	Scan desired range	CID	Scan range shifted by Δm to low mass
5	Multiple-reaction Monitoring, define m_1 and m_2	No scan, select m_1	CID	No scan, select m_2

Table was adapted from [124].

[#]Masses for reaction $m_1 = m_2 + n$, except for 1) Q1 scan.

m_1 and m_2 are any mass of interest chosen by the user whereas n is equivalent to the difference between m_1 and m_2.

1.5 Research Interest

Both glycosylation with *O*-GlcNAc and phosphorylation, are post-translational modifications found on the microtubule-associated protein tau (MAPT). The levels of these two post-translational modifications on tau have been found to vary reciprocally. This is thought to be due to the fact that they both occur on either the same or nearby hydroxyl groups of certain serine and threonine residues. It has long been proposed that hyperphosphorylation of tau leads to its aggregation, which in turn generates paired helical filaments, and leads to the eventual formation of neurofibrillary tangles, a distinctive feature of Alzheimer's disease. Therefore, by increasing the level of *O*-GlcNAc modification on tau, it may be possible to prevent or slow its

hyperphosphorylation, thus altering progression of disease in patients suffering from tauopathies, which include Alzheimer's disease[74].

Thiamet-G inhibits the activity of the glycoside hydrolase, OGA. OGA is the enzyme responsible for removing the *O*-GlcNAc modification from tau. When OGA function is impaired, the levels of *O*-GlcNAc will increase at all sites of modification but, most relevantly for tau, at sites that are either potential targets for phosphorylation or adjacent to such sites, thus helping to prevent the formation of neurofibrillary tangles. Thiamet-G is able to cross the blood brain barrier, and it has been demonstrated that this inhibitor can decrease the phosphorylation of tau *in vivo*. An animal pharmacodynamic study, which reveals what the drug does to the body, has been recently carried out using Thiamet-G. However, no pharmacokinetics for Thiamet-G have been described nor is there a published bioanalytical method for characterizing its pharmacokinetics behaviour[74].

As discussed earlier, the PK of a molecule describes how it is liberated, absorbed, distributed, metabolized, and excreted from a body[133]. In an animal study, scientific investigation of how fast the drug is being distributed and eliminated from the body is of importance since this is a key factor in designing safe and effective therapeutics[133]. After administration of a drug, one way to quantitate remaining drug in the body is by monitoring its concentration in plasma over time[133]. The development of a highly sensitive and reproducible bioanalytical method for quantifying and characterizing the drug present in the plasma of an animal is therefore a critical step in establishing its PK.

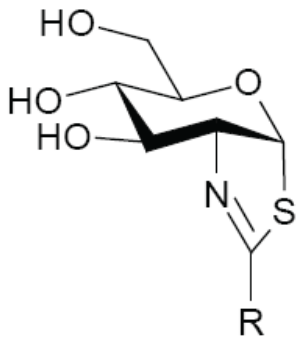

Figure 1.16. Structures of Thiambu-G (R = NHBu), Thiampro-G (R = HNPr), Thiamet-G (R = NHEt), Thiamme-G (R = HNMe), and ThiamH-G (R = NH_2).

Five analogues shown in Figure 1.15, Thiambu-G (R = NHBu), Thiampro-G (R = HNPr), Thiamet-G (R = NHEt)[74], Thiamme-G (R = HNMe), and ThiamH-G (R = NH_2), were developed in the Vocadlo laboratory. Progress toward developing a bioanalytical method for use in PK studies of the analogues is described in Chapter 2 of this thesis. The bioanalysis was carried out using high performance liquid chromatography (HPLC) coupled to a tandem mass spectrometer. In the MS/MS, MRM was used to monitor the transition of parent ions of the compounds to diagnostic product ions, which are generated by collision induced dissociation. A validated bioanalytical method was developed so that rat PK parameters from oral and intravenous administration of Thiamet-G, Thiampro-G, and Thiamme-G, can be determined and is described in Chapter 3. Optimization of the bioanalytical method cycled among the following areas until a reliable and reproducible method was realized: 1) MS optimization, 2) HPLC separation of the analytes, and 3) sample cleanup of samples mimicking genuine PK samples. With the PK data and an effective bioanalytical method, important parameters, such as the therapeutic effective concentration range of the compounds and the half-life of these molecules *in vivo* can be determined.

CHAPTER 2: METHOD DEVELOPMENT

2.1 Scope of Work

The work was directed toward devising a sensitive and reproducible bioanalytical method optimized in three areas: 1) MS analysis, 2) HPLC separation of the analogues, and 3) sample cleanup. The process of method development cycled among these three areas until a well polished method had evolved.

2.2 Optimization of MS for Quantitation

The system used was a Dionex Ultimate 3000 HPLC system coupled to an Applied Biosystems Sciex 4000 QTRAP quadrupole linear ion trap tandem mass spectrometer equipped with a turbo ion spray ion source. Analyst 1.4.2 software was used for data acquisition and processing. A less sensitive mass spectrometer, the AB Sciex API 2000 triple quadrupole tandem mass spectrometer was also employed in various studies. The API 2000 was coupled to a PerkinElmer Series 200 HPLC system. Unless mentioned specifically, the work presented was performed using the API 4000 QTRAP.

2.2.1 Establishment of the MRM Transitions for the Analytes

The first step in developing the LC-MS/MS method was to determine the polarity of ionisation to be used for detection of Thiamet-G, Thiampro-G, Thiamme-G, and Thiambu-G[134]. The type of ionisation used was based on which mode gave a higher ion count. Simultaneously, the ESI operating parameters were optimized during the

infusion of a standard of mixed analogues, Thiamet-G, Thiampro-G, Thiamme-G, and Thiambu-G. Parameters were optimized to give high signal intensity of both molecular and fragments ions. This allowed the parameters for the MRM scan analysis to be determined concurrently for all four analogues.

2.2.1.1 Polarity of Ionisation

A mixture of the compounds was infused directly into the MS with an external pump for the Q1 scan analysis. The total ion chromatogram (TIC) that was generated is a type of Q1 chromatogram that depicts the signal intensity over the entire range of all m/z plotted against time. The extracted ion chromatogram (XIC) for each corresponding compound was generated by extracting the ion of interest from the TIC. The XIC is the chromatogram with the signal of just one single ion plotted against time. Determination of the fragmentation pattern of the compounds was elucidated after consolidating the preferred instrumental parameters for ionizing the ions. See Method 1 for the experimental details (Section 2.5.1).

Results

All the analytes were observed when positive ionisation was chosen in the acquisition method during the Q1 scan analysis. The positive ions characterized in the chromatograms are shown in Table 2.1, and the spectra obtained for Q1 scan analysis is shown in Figure 2.1 (I). The consistent signal in the XIC supported the fact that the compounds were constantly infused into the MS and could readily be detected simultaneously. An attempt was made to detect the compounds using negative ionisation, but no predicted negative ions for the corresponding compounds were observed. Table 2.1 also shows the predicted molecular ions that were expected if negative ionisation was

chosen in the acquisition method of the MS. The XIC for these ions was extracted independently as shown in Figure 2.1 (II), but lack of signal suggested that these compounds did not ionise to yield the predicted negative ions.

Table 2.1. Determination of the Ionisation Polarity of the Analogues.

Analogue	Ion (m/z) Acquired with Positive Polarity	Ion (m/z) Expected to be Observed with Negative Polarity
Thiamet-G	249	247
Thiambu-G	277	275
Thiampro-G	263	261
Thiamme-G	235	233

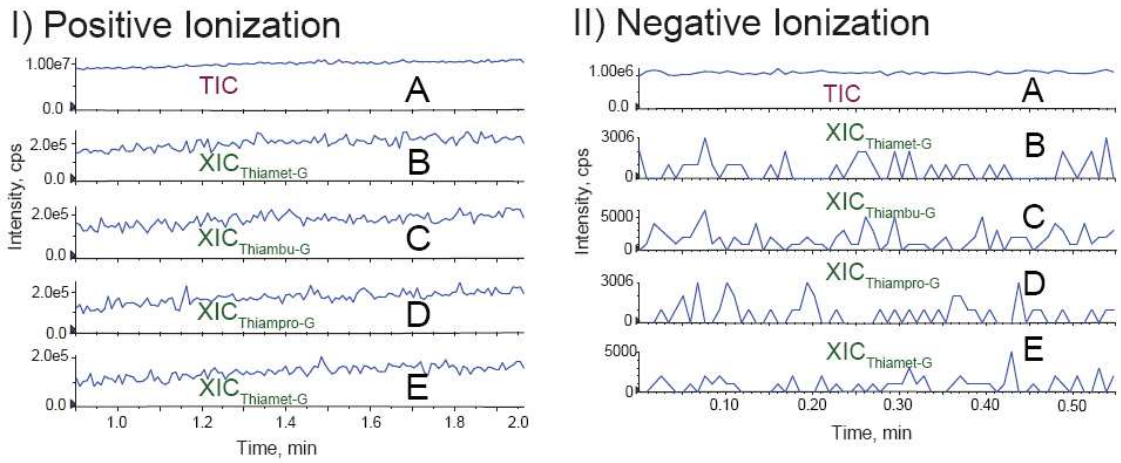

Figure 2.1. Q1 scans in Positive and Negative Ionisation Modes for Thiamet-G and its Analogues.
A mixture of the analogues was infused directly into the MS using an external pump after the acquisition was started. (I) Positive ionisation mode: (A) The TIC for all the expected molecular ions (B – E) and the XIC for each analogue; (B) Thiamet-G, (C) Thiambu-G, (D) Thiampro-G, and (E) Thiamme-G. The consistent signal in the XIC indicates the compounds were constantly infused into the MS and are being detected simultaneously. Repeat (II) Negative ionisation mode: In all the XIC collected (B – E), the signal intensity of the negative ions was much lower than the signal intensity of the TIC (A). This suggests that the predicted negative molecular ions were not detected.

2.2.1.2 Fragmentation Pattern of the Analogues

Product-ion scans have to be determined individually for each compound in order to determine the most representative or intense product ion that results after fragmenting the analogue precursor ion. The specificity of the analytical method can be vastly increased by monitoring a distinct fragmentation process for each compound in order to realize absolute quantitation. The MRM scan mode has been adopted for this purpose in this thesis.

Thiamet-G and its analogues were infused into the MS for the product-ion scan analysis. The precursor ion of each compound was selected for fragmentation with the optimized collision energy (CE) to generate a series of MS/MS chromatograms, which are plots of the signal intensity against the m/z of the remaining precursor ions and the resulting daughter ions. See Method 2 for the experimental details (Section 2.5.2).

Results

The precursor ion for each compound as reported in Table 2.1 was independently selected for product-ion scan analysis. The MS/MS spectra of these analogues are shown in Figure 2.2.

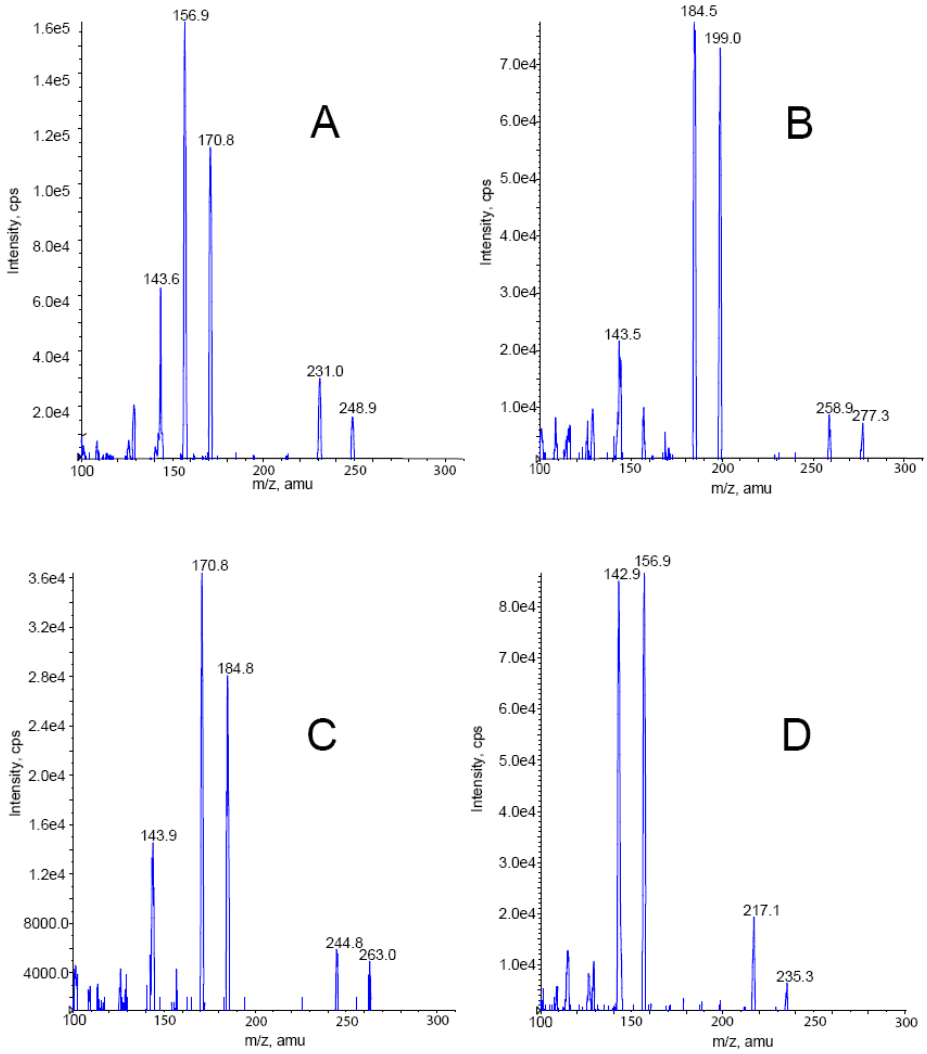

Figure 2.2. MS/MS Spectra for Thiamet-G and its Analogues.
Collision-induced dissociation mass spectra of each compound were generated by using the product-ion scan mode with positive ionisation chosen as the acquisition method. A mixture of the analogues was infused into the MS. The MS/MS chromatograms are (A) Thiamet-G, (B) Thiambu-G, (C) Thiampro-G, and (D) Thiamme-G.

As shown in the MS/MS spectra, fragmentation of the precursor ion of each compound generated two daughter ions both having high intensities. For each analogue, one of the two daughter ions was chosen for the MRM analysis. The pair of ions, precursor ion, and the selected daughter ion for all the analogues are tabulated in Table 2.2.

Table 2.2. The MRM transitions of the Analytes using Positive Polarity.

Analogue	Precursor Ion (m/z)	Daughter Ion with the Highest Intensity (m/z)
Thiamet-G	249.00	171.00
Thiambu-G	277.00	199.00
Thiampro-G	263.00	185.00
Thiamme-G	235.00	157.00

2.2.2 Optimization of the MS Parameters for each Analytical Column

The ideal method for use with each analytical column studied was optimized by using a mixing tee with two inlet ports and one outlet port, which connects to the turbo ion spray ion source on the MS. Optimization of each column method was achieved by infusing the mixture of standards into one inlet port by using an external pump (at a flow rate of 10 µL / min) and, at the same time, pumping the mobile phase into the other inlet port using the HPLC pump at the flow rate that was going to be used during the subsequent experiments. Consult Figure 2.3 for an illustration of the configuration.

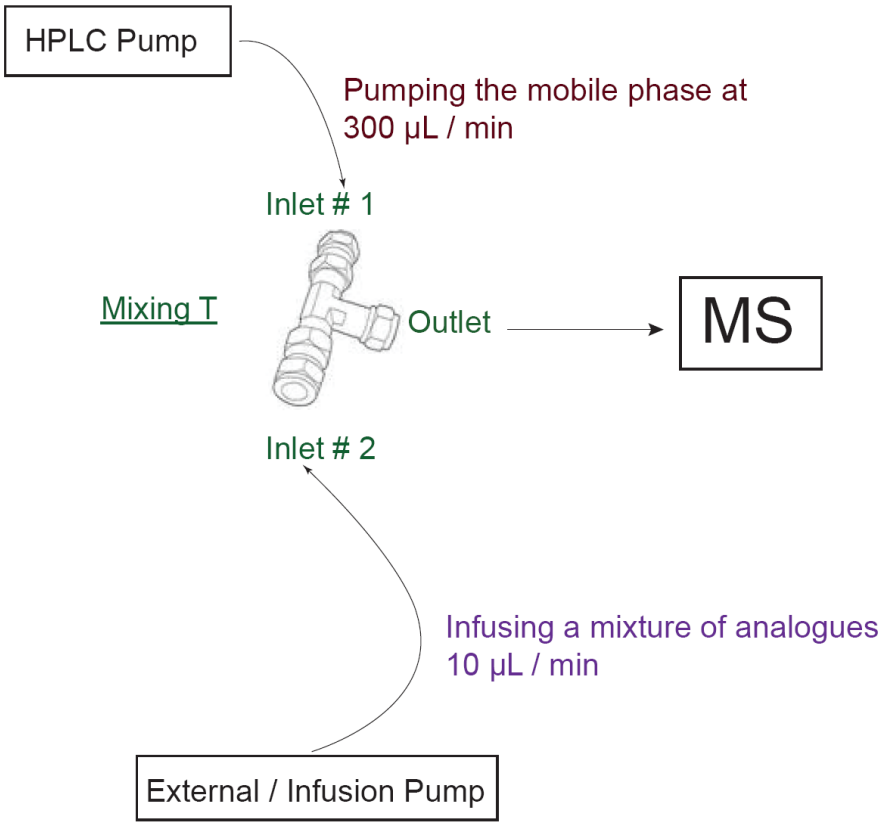

Figure 2.3. The Setup of the MS Using a Mixing T for Optimization of the System Parameters for Column.
The delivery rate of the mobile phase from the HPLC is set to 300 µL / min as an example. A column does not have to be incorporated in the configuration.

Results

MS parameters for two analytical columns, TSKgel and ZIC-HILIC, were subject to optimization. The optimized methods are summarised in Method 3 and Method 4 for TSKgel (Section 2.5.3) and ZIC–HILIC (Section 2.5.4) respectively.

2.3 Column Phase Selection for HPLC Separation

A stationary phase is compatible with the MS when solvent passed through it produces a low background signal in the MRM chromatogram since this indicates that the column is not bleeding materials into the MS. The column of choice should separate

analytes of interest with high resolution and enable their sensitive detection. Therefore, when comparing different stationary phases, sharp and tall peaks for the target analytes in the resulting chromatograms are preferred.

Reverse phase columns have been reported to be suitable for compounds with a variety of properties. The first column investigated was a reverse phase column. Two other types of columns, hydrophilic interaction (HILIC) and porous graphite carbon (PGC) were also tested. Table 2.3 summarises the properties of the different stationary phases.

Table 2.3. Properties of the Tested Stationary Phases.

Types of Chromatography	Stationary Phase	Able to Retain	Solvent Strength
Reverse phase	Alkyl chains	Nonpolar analytes, analytes with minor polarity	ACN > H_2O
Hydrophilic Interaction (HILIC)	Polar groups	Polar analytes	H_2O > ACN
Porous Graphitic Carbon (PGC)	Spherical and porous carbon	Planar or polar analytes	ACN > H_2O

2.3.1 Ranking the Stationary Phases

A mixture containing the analogues was injected into each of the different columns and the performance of each column was evaluated by examining the resulting MRM chromatograms. The protocols used for each column were initially based on those established in the literature.

Table 2.4. Literature Methods for Columns of Interest.

Column	Reference
Synergi Fusion-RP C_{18} reverse phase - alternated with hydrophobic and polar embedded groups on a silica surface	[135, 136]
Agilent Zorbax Eclipse XDB C_{18} reverse phase – alkyl chains on a silica surface	[137]
TSKgel Amide-80 HILIC - carbamoyl group covalently linked to a silica gel matrix	[120, 138-140]
ZIC-HILIC HILIC - zwitterionic functional groups covalently attached on a porous silica surface	[134, 141, 142]
Hypercarb PGC – flat sheets of hexagonally arranged carbon atoms, porous	[114, 116]

The performance of each column was evaluated based on: 1) its ability to retain the polar compounds on the stationary phase, 2) the level of background in the chromatogram, 3) the peak shapes of the analytes, and 4) integration of the signal corresponding to each analyte.

2.3.2 Optimization of Retention and Analyte Resolution of the Column(s)

Optimum conditions were established to enable a column to adequately retain all the analytes. The ideal capacity factor for the analytes (also called the retention factor) is greater than 0.5 and less than 10[143]. Optimization of various compositions of mobile phase was carried out to improve the resolution of the peaks. The aim was to identify a mixture of ACN / H_2O where the compounds were retained on the stationary phase yet elution did not take overly long. Adjustment of the pH and the addition of ion pairing reagents also affected the retention time of the analytes. Since there were multiple

analytes in the matrix, separating the analytes from each other and also from the matrix was desirable.

2.3.2.1 Results Obtained by Separating the Analytes with Different Types of Stationary Phases

A mixture of the analogues was injected into the LC-MS system for MRM analysis using the MRM transitions tabulated in Table 2.2. Chromatographic separation was carried out using the different columns so that separation and retention of the compounds can be evaluated for each stationary phase. Only the data obtained using the HILIC columns are shown in this chapter. The data obtained using other columns are shown in Appendix A 3.1 and A 3.2.

HILIC Columns

2.3.3.1 TOSOH Bioscience TSKgel Amide-80, 3 µm (TSKgel column)

TSKgel was the first HILIC column tested. The stationary phase has a carbamoyl group covalently linked to a silica gel matrix. This group is non-ionic (Figure 2.4).

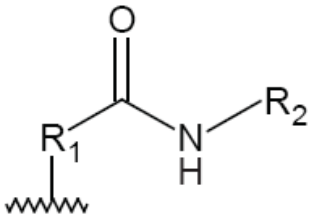

Figure 2.4. Functional Group on the TSKgel column.

Figure 2.5 shows the MRM chromatogram of the analogues and reveals that all the ion peaks afford a Gaussian peak shape. The column volume of the empty TSKgel column (CV_{empty}) was 503 µL. In general, the void volume (V_0) is assumed to be 60-70

% of the empty column, and 30-40% is assumed to be the space taken up by the packing material[144].

$$V_0 = 0.65 \times CV_{empty} \quad (1)$$

$$T_0 = V_0 / \text{flow rate} \quad (2)$$

The void time (T_0) was calculated to be 1.63 min. It is recommended that analytes of interest are eluted with at least 1.5 void volumes in order to provide sufficient time for the analytes to interact with the stationary phase[111]. Hence, the time recommended for eluting the least retained analogue ($T_{recommended}$) is 2.45 min.

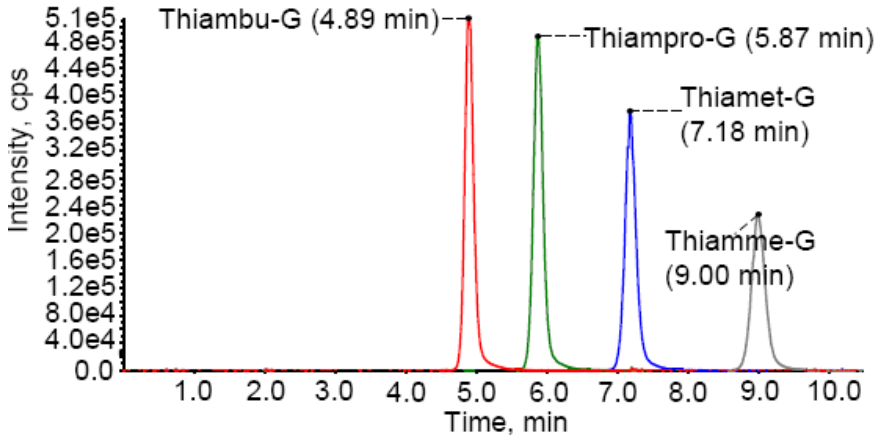

Figure 2.5. Separation of the Four Analytes Using the TSKgel column. Concentration of the mixture of analytes was 210 ng / mL. (Column: 2.0 mm x 15 cm; guard: 2.0 mm x 1.0 cm, flow rate: 200 µL / min, elution with: 0.1 % FA + 80 % ACN / H_2O)

The TSKgel column provided retention as well as separation of the compounds. In contrast to the reverse phase column, the least polar compound, Thiambu-G, eluted first while the most polar compound, Thiamme-G, was retained on the stationary phase for the longest time. Thiambu-G eluted at about 5.0 min, hence analytes were retained sufficiently on this column. In this thesis, the term background is defined as chemical noise which arises from the signals corresponding to species other than the analytes

present in the analytical system[145]. The term noise refers to electronic signal produced by the analytical instrumentation[146] and is defined as the change in detector response over a specified time period without the introduction of solvent or samples[145]. Notably, the documented maximum S / N of the instrument used in this thesis is less than 20. As a result, the instrument noise is insignificant when compared to the background noise.

The level of background noise in the chromatogram of Figure 2.4 was generally lower than 200 cps. Compared to the intensity of the analogues, the background level was a thousand times lower. In Table 2.5, the minimum S / B measured is reported in Table 2.5 and is greater than 6000. Thus, the column provides suitable sensitivity.

Table 2.5. S / B Ratios for the Separation and Detection of Thiamet-G and its Analogues on a TSKgel Column.

Analyte	S / B	Intensity of Analyte (cps)	Maximum Levels of Background (cps)
Thiamet-G	1.1×10^4	1.8×10^6	2.8×10^2
Thiambu-G	2.8×10^4	2.7×10^6	1.6×10^2
Thiampro-G	2.7×10^4	2.4×10^6	1.7×10^2
Thiamme-G	6.2×10^3	1.2×10^6	3.1×10^2

Levels of background were measured from 0 to 0.5 min.
Separation as shown in Figure 2.5.

As shown in Table 2.6, the retention factors, k′, for all the analytes ranged from 1.92 to 3.26 and were within the range (0.5-15) suggested by the literature[143]. The peaks were separated as shown in Figure 2.5. The measured resolution values confirm that there is an excellent separation between the peaks.

Table 2.6. Calculation of the k' Values and the Chromatographic Resolution of the TSKgel Column.

Analyte	RT (min)	k'A	Selectivity	Half Peak Width (min)	N_t	Resolution
Thiambu-G	4.90	2.01		0.14	3.0×10^3	
Thiampro-G	5.88	2.61	1.30	0.15	4.3×10^3	3.0
Thiamet-G	7.19	3.41	1.31	0.17	5.7×10^3	3.8
Thiamme-G	9.00	4.52	1.33	0.22	6.5×10^3	4.5

Separation as shown in Figure 2.5.

Stability of the TSKgel Column

A standard solution containing the four analytes at a concentration of 210 ng / mL each was analysed using the TSKgel column at the beginning and at the end of each set of analyses. In between analyses of these two sets of standard solutions, samples containing plasma were separated using the column and analysed by MRM using the MS/MS. Table 2.7 tabulates the peak area counts and retention times of the standard solutions. Within a group of samples containing 62 individual samples (about 11 h of analysis time), the drifting of the retention time for the analytes was less than 4%. The peak area counts of the two standard samples were very similar with less than 5 % difference in all cases. The data demonstrates that the TSKgel column is stable based on the reported retention times and peak area counts.

Table 2.7. Comparison of the Peak Area Counts of the Samples Analysed over the Course of 11 h.

Analyte	Standard (Sample 3) (min)	Standard (Sample 63) (min)	% Change in RT	Peak Area of Standard (Sample 3) (cps)	Peak Area of Standard (Sample 63) (cps)	% Change in Peak Area
Thiamet-G	5.87	5.64	3.92	6.39×10^6	6.61×10^6	3.44
Thiambu-G	4.13	3.99	3.39	$7.85e \times 10^6$	8.33×10^6	6.11
Thiampro-G	4.88	4.71	3.48	$7.30e \times 10^6$	7.68×10^6	5.21
Thiamme-G	7.29	7.05	3.29	$5.12e \times 10^6$	5.25×10^6	2.54

% shift in X (peak area or RT) = (|X of Sample 3 - X of Sample 63| / X of Sample 3) x 100 %.

2.3.3.2 Merck SeQuant ZIC-HILIC, 5 µm 200Å PEEK with PEEK frits (ZIC-HILIC column)

ZIC-HILIC is another type of HILIC column that is similar to the TSKgel column. It has a stationary phase covalently bonded with zwitterionic functional groups on the surface (Figure 2.6). Due to the overall neutral charge state of the functional group, a charged analyte will have weak electrostatic interactions with the stationary phase.

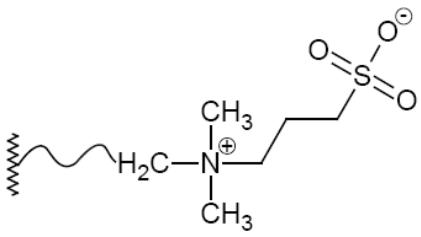

Figure 2.6. Functional Group on the ZIC-HILIC Column.

All analytes showed Gaussian peak shapes in the chromatogram. Based on the column volume, the minimum time required to elute the least retained analyte is 1.35

min. The least polar compound, Thiambu-G, took 3.45 min to elute. The chromatogram is reported in Figure 2.7.

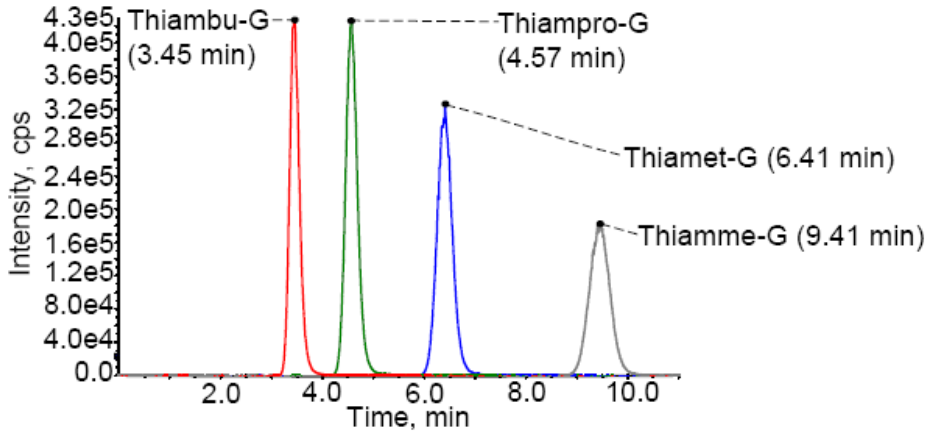

Figure 2.7. Separation of the Four Analytes Using the ZIC-HILIC Column.
Concentration of the mixture of analytes was 210 ng / mL. (Column: 2.1 x 100 mm; guard: 2.1 x 20 mm, flow rate: 300 µL / min; elution with: 0.1 % FA + 85 % ACN / H_2O)

The levels of background in the chromatogram were generally lower than 200 cps. The numerical data shown in Table 2.8 demonstrates the signal of the analytes was well above the background noise.

Table 2.8. S / B Ratios for the Separation of Thiamet-G and its Analogues Using a ZIC-HILIC Column.

Analyte	S / B	Intensity of Analyte (cps)	Maximum Levels of Background (cps)
Thiamet-G	3.80×10^3	3.20×10^5	9.50×10^1
Thiambu-G	4.51×10^3	4.30×10^5	1.10×10^2
Thiampro-G	6.60×10^3	4.30×10^5	7.00×10^1
Thiamme-G	1.17×10^3	1.80×10^5	2.60×10^2

Levels of background were measured from 0.5 to 1 min.
Separation as shown in Figure 2.7.

Based on equation 1, T_0 was determined to be 0.90 min. As shown in Table 2.9, the retention factors, k′, for all the analytes were within the range (0.5-15) as suggested by the article, "HPLC Method Development and Validation for Pharmaceutical Analysis"[143]. The peaks were greater than 2.5 as shown in Figure 2.7. The suitable resolution confirmed that there was an excellent separation between the peaks.

Table 2.9. Calculation of the k′ Values and the Chromatographic Resolution of the ZIC-HILIC Column.

Analyte	RT (min)	k'A	Selectivity	Half Peak Width (min)	N_t	Resolution
Thiambu-G	3.44	2.82		0.21	7.8×10^2	
Thiampro-G	4.57	4.08	1.44	0.26	1.14×10^3	2.4
Thiamet-G	6.41	6.12	1.50	0.33	1.52×10^3	3.3
Thiamme-G	9.46	9.51	1.55	0.46	1.96×10^3	4.3

Separation as shown in Figure 2.7.

A standard solution, containing the four analytes at a concentration of 210 ng / mL, was analysed on the ZIC-HILIC column at the beginning and at the end of analysis. Plasma samples were analysed during the period in between collecting data on these two

sets of standards. Table 2.10 tabulates the peak area counts and retention times of the samples. An increase in peak area response was observed for sample 63. The apparent increase in concentration might be due to evaporation of the ACN in the sample vial although this effect was not observed when using the TSKgel column. With a time gap of more than 11h, the shifting of the retention time for the analytes was significant; the smallest shift in retention time for the analogues was found to be over 20 %. A possible reason that could account for this effect is that left over matrix ions present inside the column may not be completely washed out prior to the injection of the next sample. The matrix ions might adhere onto the stationary phase and thereby alter the properties of the column. Consult the experimental data in Appendix A4.3.4 for further investigations regarding the stability of the ZIC-HLIC column.

Table 2.10. Stability of the ZIC-HILIC Column.

Analyte	Standard (Sample 3) (min)	Standard (Sample 63) (min)	% Change In RT	Peak Area of Standard (Sample 3) (cps)	Peak Area of Standard (Sample 63) (cps)	% Change in Peak Area
Thiamet-G	3.45	4.32	25.2	5.25×10^6	5.88×10^6	12.0
Thiambu-G	2.16	2.61	20.8	6.11×10^6	6.92×10^6	13.3
Thiampro-G	2.64	3.28	24.2	5.69×10^6	6.21×10^6	9.14
Thiamme-G	4.81	6.10	26.8	4.58×10^6	5.18×10^6	13.1

% shift in X (peak area or RT) = (|X of Sample 3 - X of Sample 63| / X of Sample 3) x 100 %.

Discussion

As discussed in Section 2.3.1, a suitable stationary phase was chosen for the analytical method based on its ability to retain the polar analogues, the level of background signal in the chromatogram, the peak shapes of the analytes, and the intensity

of the signal corresponding to each analyte. Both the TSKgel and ZIC-HILIC columns show an ability to fulfill the above criteria. Although for both columns, there were difference in peak area responses among the compounds, the relative peak area responses for the compounds were consistent among all the chromatograms. These two columns were therefore considered as possible candidates for future use. Further optimization of the sample cleanup procedure is discussed below.

2.4 Sample Cleanup of Model Samples

As described in Section 1.3.2, samples containing a biological matrix, such as rat plasma, have to undergo some kind of cleanup process before being injected into an analytical system for analysis. The higher the extent of interference from the matrix, the lower the efficiency of the ionisation of the analytes. Thus, the removal of matrix interference required optimization of sample cleanup procedures.

Various types of samples were prepared to mimic PK samples and these contained a known concentration of a mixture of the analogues. These samples were used to assess each of the sample cleanup processes tested. The blank rat plasma was purchased from a commercial supplier with sodium heparin as the anticoagulant.

Sample preparation: types of samples.

1. **Standard**: Thiamet-G and its analogues diluted from stock solution into ACN / H_2O mixture (composition dependent on experimental setup).
2. **Control sample** (positive control): Thiamet-G and its analogues were spiked in water.
3. **Blank sample** (negative control): plasma spiked in water.

4. **Plasma sample**: Thiamet-G and its analogues were spiked into plasma diluted with water.

All the samples went through the sample cleanup processes except for the *standard*.

2.4.1 Assessment of each Sample Preparation Process During Method Development

a) % Recovery = (sample peak area / standard peak area) x 100 %

The comparison of peak area response between the sample and the standard yielded the percent ratio of the recovery of the analytes. This value provides an estimate of the loss of analytes during the sample cleanup process. The desired % recovery is above 80 %.

b) % Matrix suppression = (plasma sample peak area / control sample peak area) x 100 %

Suppression of the analogue ions is caused by matrix ions coeluting with the target analytes. The percent ratio of matrix suppression reflects the influence of matrix ions present in the rat plasma on the analyte signal intensity. A percent ratio of less than 100 % indicates that matrix present in the sample is suppressing ionisation and detection of the analyte. A percent ratio of over 100 % could be caused by an ionisation enhancement effect, in which analyte is lost in the absence of matrix during analysis[147].

c) % RSD = (standard deviation of x / average of x) x 100 %

x = either the peak area response or retention time of the analytes

The percent ratio of relative standard deviation (RSD) measures the repeatability of the peak area or retention time (RT) during repeated sample runs of the analytes within

the same batch. The desired % RSD for the peak area is less than 10 % and the desired % RSD for the RT is less than 2 %.

d) Q1 scan (Scanning with the second quadrupole)

Comparison of the Q1 scan of the control sample and plasma sample reveals the matrix ions present in the plasma sample.

2.4.2 Results with Different Sample Preparation Procedures

Several sample cleanup procedures were attempted in order to remove proteins and other matrix components that were present in the model samples so that these samples could be ionised efficiently for the MS analysis. Through the comparison of the chromatograms between the control and plasma samples, ion suppression was observed for Thiamet-G and Thiamme-G, in particular, in the absence of sample clean up. This is evident from the high % matrix suppression and the distortion of peak shapes of the analytes in the chromatograms of the plasma sample (Appendix Section A 4). As discussed in Appendix Section A4.3.2, one set of samples was prepared using procedure 4 and was analysed using the ZIC-HILIC column. Although ion suppression was not observed for the analytes, using this sample preparation procedure yielded poor % recovery for both the control and plasma samples. All the detailed experimental results are summarised in Table 2.11 and are reported in greater detail in Appendix A4.

Table 2.11. Preliminary Methods for Sample Preparation and other Types of Method Development.

	Sample Cleanup Procedure	Description	Result
1	Protein Precipitation	Experimented with different organic solvents for precipitating the protein from plasma extracts.	Phospholipids and salts remained and caused ion suppression.
2	Different eluents as mobile phase	1. Combination of ACN / H_2O + 0.1 % FA. 2. Combination of MeOH / H_2O + 0.1 % FA.	2: The compounds were not retained on the stationary phase likely due to interactions between the compounds and the eluent.
3	Ultrafiltration	Obtained the filtrate using an ultra filtration device while removing the proteins in the filtrand.	Salts and other components remained and caused ion suppression. Phospholipids were removed.
4	Ultrafiltration + LLE	Extracted out the non polar matrix ions present in the filtrate that can interfere with analysis.	Salts were present resulting in ion suppression. Phospholipids were removed.

See Appendix A4 for full details.

In Table 2.12, results obtained from sample cleanup procedures involving solid phase extraction devices have been summarised. None of the procedures yielded good results except for the Hypercarb offline 1 mL SPE cartridge. In the following section the results obtained from using this particular cartridge are discussed in more detail. The detailed results for procedures 1, 3, 4 are reported in Appendix A5. Since Thiamme-G and Thiampro-G were not retained on the Supelclean ENVI-Carb SPE tube when washing the cartridge with 100 % water, procedure 2 was not pursued further. All these experiments were performed using a ZIC-HILIC column because only minor suppression was

observed for the analytes when using this column. In contrast, when using the TSKgel column, detection of the analytes suffered from severe matrix suppression.

Table 2.12. Sample Preparation Using Solid Phase Extraction Devices.

	Sample cleanup procedure	**Description**	**Result**
1	Ultrafiltration + ZiptipC_{18}	Filtrate collected from the ultrafilter was further cleaned up by the C_{18} cartridge in the ziptip.	Analytes were lost in the ZiptipC_{18}.
2	Supelclean ENVI-Carb 1 mL SPE tube	Nonporous graphite cartridge (NPGC) used after ultrafiltration.	Compounds eluted out at 100% water limiting usefulness.
3	Sigma Hybrid SPE 1 mL	Lipid remover was used after protein precipitation.	Lipids were removed but salts were still present.
4	Captiva ND^{lipid}	Lipid remover was used after protein precipitation.	Lipids were present in the final samples. The cartridge was not compatible with solvent composed of high organic composition.
5	Hypercarb offline 1 mL SPE cartridge	Porous graphite cartridge (PGC).	Analogues were obtained with low carryover of matrix.

See Appendix A5 for full details.

Hypercarb SPE Cartridge

Figure 2.8 shows the analyses of the samples using the ZIC-HILIC column after they have undergone the sample cleanup process using the Hypercarb SPE cartridges. As shown in Figure 2.8, Gaussian shapes were observed for the analytes. The plasma sample was analysed followed by nine samples, standards, and other plasma samples, before analysis of the control sample. The peak area counts of the analytes from both chromatograms were very similar.

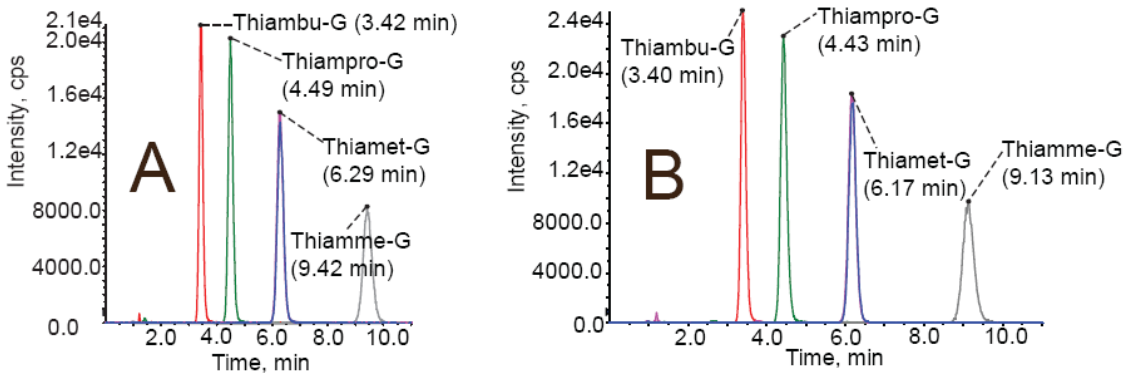

Figure 2.8. Use of Hypercarb SPE Cartridge for Sample Cleanup on Plasma Samples Containing Thiamet-G and its Analogues.
Chromatogram (A) and (B) were the control and the plasma samples respectively. These samples were separated using a ZIC-HILIC column after sample cleanup. Separation conditions: Step 1) 0 - 10 min, 300 µL / mL, 84 % B, Step 2) 10.5 – 13 min, 600 µL / mL, 30 % B, Step 3) 13.5 – 16 min, 600 µL / mL, 84 % B, Step 4) 16.5 - 18 min, 300 µL / mL, 84 % B (A = 0.5 % FA + 5 % ACN + H_2O, B = 0.1 % FA + ACN).

To evaluate the % matrix suppression following sample clean up, analogues were added into both the control and plasma samples prior to the sample cleanup process. The % matrix suppression was calculated based on the chromatographic separation as shown in Figure 2.8. The percent ratio close to 100 % demonstrated that no matrix suppression occurred for any of the analytes when contained in the plasma sample and cleaned up by Hypercarb SPE (Table 2.13). As indicated in the chromatograms, any changes in retention time were small.

Table 2.13. Comparison of the Peak Area Counts of Thiamet-G and its Analogues Prepared in Water versus Plasma.

Analyte	Control Sample (cps)	Plasma Sample (cps)	% Matrix Suppression
Thiambu-G	2.08×10^5	2.31×10^5	111
Thiamet-G	2.24×10^5	2.36×10^5	105%
Thiampro-G	2.40×10^5	2.60×10^5	108%
Thiamme-G	1.86×10^5	1.96×10^5	105%

% Matrix suppression = peak area counts of (plasma /control) x 100 %.
Separation as shown in Figure 2.8.

A % recovery experiment was carried out, and the results are reported in Table 2.14. The peak area counts were compared between the plasma sample and a blank sample that was spiked with the compounds at the same concentration as the plasma sample that had undergone the sample cleanup process. The purpose of this comparison was to test the efficiency of the sample extraction process. As shown in Table 2.14, the % recovery ranged from 93.4 to 98.0 %. A % recovery of close to 100 % suggests that the extraction process was efficient.

Table 2.14. % Recovery of the Analogues.

Analyte	Plasma Sample (cps)	Plasma Spike (cps)	% Recovery
Thiambu-G	2.31×10^5	2.39×10^5	96.6 %
Thiamet-G	2.36×10^5	2.53×10^5	93.4 %
Thiampro-G	2.60×10^5	2.66×10^5	97.6 %
Thiamme-G	1.96×10^5	2.00×10^5	98.0 %

Separation as shown in Figure 2.8.

Stability of the ZIC-HILIC Column

In Figure 2.8, the elution time of Thiamme-G in chromatogram (A) was different when compared to chromatogram (B). The retention times for the other three compound ions in both chromatograms were similar. From experience in using the ZIC-HILIC column, changing in retention times of analytes were observed throughout the time it took to analyse one batch of samples. However, the deviation of the retention time for Thiamme-G was often the greatest. A possible explanation is that some matrix ions were still present in the column even though a wash cycle was incorporated in the run. As a result, the elution time of the analytes, particularly Thiamme-G, might be affected by the co-eluted matrix ions. Another possible reason was that the stationary phase might become more polar due to frequent exposure to the polar matrix ions. As described in Section A4.1.2, a similar observation was seen for other experiments carried out using a ZIC-HILIC column.

During method development, it was not known whether the samples needed to undergo deproteinisation prior to loading onto the cartridge or not. Analytes present in the samples that were directly applied onto the Hypercarb SPE cartridges were better retained on the bulk material and did not elute out during washing with 100 % water (data not shown). When proteins were first removed from the samples by protein precipitation, elution of Thiamme-G occurred when the cartridge was washed with water using 6.5 times of the bulk material volume. Thiamet-G also eluted out when the cartridge was washed with water using 8.5 times the bulk material volume. When the samples were first passed through an ultrafilter, elution of Thiamme-G occurred when the cartridge was washed with 8.5 times of the bulk material of 100 % water. Interestingly, when directly applied to the column, the analytes were still able to bind on the cartridge when washing with 100 % water using 20 times of the bulk material volume. Nevertheless, in Q1 scan analysis, the same matrix ions co-eluting with the analytes were observed regardless of which of the three sample cleanup processes (protein precipitation, ultrafiltration, direct application to cartridge) was employed. Based on these data it was decided to use Hypercarb SPE alone for sample clean up since this was rapid and enabled a good balance between retention of the analytes and ease of elution from the cartridge. Further, this approach to clean up, along with use of the ZIC-HILIC column, showed little matrix suppression and demonstrated good run to run reproducibility.

2.4.3 The Optimized Method

An optimized analytical method was developed. The optimized method used Hypercarb SPE cartridges as the cleanup tool and a ZIC-HILIC column as a compatible stationary phase. The analytical system for LC–MS/MS analysis consisted of a Dionex

Ultimate 3000 HPLC system coupled with an AB Sciex 4000 QTRAP quadrupole linear ion trap tandem mass spectrometer equipped with a turbo ion spray ion source.

2.5 Method Section

2.5.1 Method 1: Generic Method for the 2000 QTRAP LC/MS system

Chemicals and reagents. HPLC grade acetonitrile and HPLC grade or LC-MS grade water were purchased from Caledon Laboratories Ltd. (Georgetown, Canada) and Mallinckrodt Baker, Inc. (Phillipsburg, USA) respectively while reagent grade formic acid was purchased from Fluka, Sigma-Aldrich Canada Ltd. (Oakville, Canada). The compounds, Thiamet-G (batch JJ-37)[74], Thiambu-G (batch JJ-1-28), Thiampro-G (batch JJ-1-47), and Thiamme-G (batch JJ-1-42) were synthesized previously in the Vocadlo lab (Simon Fraser University, Burnaby, BC).

Instrumentation. The 2000 QTRAP LC/MS system consisted of the 2000 QTRAP mass spectrometer (Applied Biosystems, Life Technologies Corporation, Foster City, USA) interfaced with a Perkin Elmer Series 200 high performance liquid chromatography (HPLC) system (Perkin Elmer Inc, Massachusetts, USA). The control software for data acquisition was Analyst version 1.4.2 (Applied Biosystems). The LC system was composed of a binary LC pump, a vacuum degasser, controlled autosampler, and a column compartment without temperature control. No analytical column was installed in the system. The mobile phase, 0.1% FA + 85% ACN + H_2O, was pumped at a flow rate of 300 µL / min.

Preparation of Standards. 7.00 mg of each analogue was weighed out individually with a five decimal place analytical balance (Fisher Scientific Company,

Ottawa, Canada) for preparation of stock solutions. Stock solutions (conc. = 70000 ng / mL) consisting of Thiamet-G, Thiambu-G, Thiampro-G, and Thiamme-G, were prepared by dissolving the compounds in water and making the volume to 100 mL using glass volumetric flasks. These stock solutions were stored at 4 ^{o}C in an amber glass bottle. Mixed compound standard solution A (conc. = 1400 ng / mL) was prepared by adding 200 µL from each stock solution to 8.5 mL ACN and making the volume to 10 mL with water using a glass volumetric flask. This solution, standard solution A1, was stored at 4 ^{o}C in a HPLC vial until analysis.

Analytical Procedure. Standard solution A was analysed using the MS in both positive ion and negative ionisation modes by continuously infusing the standard using a Harvard syringe pump at a flow rate of 10 µL / min into the turbo ion spray ion source of the MS. Through a mixing tee, 300 µL / min of the mobile phase was concurrently delivered into the turbo ion spray ion source using the HPLC pump. Q1 scan analysis was the selected acquisition method. The scanning range of the mass range was set from 230.00 amu to 280.00 amu, and the dwell time was set to 0.500 sec. The resolution of Q1 was set to be 1 unit mass resolution. In positive ionisation mode set, the set parameters were CUR (25.00 psi), IS (4500.00 V), TEM (100.00 °C), GS1 (55.00 psi), GS2 (40.00 psi), DP (42.50 V) FP (200.00 V), and EP (7.00 V). In negative ionisation mode set in the acquisition method, the set parameters were CUR (25.00 psi), ISP (- 4500.00 V), TEM (100.00 °C), GS1 (55.00 psi), GS2 (40.00 psi), DP (- 42.50 V), FP (- 200.00 V) and EP (- 7.00 V).

2.5.2 Method 2: Generic Method for the 4000 QTRAP LC/MS system

Chemicals and reagents. See Method 1 (Section 2.5.1).

Instrumentation. The 4000 QTRAP LC-MS/MS system consisted of the 4000 QTRAP mass spectrometer (Applied Biosystems) and the Ultimate 3000 HPLC system (Dionex Corporation, Bannockburn, USA). The LC system was composed of a binary LC pump, a vacuum degasser, a temperature controlled autosampler, and a thermostated column compartment set at 40 ^{o}C. The control software for data acquisition was Analyst version 1.4.2, Dionex Chromatography Mass Spectrometry Link software version 2.0.0.2315, and Chromeleon version 6.80 SP2 (Dionex Corporation). The mobile phase, 0.1% FA + 85% ACN + H_2O, was pumped at a flow rate of 300 µL / min.

Preparation of Standards. 7.00 mg of compounds were weighed out separately with a five decimal place analytical balance for preparation of stock solutions. Stock solutions (conc. = 70000 ng / mL) containing Thiamet-G, Thiambu-G, Thiampro-G, and Thiamme-G were prepared by dissolving the compounds in water and making the volume up to 100 mL using volumetric flasks. These stock solutions were stored at 4 ^{o}C. Mixed compound standard solution B (conc. = 1400 ng / mL) was prepared by adding 200 µL from each of the stock solutions into a 10 mL glass volumetric flask and making the volume up with water. Standard solution B was stored at 4 ^{o}C in a glass vial. Mixed compound standard solution C (conc. = 10 ng / mL) was prepared by transferring 10 µL of solution B into a HPLC vial. To this vial, 980 µL of ACN and 410 µL H_2O were added to yield solution C with a final composition of 70 % ACN / H_2O. Standard solution C was stored at 4 ^{o}C in a HPLC vial prior to analysis.

Analytical Procedure. 10 µL of standard solution C was injected by the autosampler of the HPLC system. Using the HPLC pump to provide the mobile phase, sample was delivered into the turbo ions pray ion source. The software began the acquisition prior to the injection of the sample. The same solution was repeatedly injected into the autosampler for the product-ion scan analysis of all the compounds. Q1 scan analysis was selected in the acquisition method. The scanning range of the mass spectrum was from 100.00 amu to 500.00 amu. The dwell time was 4.00 sec. The resolution of Q1 was unit and Q3 was low. In positive ionisation mode set in the acquisition method, the other parameters were CUR (30.00 psi), ISP (4500.00 V), TEM (200.00 ^{o}C), GS1 (20.00 psi), GS2 (20.00 psi), DP (65.00 V), CAD (7.00 psi), EP (8.00 V), and CXP (10.00 V). The settings for CE were 32, 33, 30, and 32 eV for Thiamet-G, Thiambu-G, Thiampro-G, and Thiamme-G respectively.

2.5.3 Method 3: Generic method for TSKgel-MS-Analysis

The method was similar to the generic method for the 4000 QTRAP LC/MS system (See Section 2.5.2) with the following changes:

Instrumentation. The analytical column for the analysis, TOSOH Bioscience TSKgel Amide-80 (South San Francisco, USA) (3 µm, 2.0 x 150 mm ID), was protected by a guard column (3 µm, 2.0 x 10 mm ID). The mobile phase, 0.1 % FA + 80 % ACN / H_2O, was pumped at a flow rate of 200 µL / min. The operating pressure of the column was approximately 47 bar.

Preparation of Standards. Mixed compound standard solution F (conc. = 1400 ng / mL) was prepared by adding 200 µL of the analogue stock solutions, prepared in

Method 2 (Section 2.5.2), into a 10 mL glass volumetric flask containing 7 mL of ACN and making the volume up with water. The standard solution F vial was stored at 4 ^{o}C in a HPLC vial prior to analysis.

Analytical Procedure. 2 µL of standard solution F was injected by the autosampler of the LC / MS system. Using the HPLC pump to provide the mobile phase, 2 µL of the sample was delivered to the turbo ion spray ion source. The MRM transitions were set according to Table 2.2, and the dwell time was set as 200.00 µsec. The resolution of Q1 and Q3 was set to be 1 mass unit resolution. In the positive ionisation mode, the other parameters were CUR (30.00 psi), ISP (4500.00 V), TEM (200.00 ^{o}C), GS1 (20.00 psi), GS2 (20.00 psi), DP (56.00 V), CAD (7.00 psi), EP (9.00 V), CE (31.00 eV), and CXP (10.00 V).

2.5.4 Method 4: Generic Method for ZIC-HILIC-MS-Analysis

The method was similar to the generic method for the 4000 QTRAP LC-MS/MS system (See Section 2.5.2) with the following changes:

Instrumentation. The analytical column used for the analyses, Merck SeQuant ZIC-HILIC column (Umeå, Sweden) (5 µm, 2.1 x 100 mm ID), was protected by a guard column (5 µm, 2.1 x 20 mm ID). The mobile phase, 0.1 % FA + 85 % ACN / H_2O, was pumped at a flow rate of 300 µL / min.

Preparation of Standards. Mixed compound standard solution G (conc. = 210 ng / mL) was prepared by adding 30 µL of the stock solutions of the analogues, prepared as in Method 2 (See Section 2.5.2), into a 10 mL glass volumetric flask containing 7 mL

of ACN and making the volume up with water. The standard solution G was stored at 4 ^{o}C in a HPLC vial prior to analysis.

Analytical Procedure. 5 µL of solution G was injected by the autosampler of the LC-MS/MS system. Using the HPLC pump to provide the mobile phase, the sample was delivered to the turbo ion spray ion source. The MRM transitions were set according to Table 2.2 and the dwell time was set as 200.00 µsec. The resolution of Q1 and Q3 was set to be 1 unit mass resolution. In the positive ionisation mode, the other parameters were CUR (30.00 psi), ISP (4500.00 V), TEM (200.00 ^{o}C), GS1 (20.00 psi), GS2 (20.00 psi), DP (56.00 V), CAD (7.00 psi), EP (8.00 V), CE (31.00 eV), and CXP (10.00 V).

2.5.5 Method 5: Generic Method for Hypercarb SPE Cleanup and LC-MS/MS Analysis

The method was similar to the method for validation (See Section 3.7) with the following changes:

Preparation of Samples: One stock solution containing Thiamet-G, Thiampro-G, and Thiamme-G (conc. = 10000 ng / mL) was prepared by dissolving 1.0 ± 0.1 mg of each standard in water and making up the volume in a 100 mL volumetric flask. A mixed standard containing 100 ng / mL of each compound was prepared by serial dilution. A separate 100 ng / mL internal standard was prepared the same way by preparing a stock solution containing only Thiambu-G (conc. = 10000 ng / mL).

To generate the plasma sample 11 µL of the 100 ng / mL mixed standard and 11 µL of the 100 ng / mL internal standard were transferred into a centrifuge tube. In addition, two portions of 11 µL of the control rat plasma and 110 µL of water were added into the tube to give a total final volume of 154 µL. After the tube was capped and

vortexed for 30 sec, it was centrifuged at 10000 rpm for 1 min at room temperature. The control sample was prepared the same way except that the rat plasma was replaced with water. A blank sample was also prepared using the same sample preparation procedure as the plasma sample except that the mixed standard was replaced with water. To a blank sample, after undergoing the sample cleanup process, was added 11 µL of the 100 ng / mL mixed standard and 11 µL of the 100 ng / mL internal standard. This sample was called the plasma spike sample. These samples were cleaned up using the Hypercarb SPE cartridge following the procedure described in the validation method (See Section 3.7). The peak area counts of the analytes reported in Table 2.14 were corrected using equation 3 to make the peak area counts equivalent to what should be observed for a blank sample spiked with 10 µL of the standards.

Analytical Procedure. 4 µL of the plasma sample was injected by the autosampler of the LC-MS/MS system after analysis of the control sample (injection volume = 4 µL) had finished. Nine samples were analysed in the time between the control and the plasma sample analyses. The plasma spike, 4 µL injection volume, was then analysed after the plasma samples.

CHAPTER 3: METHOD VALIDATION

A highly selective, sensitive, and reproducible method is needed for quantifying potential therapeutics and their metabolites within biological samples for biopharmaceutical studies. The main objective of validating the current method is to demonstrate a bioanalytical method suitable for quantifying Thiamet-G and its analogues in rat plasma. From this quantification, a PK curve can be generated for each of the compounds that were dosed into rats by either oral administration or intravenous administration. According to the industrial guidance for bioanalytical method validation, the fundamental parameters for validation consist of linearity, ,specificity, accuracy, precision, recovery, matrix effect, stability, and sensitivity [148]. Limit of detection (LOD) and limit of quantitation (LOQ) are critical factors that need to be determined[148]. The method created here (See 2.5.5 Method 5) was tested to ensure that it met these general criteria.

Specific samples were prepared for validation purposes. The same amount of internal standard (10 µL of 100 ng / mL), Thiambu-G, was spiked into all three types of solutions.

1) Control standard solution (CSS): Thiamet-G, Thiampro-G, and Thiamme-G were spiked into neat solvent (70 % ACN / H_2O). This solution did not go through the sample extraction process and serves as a positive control.
2) Blank plasma solution: Plasma (diluted with water) that has undergone the sample extraction process. This solution serves as a negative control.

3) Working calibration standard solution (WCSS): Thiamet-G, Thiampro-G, and Thiamme-G were spiked into plasma diluted with water. The solution went through the sample clean up process.

3.1 Selectivity/Specificity, General Considerations

A method is selective when it can be used to quantify the analyte in the sample in the presence of other components[148]. It is important to maintain selectivity at the lower limit of the quantification (LLOQ)[148]. Specificity is crucial for identifying the correct analytes. For this project, compounds of closely related structures were present in certain mixtures. The method being developed and used should enable monitoring the response of one analyte and its specific detection over other analytes, providing that representative chromatograms are available for each analyte. Bioanalytical validation practices recommend that analyses of blank samples collected from biological matrices should be obtained from at least six sources[148]. However, other sources state that a single source of matrix may be used when the bioanalytical method is able to maintain its selectivity[147]. A single matrix source was used here since the method was being developed for plasma.

3.1.1 Results

As discussed earlier, a QTRAP tandem mass spectrometer was the chosen analytical technique for analysis of Thiamet-G and its analogues. The use of a tandem mass spectrometer (MS/MS) enables the use of MRM. The analytical method was readily able to discriminate between compounds of closely related structures by using the MRM scan mode. Chromatograms (A), (B), and (C) in Figure 3.1 were obtained using

LC-MS/MS analysis of the following solutions, the CSS, the blank, and the WCSS. The blank sample was used to determine any interference present in the blank plasma solution. Supporting data shows a positive peak response when a mixture of compounds was separated (chromatogram A), and no response when analysing samples that did not contain the analytes (chromatogram B). The spectra demonstrated the specificity of the analytical method in the presence of the matrix ions present within the samples (chromatogram C).

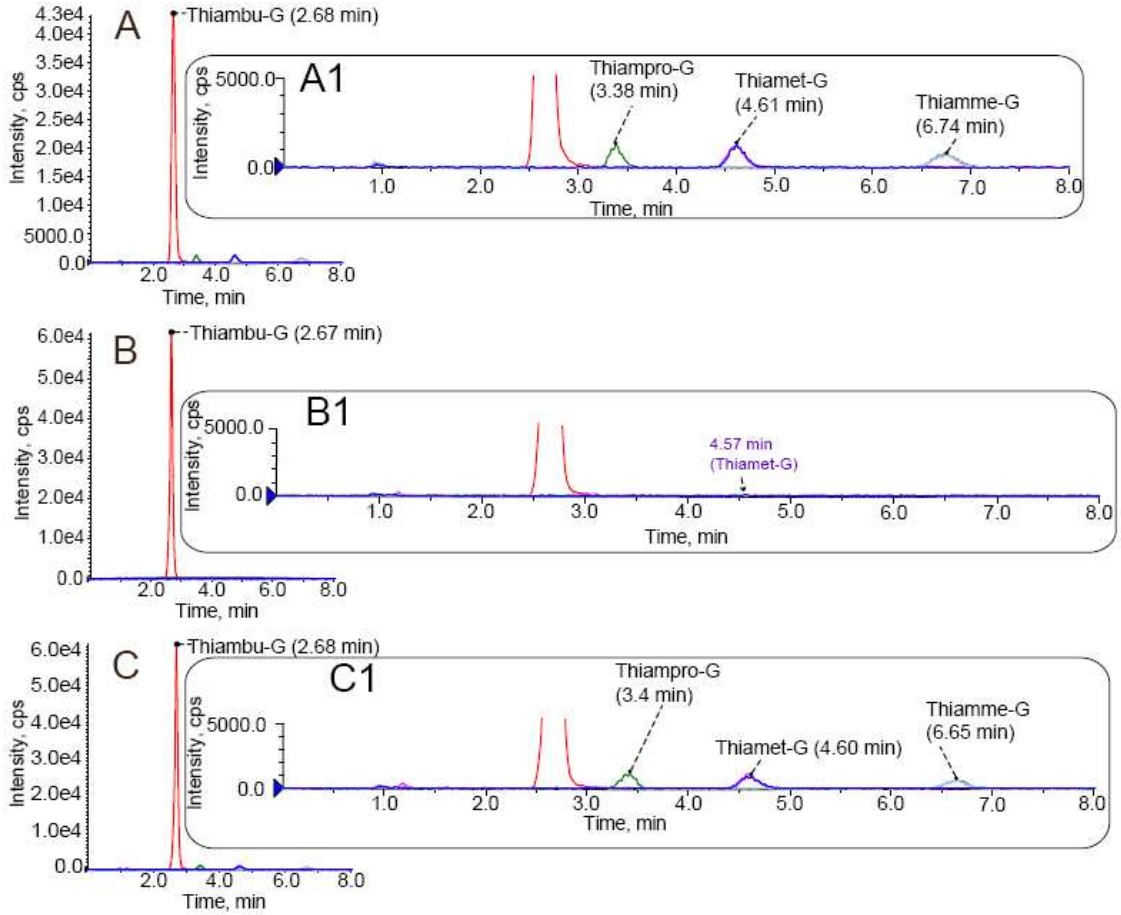

Figure 3.1. Thiamet-G, Thiampro-G, and Thiamme-G were Easily Separated in the Presence of the Matrix Plasma.
Chromatogram (A) was obtained using the CSS sample. Chromatogram (B) and (C) were blank samples containing the internal standard (Thiambu-G) and the WCSS sample, respectively. A1, B1, and C1 are the expanded version of the corresponding chromatograms. In all cases, the large off scale peak is Thiambu-G which was used as an internal standard.

3.2 Linearity

The linearity of the method is the ability of the procedure to relate the signal responses obtained during analysis directly to the concentration of analytes in the samples in a proportional manner within a specified range. A calibration curve relates the detector response with a series of known concentrations of the analyte of interest. A calibration curve is constructed from a blank sample lacking the internal standard, a zero sample containing the internal standard, and at least six standards covering the analyte of

concentration range expected to be present in the experiments to be analysed. All standards used for the calibration curve should be prepared in the same biological matrix as the actual samples. The concentrations of the working calibration standards are based on the concentration ranges used in the actual study.

Linearity is assessed by visual inspection of a plot of signal response against the concentration of analytes and more quantitatively by taking the data from the regression line and determining the degree of linearity[148]. The Pearson product moment correlation coefficient, r, is often used during linear regression analysis to relate a dependent variable to an independent variable[149]. For a set of data points, linear regression generates a formula for the trend line that most closely matches those points. It also gives an r value to demonstrate how much of the variability of the dependent variable is explained by the independent variable. A r value close to 1 indicates the signals are well correlated with the actual concentration of the analytes[149]. The acceptable r value for this method is above 0.99.

3.2.1 Results

Calibration standard solutions (CSSs), composed of Thiamet-G, Thiampro-G, and Thiamme-G, were diluted from a stock solution, $stock_{mixed}$, by serial dilution. A set of WCSS samples with a final concentration of 0.5, 1, 10, 100, 500, and 1000 ng / mL of the analytes were prepared using the CSSs. As mentioned earlier, WCSS samples were spiked into blank rat plasma using a constant amount of the internal standard in order to offset the variation of instrumental responses due to the instability of the system.

Out of the various possible weighting factors commonly used, $1/y^2$ yielded the best fitting WCSS curves and this weighting was used for all analytes. The plots below show the peak area ratio versus concentration plot, the working curve, for each compound.

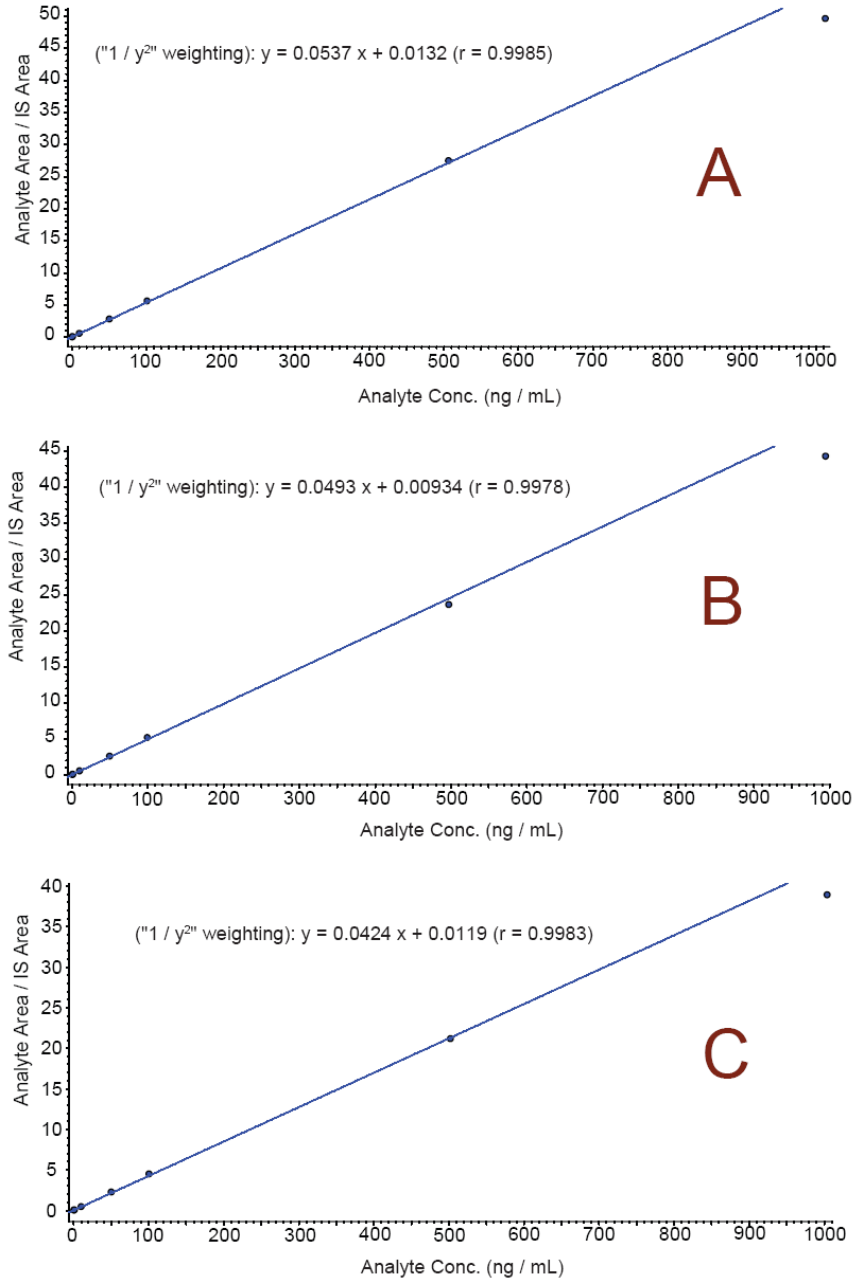

Figure 3.2. Working Curves. Plots of Peak Area Ratios versus Concentration of the WCSS Samples for (A) Thiamet-G, (B) Thiampro-G, and (C) Thiamme-G.

The r value was greater than 0.99 in all cases. The data suggested that the recorded signals can be well correlated with the actual concentration of the analogues, and one can directly predict the concentration of the analytes from the curve over a

concentration range of the analyte ranging from 0.5 to 1000 ng / mL.

One observation in the working curves is that there appears to be curvature at the higher end (Figure 3.2), which results in systematic underestimation of the concentration at the higher concentrations. The sample at 1000 ng / mL noticeably deviates from the line and it is possible that the response from the MS detector is becoming saturated at higher concentrations. Since data for QC at high concentrations (QC_H = 800 ng / mL) are accurate (Section 3.4.1) and precise (Section 3.4.2), the results suggest that the working curves are still maintaining linearity at around 800 ng / mL. Further, the expected range of analytes should be less than 800 ng / mL. Therefore, we felt that these working curves were adequate for our analyses.

3.3 Limits of the Method

3.3.1 Lower Limit of Detection (LOD)

LOD is the minimum concentration of analyte that is detectable using the analytical system being employed. However, at the LOD, the signal does not have to be quantifiable. In equation 4, Cm is the concentration at the detection limit[146]. $\bar{S}_{bl}$ is the mean background signal obtained by averaging the peak height of a blank sample in multiple mass spectra. S_{bl} is the calculated standard deviation of the peak height responses recorded in the mass spectra. Sm in equation 4 is the minimum distinguishable analytical signal and the m in equation 5 is the slope of the calibration curve.

$$Sm = \bar{S}_{bl} + (k \times s_{bl}), \text{ where } k = \text{variation of blank due to random errors} \quad (4)$$

$$Cm = (Sm - \bar{S}_{bl}) / m \quad (5)$$

By substituting equation 4 into equation 5, one obtains:

$$Cm = (k \times_{sbl}) / m, \text{ where } k = 3.3 \text{ [146]} \quad (6)$$

Confirmation of the LOD can be done by using statistical techniques along with the signal-to-background ratio (S / B) [150]. Equation 7 shows the relationship that one can practically draw between % RSD (introduced in Section 2.4.1) and S / B. The commonly accepted S / B ratio for the LOD is between 2 to 3[151].

$$\% \text{ RSD} = 50 / (S / B) \quad (7)$$

By inputting the numerical value 3 for S / B in equation 7, the % RSD is about 17 %. This means that by injecting six replicates of a sample at the LOD, if the calculated % RSD for peak height is around 17 %, then the samples prepared were approximately at the LOD[150].

3.3.2 Limit of Quantification (LOQ)

LOQ is the minimum concentration of analyte that is quantifiable. In principle, the theoretical value of LOQ can be calculated with equation 8[150].

$$LOQ = (10 \times_{sbl}) / m \quad (8)$$

The signal response at the LOQ should be at least five times higher than a blank response[148]. Analyses of replicates at this concentration level should yield quantifiable results with precision and accuracy[148]. In practice however, the commonly accepted S / B ratio for the LOQ is 10-20[151]. By inputting the numerical value 10 for S / B in equation 6, the % RSD obtained is about 5 %. In other words, the % RSD of six injected replicates should be less than 5 % at the LOQ.

LOD and LOQ are illustrated in Figure 3.3. Bioanalytical validation recommendations and the actual data for LOQ are discussed in the Result sections of

accuracy and precision (See Section 3.4.1.1 and 3.4.2.1). According to the guidance, % accuracy for LOQ should not deviate from the nominal concentration by more than 20 % and the precision data for LOQ should be within 20 %[148].

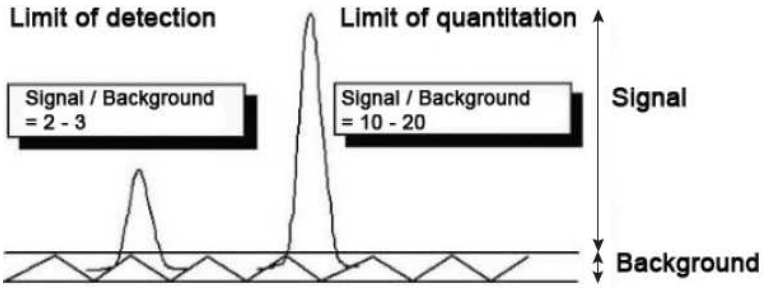

Figure 3.3. Limit of Detection and Limit of Quantitation Expressed in Signal-to-Background Ratios.
Adapted from [151].

LOQ is also the lowest working calibration standard for constructing the calibration curve[148]. For this project, the desired LOQ in the plasma is less than or equal to 2.5 ng / mL, since this is the lowest concentration at which most therapeutics are useful. The lowest calibration standard for constructing the working calibration curve is 0.5 ng / mL. The concentration is equivalent to 1.25 ng / mL in the undiluted rat plasma.

3.3.2.1 Result

The background level ($\bar{S}_{bl}$) measured from the blank mass spectra was 1×10^1 cps while the standard deviation of the background levels ($_{sbl}$) was 1×10^1 cps. The calculated LOD and LOQ are summarised in Table 3.1. The LOD from the experimental result is found to be 0.05 ng / mL for all three compounds. The working curves used to quantify the respective analytes are shown in Figure 3.2.

Table 3.1. The Calculated LOD and LOQ.

Analyte	LOD (ng / mL)	LOQ (ng / mL)
Thiamet-G	0.0210	0.0700
Thiampro-G	0.0175	0.0585
Thiamme-G	0.0307	0.1025

3.4 Accuracy, Precision, Recovery, and Range

The accuracy, precision, recovery, and the range of the method are determined based on the quality control (QC) samples. A minimum of five replicates of QC samples (n = 5 for 3 different concentrations) are recommended to be included in each batch of runs[152]. A group of samples that are analysed within the same run is called a *batch*. Each sample is analysed one after the other with no machine idle time in between.

During validation, the QC samples were prepared as follows: The lowest concentration level of QC samples (QC_L, conc. = 1 ng / mL) was prepared at a concentration level close to the LOQ. The medium concentration level (QC_M, conc. = 400 ng / mL) was at the midrange of the calibration curve. Lastly, the high QC sample (QC_H, conc. = 800 ng / mL) was at a concentration close to the upper level of quantification (ULOQ). During validation, six replicates of QC samples were run throughout the batch along with a freshly prepared WCSS. The concentrations of the QC samples were determined by interpolating from the working curves. The QC samples and the WCSS samples were freshly prepared for each batch analysed.

3.4.1 Quantification of QC Samples

Four batches of samples were analysed. Tables 3.2 through 3.5 summarise the resulting data after quantifying the QC samples for each batch of analysis. The reported

information are the nominal concentration of the analytes, the mean concentration of the replicates, and the SD of the concentration of the replicates. The nominal concentration was the theoretical concentration of the QC samples, which was determined by the weight of the analyte added to the stock solution and the dilution factors. The mean concentrations of the analytes at three different levels were determined to be close to the nominal concentration in all four batches of samples. Some QC samples were not included the calculations due to verifiable injection failures.

Table 3.2. Mean Concentration and SD of QC Samples for Thiamet-G and its Analogues in Sample Batch #1.

	Thiamet-G				Thiampro-G				Thiamme-G			
intraday	nominal conc.	n	mean	SD	nominal conc.	n	mean	SD	nominal conc.	n	mean	SD
	(ng / mL)		(ng / mL)		(ng / mL)		(ng / mL)		(ng / mL)		(ng / mL)	
QC_L	1.01	6	1.14	0.03	0.99	6	1.07	0.05	1.0	6	1.1	0.1
QC_M	405	6	395	5	398	6	376	9	402	6	3.4×10^2	0.2×10^2
QC_H	810	6	7.6×10^2	0.2×10^2	796	6	7.3×10^2	0.2×10^2	803	6	7.6×10^2	0.3×10^2

QC samples were cleaned up using Hypercarb SPE cartridges. These samples were then analysed using a LC equipped with a ZIC-HILIC column coupled with the MS. Separation conditions: Step 1) 0 - 10 min, 300 µL / mL, 84 % B, Step 2) 10.5 – 13 min, 600 µL / mL, 30 % B, Step 3) 13.5 – 16 min, 600 µL / mL, 84 % B, Step 4) 16.5 - 18 min, 300 µL / mL, 84 % B (A = 0.5 % FA + 5 % ACN + H_2O, B = 0.1 % FA + ACN). See the Methods for Validation (Section 3.7) for details.

Table 3.3. Mean Concentration and SD of QC Samples for Thiamet-G and its Analogues in Sample Batch #2.

	Thiamet-G				Thiampro-G				Thiamme-G			
intraday	nominal conc.	n	mean	SD	nominal conc.	n	mean	SD	nominal conc.	n	mean	SD
	(ng / mL)		(ng / mL)		(ng / mL)		(ng / mL)		(ng / mL)		(ng / mL)	
QC_L	1.01	6	0.98	0.03	0.99	6	1.07	0.07	1.0	6	0.9	0.1
QC_M	405	6	4.0×10^2	0.1×10^2	398	6	428	7	402	6	3.8×10^2	0.3×10^2
QC_H	810	6	7.8×10^2	0.2×10^2	796	6	8.1×10^2	0.2×10^2	803	6	7.5×10^2	0.4×10^2

Same conditions as described for sample batch #1 above.

Table 3.4. Mean Concentration and SD of QC Samples for Thiamet-G and its Analogues in Sample Batch #3.

	Thiamet-G				Thiampro-G				Thiamme-G			
intraday	nominal conc.	n	mean	SD	nominal conc.	n	mean	SD	nominal conc.	n	mean	SD
	(ng / mL)		(ng / mL)		(ng / mL)		(ng / mL)		(ng / mL)		(ng / mL)	
QC_L	1.01	4	1.02	0.02	0.99	5	1.04	0.05	1.0	5	1.0	0.05
QC_M	405	6	404	9	398	6	381	4	402	6	4.2×10^2	0.3×10^2
QC_H	810	6	7.5×10^2	0.1×10^2	796	6	6.9×10^2	0.1×10^2	803	6	8.0×10^2	0.4×10^2

Same conditions as described for sample batch #1 above.

Table 3.5. Mean Concentration and SD of QC Samples for Thiamet-G and its Analogues in Sample Batch #4.

	Thiamet-G				Thiampro-G				Thiamme-G			
intraday	nominal conc.	n	mean	SD	nominal conc.	n	mean	SD	nominal conc.	n	mean	SD
	(ng / mL)		(ng / mL)		(ng / mL)		(ng / mL)		(ng / mL)		(ng / mL)	
QC_L	1.01	5	1.03	0.04	0.99	6	1.07	0.05	1.0	6	0.98	0.04
QC_M	405	6	394	8	398	6	388	9	402	6	4.0×10^2	0.1×10^2
QC_H	810	6	7.7×10^2	0.3×10^2	796	6	7.4×10^2	0.2×10^2	803	6	7.8×10^2	0.5×10^2

Same conditions as described for sample batch #1 above.

3.4.1 Accuracy

The accuracy of a method describes the deviation of the mean test results from the true concentration of the analyte[148]. Using a calibration curve constructed with freshly prepared standards, one can determine the *measured* concentrations of the QC samples (n = 6). The mean *measured* concentrations of the QC samples were compared to the nominal concentrations to determine the % accuracy.

$$\% \text{ accuracy} = (\text{mean measured conc. of the replicates} / \text{nominal conc.}) \times 100 \% \quad (9)$$

3.4.1.1 Results

Four batches of samples were analysed. Six replicates of QC samples for three concentration levels, 1, 400, and 800 ng / mL were acquired for each batch. Each batch of samples was freshly prepared prior to analysis. The accuracy data for Thiamet-G (Et), Thiampro-G (Pro), and Thiamme-G (Me) that were obtained from the four batches of QC

samples ranged from 86.5 % to 113 % (Table 3.6).

Table 3.6. Accuracy Data for QC Samples of Thiamet-G and its Analogues.

	% Accy QC_L (1 ng / mL)			% Accy QC_M (400 ng / mL)			% Accy QC_H (800 ng / mL)		
	Et	Pro	Me	Et	Pro	Me	Et	Pro	Me
Batch 1	113%	107%	112%	97.6%	94.5%	96.6%	93.8%	91.8%	94.5%
Batch 2	96.7%	108%	93.9%	99.6%	108%	95.6%	96.8%	102%	93.6%
Batch 3	101%	104%	104%	100%	95.6%	105%	93.0%	86.8%	99.4%
Batch 4	102%	107%	98.0%	97.2%	97.6%	99.1%	94.9%	92.4%	97.4%

According to the FDA guidance, % accuracy for all the concentration levels is suggested to be within 15 % of the nominal concentration, and the LOQ is suggested to not deviate from the nominal concentration by more than 20 %[148]. As shown in Table 3.6, the analytical method developed here provides an accurate means of quantifying Thiamet-G and its analogues that is consistent with FDA guidances.

During the collection of data for the second batch of samples, the run was interrupted due to a setup error. The run was resumed by acquiring data for six aliquots of system suitability (SS) samples to ensure the instrument was stable, and the data that were obtained after the analyses of the SS samples were labelled SS_2. SS_1 were obtained in the same way as SS_2, but they were collected at the beginning of the run prior to interruption. SS was a solution composed of all the analogues including the internal standard with the same solvent compositions as the QC samples (70 % ACN / H2O), except that SS was not treated with plasma. The main purpose of analysing SS samples is to monitor the stability of the instrumentation within a run. The data for SS_2 were compared with the data of SS_1 as shown in Table 3.7. The precision data for both sets of CV are less than 2 %. The average signal response data for SS_1 and SS_2 also are very

similar. The percent ratio tabulated in the last column shows that the average peak area responses for each compound deviates by no more than 7 % between the two sets of data. As a result, the instrument was shown to be stable throughout the entire period spanning the interruption. Furthermore, no outlier was detected for the replicates of the QC samples as evaluated by performing the Grubbs' Outlier Test.

Table 3.7. Comparison of the Data of SS_1 and SS_2 for QC Samples of Thiamet-G and its Analogues.

	Analyte	Average Peak Area (cps)	SD	CV	% (Peak Area of SS_1/ Peak Area of SS_2)
SS_1	Thiamet-G	2.35×10^5	0.03×10^5	1 %	94.2%
	Thiampro-G	1.99×10^5	0.04×10^5	2%	93.4%
	Thiamme-G	2.04×10^5	0.04×10^5	2%	94.1%
	Thiambu-G (IS)	2.26×10^5	0.04×10^5	2%	93.9%
SS_2	Thiamet-G	2.50×10^5	0.03×10^5	1%	
	Thiampro-G	2.13×10^5	0.03×10^5	1%	
	Thiamme-G	2.16×10^5	0.02×10^5	1%	
	Thiambu-G (IS)	2.41×10^5	0.02×10^5	1%	

3.4.2 Precision

The precision of a method demonstrates the deviation in measurements of the analyte when it is at a known constant concentration[148]. Precision is expressed as the percentage of relative standard deviation, % RSD, or coefficient of variation, CV.

$$CV = (\text{SD of measured conc.} / \text{mean measured conc.}) \times 100\ \% \quad (10)$$

Validation of precision can be further classified as intra-batch (within-run) and inter-batch (between-run).

The intra-batch analysis involves the measurement of a group of samples under the same operating conditions for a short period of time, or samples within the same batch. The QC samples being analysed are prepared separately for each run. The purpose of the intra-batch analysis is to determine the repeatability of the sample preparation procedure through comparison of the precision of the QC samples within batches. The inter-batch analysis involves varying the analytical method while assessing the precision of the QC samples during the run. Differences in the analysts, equipment, and day of analysis all contribute to variation[148]. A minimum of three batches of samples are recommended for carrying out the inter-batch analyses[152].

3.4.2.1 Results

Precision for a Single Run

A total of four batches of samples were run. In each batch run, QC samples (n = 6) at three different concentration levels were analysed. Since these QC samples were extracted individually, the precision measurement took into account possible human errors and any sources of deviations that could arise during the sample preparation procedures.

The resulting precision data are shown in Table 3.8. According to the guidances, the % RSD for all the concentration levels should be within 15 % and the LOQ should be within 20 %[148]. A low percentage indicates the deviation among the QC replicates was low. In the data, all CV values are below 10 %. The data suggests that by following

the sample preparation procedure, the analytical method was able to reliably produce precise data that is consistent with the FDA guidances.

Table 3.8. Precision Data for QC Samples of Thiamet-G and its Analogues.

	CV QC_L (1 ng / mL)			CV QC_M (400 ng / mL)			CV QC_H (800 ng / mL)		
	Et	Pro	Me	Et	Pro	Me	Et	Pro	Me
Batch 1	3%	5%	9%	1%	2%	6%	2%	2%	4%
Batch 2	3%	6%	8%	2%	2%	7%	2%	2%	6%
Batch 3	2%	5%	4%	2%	1%	7%	2%	1%	5%
Batch 4	4%	5%	4%	2%	2%	3%	4%	3%	6%

Intermediate Precision

Two types of analyses were performed to validate for intermediate precision. One was called the day-to-day analysis, and the other one was called the column-to-column analysis.

Day-to-day Analysis

The numerical data that were obtained on different days of analysis are reported in Table 3.9. For each day of the analysis, samples were freshly prepared and analysed using the LC-MS/MS as an individual batch. Since these batches of samples were all analysed with column # 1 installed in the system, the parameter that was monitored was the repeatability of the sample preparation process. The mean accuracy data, calculated by averaging the % accuracy of the QC samples from the four batches of analyses, are close to 100 %. The results for the QC samples are similar for all three compounds at three different concentration levels. The precision data show a CV below 10 %. These results demonstrate the sample extraction process was highly reproducible over different days.

Table 3.9. Precision Data for QC Samples of Thiamet-G and its Analogues in Different Batches of Samples over Different Days.

QC Samples	% Accy				Mean % Accy (%)	SD	CV
	Batch # 1	Batch # 2	Batch # 3	Batch # 4			
$QC_{L(Thiamet-G)}$	113%	96.7%	101%	102%	103%	0.07	7%
$QC_{L(Thiampro-G)}$	107%	108%	104%	107%	107%	0.02	2%
$QC_{L(Thiamme-G)}$	112%	93.9%	104%	98.0%	102%	0.08	8%
$QC_{M(Thiamet-G)}$	97.6%	99.6%	100%	97.2%	98.7%	0.02	2%
$QC_{M(Thiampro-G)}$	94.5%	108%	95.6%	97.6%	98.8%	0.06	6%
$QC_{M(Thiamme-G)}$	96.6%	95.6%	105%	99.1%	99.1%	0.04	4%
$QC_{H(Thiamet-G)}$	93.8%	96.8%	93.0%	94.9%	94.6%	0.02	2%
$QC_{H(Thiampro-G)}$	91.8%	102%	86.8%	92.4%	93.2%	0.06	7%
$QC_{H(Thiamme-G)}$	94.5%	93.6%	99.4%	97.4%	96.2%	0.03	3%

Column–to–column Analysis

In the column–to–column analysis, the same batch of QC samples were analysed with different lots of the same stationary phase. Each sample in batch #4 was divided into two HPLC vials before the LC-MS/MS analysis. One set of samples were analysed using column # 1 (column # SB80414) installed on the analytical system and interfaced with the MS/MS. After the completion of the analysis, the other set of samples were analysed in the same way but using column # 2 (column # SB81229) installed on the analytical system. The purpose of this experiment was to see whether the analyses of the

same samples using different lots of the same stationary phase would lead to differences in accuracy and precision. The data are reported in Table 3.10. On both days of analyses, the accuracy data were close to 100 %. The CV values for all concentration levels of the analytes were within 10 %. The recorded data therefore suggests that using different lots of columns did not produce differences in the data.

Table 3.10. Precision Data for QC Samples of Thiamet-G and its Analogues with Different Lots of Stationary Phase.

QC Samples	% Accy		Mean % Accy	SD	CV
	Column #1	Column #2			
$QC_{L(Thiamet\text{-}G)}$	102%	107%	105%	0.04	4×10^0 %
$QC_{L(Thiampro\text{-}G)}$	107%	112%	110%	0.03	3×10^0 %
$QC_{L(Thiamme\text{-}G)}$	98.0%	111%	105%	0.09	9×10^0 %
$QC_{M(Thiamet\text{-}G)}$	97.3%	106%	102%	0.06	6×10^0 %
$QC_{M(Thiampro\text{-}G)}$	97.6%	102%	99.9%	0.03	3×10^0 %
$QC_{M(Thiamme\text{-}G)}$	99.1%	111%	105%	0.08	8×10^0 %
$QC_{H(Thiamet\text{-}G)}$	94.9%	110%	102%	0.1	1×10^1 %
$QC_{H(Thiampro\text{-}G)}$	92.4%	99.7%	96.0%	0.05	5×10^0 %
$QC_{H(Thiamme\text{-}G)}$	97.4%	111%	104%	0.09	9×10^0 %

Stability of the ZIC-HILIC Column

20 SS samples were injected into the analytical system using a newly installed ZIC-HILIC column (Column #2). The peak area responses and retention times of these analogues are summarised in Table 3.11. Although the CV values for the peak area ratios

for Thiamet-G and Thiampro-G were low, suggesting that the system was reproducible, for Thiamme-G, the CV value was somewhat high. This indicates that the behaviour of Thiamme-G on this column is to some extent less stable. The retention time ratio for all three compounds had a small CV value indicating the retention times were constant when no plasma was present in the sample.

Table 3.11. Consistency of Peak Area and RT Ratio of Thiamet-G and its Analogues over 19 h of Analysis Time.

Analyte	Peak Area Ratio			RT Ratio		
	Average	SD	CV	Average	SD	CV
Thiamet-G	0.94	0.04	4%	1.8	0.005	0.3%
Thiampro-G	0.88	0.02	2%	1.3	0.005	0.4%
Thiamme-G	0.72	0.06	8%	2.6	0.009	0.3%

A separate experiment was carried out to demonstrate the behaviour of a new ZIC-HILIC column (column # 2) when it was first exposed to WCSS samples. Five QC samples were prepared in triplicate in plasma at 0.5, 1, 10, 100, and 1000 ng / mL. When these QC samples were first exposed to the new column, the elution times of all three compound ions changed. The trend of the elution time could not be tracked during these experiments. This same batch of samples were also analysed using column # 1, and the results indicated all three analytes had stable retention times on column # 1. It was found that after analysing at least two batches of samples on column #2, the precision and accuracy improved to acceptable levels, suggesting that the column requires a period of conditioning of approximately 70 QC samples before reproducible results are obtained.

3.4.3 Recovery

Recovery describes the comparison of the detector response for analytes added to and then extracted from the biological matrix to the detector response for samples of authentic analytes of known concentration. The recovery of analytes and the internal standard should be both consistent and reproducible[148].

An experimental design was proposed by Chambers *et al*[153]. Recovery was expressed in % recovery.

> % Recovery = (signal response of sample spiked before extraction / signal response of sample spiked after extraction) x 100 %
>
> (11)

The FDA guidances suggest that % recovery does not need to be 100%, but the ability of the method to maintain consistency, precision, and reproducibility is the main objective[148]. For this analytical method, the expected range for % recovery was 80 to 120 %.

3.4.3.1 Results

Samples at two different concentration levels (low and high) were measured. The obtained data for the WCSS samples were compared with blank samples that were spiked with the same amount of analytes as the plasma samples. The recovery data are reported in Table 3.12. The results are within the expected range. We are able to demonstrate the sample extraction process is efficient as only minimal sample is lost during the process. Consequently, the method yields good recovery.

Table 3.12. Recovery Data for QC Samples of Thiamet-G and its Analogues.

Analyte	QC_L	QC_H
Thiamet-G	83.8%	97.4%
Thiampro-G	85.1%	83.4%
Thiamme-G	86.3%	100%
Thiambu-G (IS)	95.0%	105%

3.4.4 Range

The range of a method is the concentration of the analytes that can be detected with a suitable level of precision, accuracy, and linearity. The range of a method is defined as the region between the upper and lower concentration levels[151]. The minimum specified ranges for assaying drug product is from 80 to 120 % of the test concentration[154].

3.4.4.1 Results

In the concentration range of 0.5 to 1000 ng / mL for Thiamet-G and its analogues, all the fundamental parameters for validation, such as precision, accuracy, and linearity, are expected to meet the guidance suggestions given the levels of analytes dosed to animals. In the analysis of the actual PK samples for Thiamet-G (Section 3.8), most of the concentrations ranged from 50 to 420 ng / mL. The lowest concentration detected was 2.8 ng / mL. 80 and 120 % of 2.8 ng / mL are 2.24 and 3.36 ng / mL respectively. As a result, the linear dynamic range, 0.5 to 1000 ng / mL, is acceptable for detecting the concentrations of the actual PK samples.

3.5 Matrix Effect

This experiment assesses the ionization efficiency of the analytes in MS-based analysis. One generic observation for MS-based analysis is that ions are either suppressed or enhanced with the presence of matrix components in the biological samples[147].

An experimental design was proposed by Chambers *et al.*

% Matrix effect = (signal response of sample spiked in plasma /
signal response of sample spiked in 70 % ACN / H_2O) x 100 %

(12)

A percent ratio of 100 % suggest that there is no effects. When the value is low, there is signal suppression; when the value is high, there is ionization enhancement.

For this analytical method, we expected the % matrix effect to be within the range of 70 to 110 %[153].

3.5.1 Results

Samples at two different concentration levels (low and high) were measured. The obtained data for the WCSS samples were compared with the CSS samples that were spiked with the same amount of analytes as the plasma samples. Data for the internal standard-normalized matrix effect are reported in Table 3.13. The results are close to the preset range. The data suggest that there were matrix ions suppressing the ionization of the analytes but the level of suppression was minor. As a result, the method is not affected by the matrix to any extent causing complications.

Table 3.13. Matrix Effect Data for QC Samples of Thiamet-G and its Analogues.

Analyte	QC_L	QC_H
Thiamet-G	84.0%	79.6%
Thiampro-G	85.3%	92.3%
Thiamme-G	77.9%	77.9%

3.6 Stability

Short and long-term compound stability experiments can also be carried out. Short-term stability tests should include 3 freeze / thaw cycles, bench top, and refrigerated stability. Short-term stability measurements are best carried out during method validation. Long-term measurements are started prior to validation and should be completed after validation[155]. The stability of analytes is dependent on the storage conditions, chemical properties of the analytes, the biological matrix, and the container used. In this work the following stability studies were carried out: stock solution, freeze-thaw, bench top, refrigerated stability, and the stability of the samples at the -20 ^{o}C prior to reconstitution. Some of the actual PK samples were stored at – 80 ^{o}C. Under different storage conditions, it is generally accepted that the sample matrix will have variable stability. Therefore, determination of the stability of the compounds in plasma at – 80 ^{o}C was also carried out[155].

3.6.1 Stock Solution Stability

The stability of both the analyte and internal standard in the stock solutions is required for evaluation at room temperature for at least 6 h. Stock solutions of analytes for the stability evaluation should be prepared in an appropriate solvent at known concentrations. Fresh stock solutions are prepared from the reference material for

determination of the stability of the compounds in the stock solution and the stock solutions that were refrigerated[152].

3.6.1.1 Results

For this method, the stock solutions were prepared in water. One fresh stock solution, $Stock_{mixed}$, was prepared for Thiamet-G, Thiampro-G, and Thiamme-G. The other stock solution, $Stock_{IS}$, was prepared for the internal standard, Thiambu-G. These fresh stock solutions were prepared from reference material to determine both the stability of analytes and the stability of the older stock solution (4 months old).

The response of a fresh stock solution at time zero, T_0, was compared with the response of the same stock solution that has been sitting at room temperature in the autosampler for 6 h, T_{6hrs}. The analysis of the stock stability was carried out individually for $Stock_{IS}$ and $Stock_{mixed}$. A percent ratio can be obtained by the following formula where T_n stands for any time point:

$$\% \text{ Ratio} = (\text{Peak Area Response of } T_n / \text{Peak Area Response of } T_0) \times 100 \% \quad (13)$$

In first row of Table 3.14, the percent ratios are tabulated for the analytes in $Stock_{mixed}$. With deviations of less than 5%, the compounds were shown to be stable within a time frame of 6 h at room temperature. In the second row of the table, the percent ratios for comparing the signal response of an older $Stock_{mixed}$ with the signal response of the T_0 sample are tabulated. The response of the older stock solution should be within 5 to 7 % of the response of the fresh stock solution[152]. The data indicates the compounds are stable for 4 months when stored at 4 ^{o}C.

Table 3.14. Stability Test for $Stock_{mixed}$.

% Peak Area	Thiamet-G	Thiampro-G	Thiamme-G
$\%(T_{6hrs} / T_0)$	105%	105%	103%
$\%(T_{4\ months\ old} / T_0)$	99.0%	100%	95.5%

A similar experiment was performed using Thiambu-G in $Stock_{IS}$. In Table 3.15, Thiambu-G was shown to be stable within a time frame of 6 h because the recorded percent ratio in the first row is close to 100 %. The recorded percent ratios in the second and the last rows are similar, except that in the last row, the recorded signal response at each time point is divided by the measured weight of Thiambu-G. A 17 % deviation is observed in the second percent ratio in the table. The reason was that the nominal concentration of the $T_{4\ months\ old}$ sample was slightly higher than T_0. Nominal concentration is determined by the weight of the analyte and the volume of the stock solution. Therefore, a 10 % deviation is seen after the correction is made. For the purpose of this project, a 10 % deviation is acceptable.

Table 3.15. Stability Test for $Stock_{IS}$.

% Peak Area Response	Thiambu-G
$\%(T_{6hrs} / T_0)$	102%
$\%(T_{4\ months\ old} / T_0)^1$	110%

[1]These samples have been corrected for the differences in their nominal concentrations. % Peak Area Response calculated based on equation 11.

Three sets of system suitability (SS) samples were run at the beginning, in the middle, and at the end of the batch analysis of the stability samples. The precision data of the three sets of SS are reported in Table 3.16. The precision data are less than 5 %, and this indicates that the system was stable during the analysis.

Table 3.16. Stability of the Analytical System Determined by System Suitability Samples.

	Peak Area			Relative RT		
	Average (cps)	**SD**	**CV**	**Average (min)**	**SD**	**% RSD**
$SS_{Thiamet\text{-}G}$	1.83×10^5	0.07×10^5	4%	4.82	0.05	1
$SS_{Thiampro\text{-}G}$	1.55×10^5	0.07×10^5	5%	3.53	0.04	1
$SS_{Thiamme\text{-}G}$	1.63×10^5	0.06×10^5	4%	7.03	0.09	1
SS_{IS}	1.88×10^5	0.09×10^5	5%	2.76	0.02	1

For the rest of the stability experiments including freeze-thaw, bench top, refrigerated stability, and the stability of the samples at -20 ^{o}C prior to reconstitution, a set of samples freshly prepared from the stock solution of analytes in an appropriate analyte-free, interference-free biological matrix were used. The replicate aliquots of stability samples were analysed along with a set of freshly prepared working calibration standard solutions (WCSS). Two concentration levels of QC samples, QC_L and QC_H, are recommended to be used in the stability experiments and we followed this guideline[155].

3.6.2 Long-term Stability Experiment

For long-term stability studies, the storage time of the QC samples should be long enough to account for the storage time of the sample analytes. At least three aliquots of QC samples were stored at the storage conditions used for the eventual sample analyses. The volumes of the stability samples are large enough such that there is adequate sample for three separate analyses. Periodic analyses of the stored samples help to monitor the stability of the compounds in plasma. The concentrations of the stability samples are calculated from the calibration curve constructed with a set of freshly prepared WCSS.

Concentrations of all the stability samples analysed on different days are compared to the mean of the samples analysed on *day 1*. The *day 1* analysis took place within 24 h after the samples were prepared. It is recommended that two consecutive assessments be carried out on two successive days to determine whether the analyte has become unstable due to its storage conditions[155].

3.6.2.1 Results for QC_H

A large volume of QC_H was freshly prepared and aliquoted into several portions. Three aliquots were analysed in batch # 1. The resulting data from analysis of these three aliquots were labelled as the *day 1 analysis*, and they are tabulated in the first row of Table 3.17. Half of the remaining aliquots were stored at – 20 ^{o}C and the other half were stored at – 80 ^{o}C.

In the day 1 analysis, the accuracy data were calculated by comparing the mean concentration of the replicates to the nominal concentration of the QC samples. All samples have % accuracy ranging from 90 to 99 %. The precision data demonstrated that the concentrations of the replicates were very close to each other. The bioanalytical validation guidelines generally suggest that the result of the day 1 analysis should not deviate from the nominal concentration by more than 5 to 7 %[155]. For this project, we have accepted the data to deviate from the nominal concentration by 10 %.

Analysis of QC_H samples that have been stored at –20 ^{o}C and –80 ^{o}C for 10 days and 6 months are also shown in Table 3.17. The precision data that are lower than 5 % showed that the replicates have only minor differences from each other. The accuracy data were calculated by comparing the mean concentration of the replicates to the

concentration obtained from the day 1 analysis. The accuracy data are mostly within 15 % of the nominal concentration. The result suggests that Thiamet-G and Thiamme-G at a high concentration level were stable in the plasma at the corresponding storage conditions. Further stability experiments should demonstrate whether Thiampro-G is unstable under these conditions since the recorded accuracy data deviated from the concentration of the day 1 analysis by more than 15 %.

Table 3.17. Long-Term Analyte Stability of QC_H for Thiamet-G and its Analogues

		Thiamet-G						Thiampro-G				
Samples[1]	Storage	n	mean (ng / mL)	SD	CV	%Accy		n	mean (ng / mL)	SD	CV	%Accy
Day 1	N / A	3	797	7	1%	98.4%		3	761	4	1%	95.7%
Day 10	-20 °C	3	750	10	2%	93.9%		3	690	20	2%	90.5%
	-80 °C	3	810	20	2%	102%		3	800	30	4%	105%
6 months	-20 °C	3	750	10	1%	94.6%		3	580	10	2%	75.5%
	-80 °C	3	740	20	2%	93.3%		3	550	20	3%	72.4%

	Thiamme-G					
Samples[1]	Storage	n	mean (ng / mL)	SD	CV	%Accy
Day 1	N / A	3	720	10	1%	90.0%
Day 10	-20 °C	3	770	30	3%	106%
	-80 °C	3	803	9	1%	111%
6 months	-20 °C	3	810	20	3%	112%
	-80 °C	3	740	20	2%	102%

[1]Replicates of QC_H was prepared and analysed on day 1. The other data are for replicates of QC_H that were stored at -20 °C and - 80 °C for 10 days and 6 months before analysis.

3.6.2.2 Results for QC_L

In the case of QC_L, the data for the day 1 analysis show high accuracy (Table 3.18). The precision data demonstrate that the concentrations of the replicates were very close to each other. The mean concentration obtained from the samples of the day 1 analysis was used for calculating accuracy data for the further long-term stability experiments.

Analysis of QC_L samples that have been stored at –20 ^oC and –80 ^oC for 10 days and 6 months are also shown in Table 3.18. The precision data that are lower than 7 % demonstrated that the replicates have only minor differences from each other. The accuracy data are mostly within 15 % of the nominal concentration. The result suggests that Thiamme-G at a high concentration level is stable in the plasma under the corresponding storage conditions. Further stability experiments should demonstrate whether Thiamet-G and Thiampro-G are unstable under these conditions since some of the recorded accuracy data deviated from the concentration of the day 1 analysis by more than 15 %.

Table 3.18. Long-Term Analyte Stability of QC_L for Thiamet-G and its Analogues

		Thiamet-G						Thiampro-G				
Sample[1]	Storage	n	mean (ng / mL)	SD	CV	%Accy		n	mean (ng / mL)	SD	CV	%Accy
Day 1	N / A	3	0.97	0.03	3%	95.8%		3	0.96	0.02	2%	96.2%
6 months	-20 °C	2	0.78	0.02	3%	80.9%		2	0.653	0.004	1%	68.3%
	-80 °C	2	0.88	0.05	5%	90.7%		3	0.69	0.02	3%	72.4%

		Thiamme-G				
Sample[1]	Storage	n	mean (ng / mL)	SD	CV	%Accy
Day 1	N / A	3	1.00	0.02	2%	100%
6 months	-20 °C	2	0.95	0.03	3%	94.6%
	-80 °C	3	0.97	0.06	6%	96.3%

[1]Replicates of QC_L were prepared and analysed on day 1. The other data are for replicates of QC_L that were stored at -20 ^oC and - 80 ^oC for 10 days and 6 months before the analyses.

3.6.3 Freeze-Thaw Stability

The stability of the analyte was determined after three freeze - thaw cycles. Three aliquots of QC samples were frozen at their storage temperature for 24 h and thawed at room temperature. Once the samples were completely thawed, the samples were frozen again for at least 12 h under the same storage conditions. The freeze - thaw cycle was repeated two more times. After the last freeze - thaw cycle, the stability samples were

analysed using the LC-MS/MS along with a set of samples that had undergone only one freeze - thaw cycle.

3.6.3.1 Results

Aliquots of QC samples were stored at –20 ^{o}C and –80 ^{o}C. Three aliquots of QC samples were removed from each of the storage conditions and were thawed at room temperature. Then, these samples were returned back to their original storage conditions. This cycle was repeated a total of three times. On the day of the analysis, three aliquots of QC samples that have been thawed only once (1 FT) were extracted and analysed along with the samples that had gone through the freeze-thaw cycles three times (3 FT). These samples were analysed along with a set of WCSS from batch #2.

The accuracy data for each type of freeze – thaw samples were calculated by comparing the mean concentration of the replicates to the nominal concentration of the QC samples. The accuracy data of close to 100 % suggests that the concentration of the replicates were very close to their actual values (Table 3.19). Variation in precision of less than 5 % further suggests that there were minimal differences between replicates.

Table 3.19. Freeze-thaw (FT) Stability of QC_H for Thiamet-G and its Analogues.

		Thiamet-G					Thiampro-G				
Storage	Sample	n	mean	SD	CV	%Accy	n	mean	SD	CV	%Accy
			(ng / mL)					(ng / mL)			
- 20 °C	3 FT	3	790	20	2%	97.7%	3	820	10	1%	103%
	1 FT	3	770	10	2%	94.8%	3	800	10	2%	100%
- 80 °C	3 FT	3	790	20	2%	97.1%	3	800	20	3%	101%
	1 FT	3	774	6	1%	95.5%	3	816	5	1%	103%

		Thiamme-G				
Storage	Sample	n	mean	SD	CV	%Accy
			(ng / mL)			
- 20 °C	3 FT	3	760	20	3%	94.3%
	1 FT	3	710	30	4%	88.6%
- 80 °C	3 FT	3	731	5	1%	91.0%
	1 FT	3	810	10	2%	101%

Replicates of QC_H were prepared and stored at -20 °C and - 80 °C. 3FT QC samples were subjected to three freeze-thaw cycles while the 1FT samples were subjected to only one freeze-thaw cycle.

In Table 3.20, the accuracy data of samples that were thawed only once are compared with the accuracy data of samples that have gone through the freeze-thaw cycle three times. The difference in percentage is in all cases less than 11 %. The numerical data showed that the compounds in plasma were stable after going through the three freeze-thaw cycles.

Table 3.20. Comparison of the Accuracy Data of QC_H for FT Samples.

Storage	Thiamet-G	Thiampro-G	Thiamme-G
-20 °C	3.0%	3%	5.7%
-80 °C	1.6%	2%	10%

Percent values = |% accuracy of 3FT - % accuracy of 1FT|

For the stability analyses for QC_L, the accuracy data for all the compounds, except for Thiampro-G, are high (Table 3.21). The percent values for all the samples being

close to 100 % suggests that the FT samples had minor deviations from the nominal concentration that were not problematic.

Table 3.21. Freeze-thaw (FT) Stability of QC_L for Thiamet-G and its Analogues.

			Thiamet-G						Thiampro-G			
Storage	**Sample**	**n**	**mean**	**SD**	**CV**	**%Accy**	**n**	**mean**	**SD**	**CV**	**%Accy**
			(ng / mL)					(ng / mL)			
-20 °C	3 FT	3	0.96	0.03	3%	94.6%	3	0.91	0.03	3%	91.6%
	1 FT	3	0.91	0.01	1%	90.2%	3	0.89	0.04	4%	89.3%
-80 °C	3 FT	3	0.93	0.04	5%	92.3%	3	0.77	0.07	9%	77.5%
	1 FT	3	0.92	0.02	3%	90.8%	3	0.77	0.01	1%	77.1%

Thiamme-G

Storage	**Sample**	**n**	**mean**	**SD**	**CV**	**%Accy**
			(ng / mL)			
-20 °C	3 FT	3	0.96	0.03	3%	95.4%
	1 FT	3	0.92	0.01	2%	91.9%
-80 °C	3 FT	3	0.95	0.06	7%	94.5%
	1 FT	3	0.93	0.02	2%	92.9%

Replicates of QC_L were prepared and stored at -20 ^{o}C and - 80 ^{o}C. QC samples for 3FT were subjected to three freeze-thaw cycles while the 1FT samples were subjected to only one freeze-thaw cycle.

In Table 3.22, the accuracy data for QC_L samples that have undergone three freeze-thaw cycles compared with samples that have undergone only one freeze-thaw cycle. The results suggest that Thiamet-G and Thiamme-G were stable in plasma after three freeze-thaw cycles at the low concentration. For Thiampro-G, the FT samples that were stored at – 20 ^{o}C had accuracy values close to 100 %. In the FT samples that were stored at – 80 ^{o}C, 1FT and 3FT had a % accuracy of less than 80 %. The precision data suggest that the measurements of the replicates were very close to each other. A possible reason for the observed result is that Thiampro-G might precipitate out when stored at

– 80 ^{o}C and then it might take additional time for Thiampro-G to redissolve at room temperature. This is a possibility that will need to be investigated further.

Table 3.22. Comparison of the Accuracy Data of QC_L for FT Samples.

Storage	Thiamet-G	Thiampro-G	Thiamme-G
-20 ^{o}C	4.4%	2.3%	3.6%
-80 ^{o}C	1.5%	0.4%	1.6%

Percent values = |% accuracy of 3FT - % accuracy of 1FT|

3.6.4 Short-term Stability Experiment

This experiment ensures that the analyte does not degrade during the sample cleanup process prior to analyses. Three aliquots of QC samples were removed from the storage conditions, thawed, and then maintained at room temperature for the period of time that the samples will be at room temperature during the proposed analytical method. The typical time for analysis is between 4 and 24 h. For this project, 24 h is used to be on the safe side since the batch analysis can take 7 h. After 24 h, another set of stability samples was removed from storage and thawed. When the second set of samples had thawed, a WCSS standard was freshly prepared and analysed along together with the two sets of samples. The accuracy data were calculated by comparing the mean concentration of the replicates to the nominal concentration of the QC samples.

Results

Three aliquots of QC_H samples were removed from each of the storage conditions and were thawed and then maintained at room temperature for 24 h. On the day of the analysis, three aliquots of QC samples were removed from the storage conditions and thawed. These freshly removed samples (1 FT) were extracted and analysed along with

the samples that had been at room temperature for 24 h (ST). These samples were analysed with a set of WCSS from batch #2.

The data for the short-term stability experiment for QC_H are reported in Table 3.23. The % accuracy and the precision data are shown to be close to 100 % and below 4 % respectively. The % accuracy of these two sets of stability samples should be within 15 % of the nominal concentration. The CV of the three replicates should be less than 15 %[155]. These data indicate the measured concentrations were close to the nominal concentrations and measurements of the replicates were in agreement with each other.

Table 3.23. Stability of QC_H for Thiamet-G and its Analogues at Room Temperature for 24 h.

		Thiamet-G					Thiampro-G					Thiamme-G				
Storage	Sample	n	mean	SD	CV	%Accy	n	mean	SD	CV	%Accy	n	mean	SD	CV	%Accy
			(ng / mL)					(ng / mL)					(ng / mL)			
- 20 °C	ST	3	780	30	3%	98.3%	3	810	20	3%	107%	3	760	30	4%	105%
	1 FT	3	770	10	2%	96.3%	3	800	10	2%	105%	3	710	30	4%	98.5%
- 80 °C	ST	3	780	10	1%	98.4%	3	796	8	1%	105%	3	760	30	4%	105%
	1 FT	3	774	6	1%	97.1%	3	816	5	1%	107%	3	810	10	2%	112%

		Thiamme-G				
Storage	Sample	n	mean	SD	CV	%Accy
			(ng / mL)			
- 20 °C	ST	3	760	30	4%	105%
	1 FT	3	710	30	4%	98.5%
- 80 °C	ST	3	760	30	4%	105%
	1 FT	3	810	10	2%	112%

Replicates of QC_H were prepared and stored at -20 °C and - 80 °C. QC samples for ST were thawed and held at room temperature for 24 h while the 1FT samples were thawed and analysed immediately afterward.

In Table 3.24, accuracy data of the samples that have thawed right away are compared with the samples that were at room temperature for 24 h. The difference in percentage is less than 7 % suggesting that the compounds in plasma were stable after sitting at room temperature for 24 h.

Table 3.24. Comparison of the Accuracy Data of QC_H for Short-term Stability Samples.

Storage	Thiamet-G	Thiampro-G	Thiamme-G
- 20 ^{o}C	2.0%	2%	7%
- 80 ^{o}C	1.2%	3%	7%

Percent values = |% accuracy of ST - % accuracy of 1FT|

Aliquots of QC_L samples were removed from the storage conditions, were thawed and maintained at 24 h, and labelled as ST. After 24 h, aliquots of freshly removed samples (1 FT) were extracted along with the ST samples that had been at room temperature for 24 h. These samples were analysed as batch # 4.

The short-term stability data for QC_L are reported in Table 3.25. For samples that were stored at -20 ^{o}C, the accuracy data for both the ST and 1 FT samples are close to 100 %, which suggests that the reported data have only minor deviations from the nominal concentration. The calculated CV values that are less than 5% indicating that the concentrations of the replicates were in agreement with each other. The data shows that the compounds were stable in plasma for 24 h at room temperature. The only exception was the samples containing Thiampro-G that was stored at – 80 ^{o}C.

Table 3.25. Stability of QC_L for Thiamet-G and its Analogues at Room Temperature for 24 h.

		Thiamet-G					Thiampro-G				
Storage	Sample	n	mean	SD	CV	%Accy	n	mean	SD	CV	%Accy
			(ng / mL)					(ng / mL)			
- 20 °C	ST	3	0.94	0.04	4%	97.2%	3	0.92	0.06	7%	95.8%
	1 FT	3	0.91	0.01	1%	93.9%	3	0.89	0.04	4%	92.8%
- 80 °C	ST	3	0.97	0.04	4%	100%	3	0.97	0.02	2%	101%
	1 FT	3	0.92	0.02	3%	94.5%	3	0.77	0.01	1%	80.1%

		Thiamme-G				
Storage	Sample	n	mean	SD	CV	%Accy
			(ng / mL)			
- 20 °C	ST	3	0.96	0.03	3%	95.5%
	1 FT	3	0.92	0.01	2%	91.8%
- 80 °C	ST	3	0.95	0.01	1%	94.9%
	1 FT	3	0.93	0.02	2%	92.9%

Replicates of QC_L were prepared and stored at -20 °C and - 80 °C. QC samples for ST were thawed at room temperature for 24 h while the 1FT samples were thawed and analysed right away.

In the case of Thiampro-G, the FT samples stored at – 80 °C are shown to have low accuracy. The samples that underwent both one and three freeze thaw cycles were observed to have the same variation. However, the ST samples that were stored at – 80 °C still maintained high accuracy. This could be because, when thawing a sample stored at – 80 °C, Thiampro-G needs more time to be redissolved at room temperature. This idea will need to be tested in the future. See Table 3.26 for the comparison between the accuracy data of 1 FT and ST samples.

Table 3.26. Comparison of the Accuracy Data of QC_L for Short-term Stability Samples.

Storage	Thiamet-G	Thiampro-G	Thiamme-G
- 20 °C	3.3%	3.0%	3.7%
- 80 °C	6%	21%	2.0%

Percent values = |% accuracy of ST - % accuracy of 1FT|

3.6.5 Post-Preparative Stability

There are two types of post-preparative stability experiments, on-instrument and extraction stability. For the on-instrument experiment, $QC_{stability}$ samples analysed at the beginning of the run were compared against $QC_{stability}$ samples analysed in between or at the end of the run[155]. For the extraction stability experiment, the stored $QC_{stability}$ samples are compared with replicates of $QC_{stability}$ samples that are prepared fresh. This evaluation is not part of the routine validation process[155]. For this project, only the on-instrument stability experiment was performed.

3.6.5.1 Results

Replicates of extracted QC samples were pooled together and aliquoted into six portions. They are referred to as the $QC_{stability}$ samples, and two concentration levels were prepared, a low concentration $QCL_{stability}$ and a high concentration $QCH_{stability}$ were prepared. These aliquots of samples were run through out the batch. The number of replicates was six. Since they were pooled together after the extraction process, the resulting data should yield a low CV. There were pooled together to eliminate the differences in concentrations during sample preparation.

In the longest on-instrument stability experiment, the time of the analysis between the first and the last $QC_{stability}$ samples was 79 h. The accuracy data were close to 100 %

(Table 3.27). The precision data were less than 8 %. All three compounds were therefore stable in the autosampler at 10 ^{o}C for 79 h.

Table 3.27. On-Instrument Stability of $QC_{stability}$ for Thiamet-G and its Analogues for 27 h.

	Thiamet-G					Thiampro-G				
intraday	nominal conc.	mean	SD	CV	%Accy	nominal conc.	mean	SD	CV	%Accy
	(ng / mL)	(ng / mL)				(ng / mL)	(ng / mL)			
QC_L	1.01	0.97	0.07	7%	96.0%	0.99	0.95	0.04	4%	95.8%
QC_H	810	760	20	3%	93.6%	796	720	20	2%	89.9%

	Thiamet-G				
intraday	nominal conc.	mean	SD	CV	%Accy
	(ng / mL)	(ng / mL)			
QC_L	1.00	1.01	0.06	6%	101%
QC_H	803	780	20	2%	97.2%

3.7 Sensitivity

Sensitivity is the assessment of the lowest concentration that can be measured using the method with acceptable accuracy and precision[152]. For this method, the LOQ is set at 0.5 ng / mL.

3.7.1 Results

Six replicates of QC samples at the concentration of LOQ were prepared. They were injected into the system one after another. The accuracy and precision data are reported in Table 3.28. The accuracy data for all three analytes are within 85 to 115 % whereas the precision data are lower than 5 %. The data support the fact that method is able to detect the lowest concentration at 0.5 ng / mL.

Table 3.28. Sensitivity Data for Thiamet-G and its Analogues.

	Expected Conc. (ng / mL)	Mean (ng / mL)	SD	CV	% Accy
Thiamet-G	0.506	0.47	0.02	4%	92.5%
Thiampro-G	0.497	0.432	0.008	2%	86.9%
Thiamme-G	0.502	0.44	0.01	3%	86.7%

3.8 Analyses of PK Samples

After completing of the validation procedure, the PK samples for Thiamet-G were analysed using the same protocol. Three rats were treated by with100 mg / kg of Thiamet-G were fed into three rats by oral gavage. Aliquots of rat plasma were collected from the animals throughout a time period extending up to 24 h. These samples were prepared as described above and analysed by LC-MS/MS. Two separate analyses were carried out for each sample. The mean concentrations and standard deviation obtained for each time point are tabulated in Table 3.29.

From the experimental results, we could determine the maximum concentration of Thiamet-G that can be absorbed into the bloodstream, C_{max}, and the time point for C_{max}. As seen in table, C_{max} and t_{max} are determined to be 370 ± 20 ng / mL and 2 h respectively.

Table 3.29. Concentration of Thiamet-G in the Pharmacokinetic Samples

Time	Rat # 1		Rat # 2		Rat # 3			
(h)	(ng / mL)							
	1st analysis	2nd analysis	1st analysis	2nd analysis	1st analysis	2nd analysis	average	SD
0	0	0	0	0	0.587	0.653	0.2	0.3
0.25	207	223	200	222	155	164	200	30
0.5	336	358	382	388	323	353	360	30
1	301	334	N/A	409	356	416	360	50
2	356	389	358	375	349	367	370	20
4	182	186	106	105	157	163	150	40
8	95.9	101	54.1	55.5	86.3	94.5	80	20
24	2.89	3.24	2.19	2.5	2.94	3.13	2.8	0.4

The total amount of compound that is absorbed into the body system can be determined by plotting the average concentrations of Thiamet-G in Table 3.29 against the range of time points for collecting the plasma samples. The result, which is a typical pharmacokinetic graph, is shown in Figure 3.4. The area under the curve (AUC) represents the average amount of Thiamet-G absorbed by the rats. The AUC was 2263 ng / mL by oral administration. In the future, additional information, such as the bioavailability, can be determined by using this data along with a pharmacokinetic study using intravenous administration.

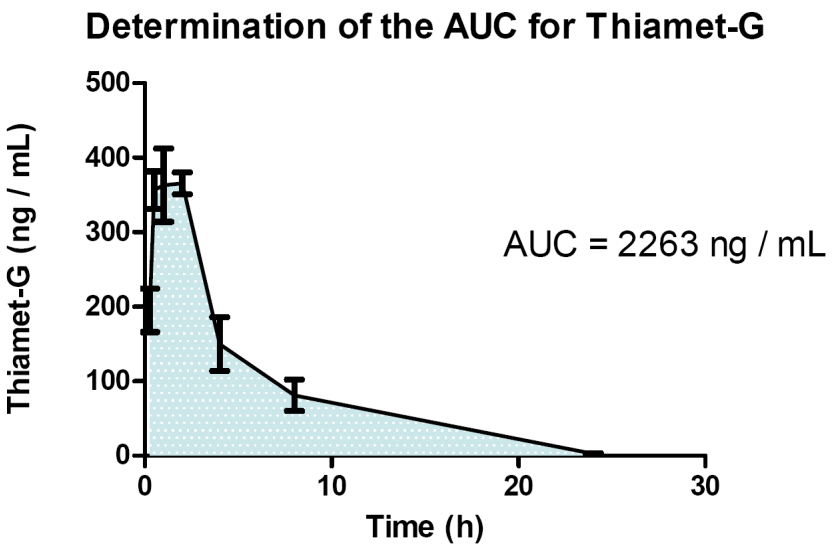

Figure 3.4. The Total Amount of Thiamet-G that was Absorbed by Rats.
Concentrations of Thiamet-G were plotted against the time points of collection. The AUC was 2263 ng / mL.

PK compartment models are often used to describe how a compound behaves in a biological system after administration. The behaviour of Thiamet-G in rat can be examined by plotting the log of concentrations of Thiamet-G versus time points. In the logarithmic graph of Figure 3.5, it exhibits an absorption phase, a distribution phase and an elimination phase are all observed. In oral administration as compared to IV injection, the compound in the blood is slower to reach C_{max} because of the absorptive processes of the GI tract[94]. Since the experiment was performed using oral gavage, these phases are not distinctive in the graph. Nevertheless, most of the points lie on the trendline. The shape of the graph resembles the curve expected for a one compartment model (Figure 1.12 B). The actual determination of the type of compartment model should be determined by administration via the intravenous route.

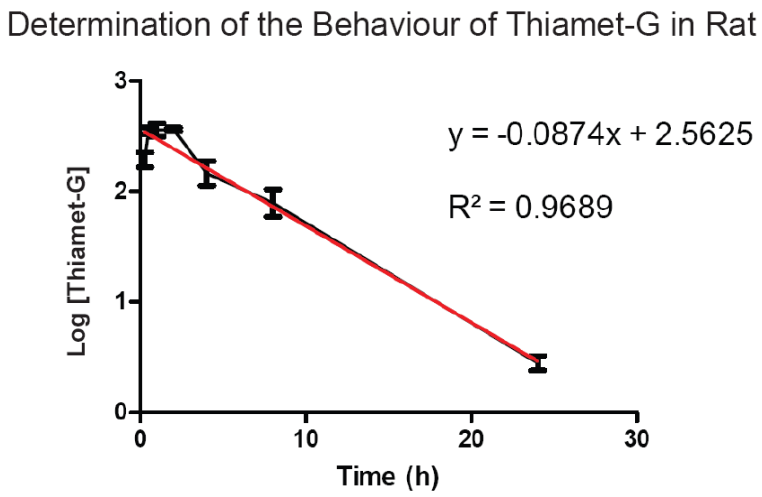

Figure 3.5. An Apparent One Compartment Model is Exemplified in the Log of Concentrations of Thiamet-G versus Time Graph.
The behaviour of Thiamet-G in the body of rat can be determined by compartment modeling. In an one compartment model, the body is considered as one unit. Once the compound reaches the body system, the compound immediately distributes throughout the body and maintain steady state between tissues. The black line is the actual data and the red line is the trendline.

The elimination rate constant, *k*, can be determined by plotting the natural log of the concentrations of Thiamet-G in the elimination phase versus time. The graph is shown in Figure 3.6. A minimum of three points are required for determining *k*[91]. A linear relationship was drawn between concentration and time with a coefficient of regression of 0.998. The plot supports the fact that the compound is eliminated from the body by a first order kinetic process. The apparent *k* can be estimated from the negative slope of the line representing the elimination phase of the graph (Figure 3.6). Hence, the apparent *k* is 0.201 ± 0.009. Using equation 14, the apparent half life, $t_{1/2}$, can be determined as well that is the time it takes for the initial concentration of the compound in the plasma to decrease to 50 %.

$$t_{1/2} = 0.693 / k \qquad (14)$$

In this study, $t_{1/2}$ is 4.977 ± 0.222 h. The $t_{1/2}$ suggests that Thiamet-G indeed partitions between the plasma and the tissues in the body and it is well absorbed by the body system.

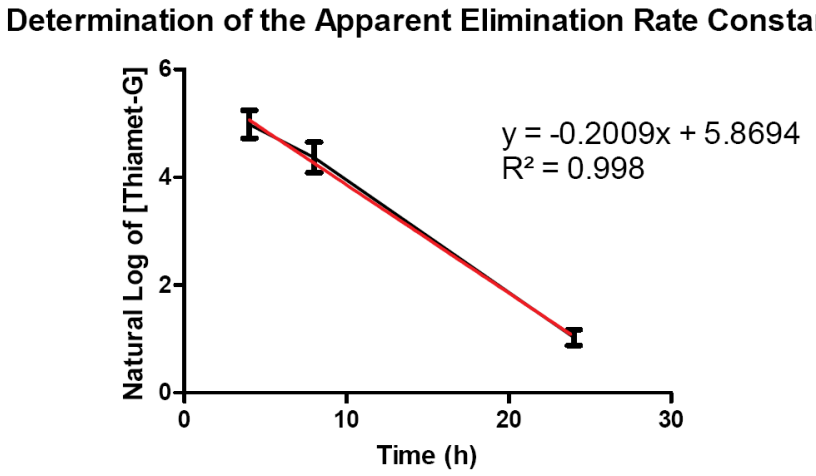

Figure 3.6. The Apparent Elimination Rate Constant can be Determined from the Natural Log of Concentrations of Thiamet-G versus Time Graph.
k is equal to the negative slope of the plot. $t_{1/2}$ can be determined once *k* is known. *k* and $t_{1/2}$ are 0.201 ± 0.009 and 5.0 ± 0.2 h respectively.

3.9 Conclusion

We have developed a LC-MS/MS method for supporting the pharmacokinetic analyses for Thiamet-G, Thiampro-G, and Thiamme-G. During method development, samples were prepared by spiking compounds in rat plasma that mimicked the make up of the actual pharmacokinetic plasma samples. Thiambu-G acted as the internal standard. The method utilized the Hypercarb offline cartridge as the sample extraction tool and the ZIC-HILIC column as the stationary phase. The instrumental settings for the bioanalytical method are summarised in Table 3.30.

Table 3.30. Summary of Validated Instrumental Settings

LC	Ultimate 3000 HPLC system (Dionex Corporation, Bannockburn, USA
MS	4000 QTRAP mass spectrometer (Applied Biosystems Life Technologies Corporation, Foster City, USA)
Column	Merck SeQuant ZIC-HILIC column (Umeå, Sweden) (5 µm, 2.1 x 100 mm ID), was protected by a guard column (5 µm, 2.1 x 20 mm ID).
Separation conditions	Step 1) 0 - 10 min, 300 µL / mL, 84 % B, Step 2) 10.5 – 13 min, 600 µL / mL, 30 % B, Step 3) 13.5 – 16 min, 600 µL / mL, 84 % B, Step 4) 16.5 - 18 min, 300 µL / mL, 84 % B (A = 0.5 % FA + 5 % ACN + H_2O, B = 0.1 % FA + ACN).
Dwell time	200.00 µsec
CUR	30.00 psi
ISP	4500.00 V
TEM	200.00 ^oC
GS1	20.00 psi
GS2	20.00 psi
DP	56.00 V
CAD	7.00 psi
EP	8.00 V
CE	31.00 eV
CXP	10.00 V

We have successfully validated the method specifically for supporting the pharmacokinetic analyses for Thiamet-G, Thiampro-G, and Thiamme-G. The method has been proven to be linear, specific, accurate, precise, sensitive, with good recovery, and not affected by matrix effect. The compounds were found to be generally stable with some exceptions at their storage conditions, - 20 ^oC and -80 ^oC. The experimental LOD

was determined to be 0.05 ng / mL for all three compounds. Precision and accuracy were maintained at the LOQ, 0.05 ng / mL. The linear dynamic range ranged from 0.05 to 1000 ng / mL.

As shown in Section 3.8, the method proved useful for analysis of the actual pharmacokinetic samples. The study was carried out by feeding Thiamet-G to rats by oral gavage. Thiamet-G was found to be absorbed with a C_{max} of 370 ± 20 ng / mL and a t_{max} of 2 h. The AUC was 2263 ng / mL. From the analysis, the apparent k and $t_{1/2}$ were determined to be 0.201 ± 0.009 and 5.0 ± 0.2 h respectively. We were conclusively able to demonstrate that the method was capable of quantifying the analytes in rat plasma from pharmacokinetic studies.

3.10 Future Plans

PK samples for other compounds and samples that were collected from intravenous administration will be analysed using the same protocol. The method can be expanded to analyse other plasma types and tissues. It should be possible to make improvements to the current sample extraction method and the chromatographic conditions. For example, the manual extraction process can be adapted to an automatic format, which will help to shorten the time required to perform the overall analysis.

3.11 Methods for Validation

Chemicals and reagents. HPLC grade acetonitrile was purchased from Caledon Laboratories Ltd. LC-MS grade or HPLC grade water was purchased from

Mallinckrodt Baker, Inc, while reagent grade formic acid was purchased from Fluka, Sigma-Aldrich. Reagent grade glacial acetic acid was purchased from Anachemia. Control rat plasma was obtained from the animal facility of Valley Biochemical, Inc. (Winchester, USA).

Instrumentation. The 4000 QTRAP LC-MS/MS system consisted of the 4000 QTRAP mass spectrometer interfaced with an Ultimate 3000 HPLC system. The HPLC system was composed of a binary LC pump, a vacuum degasser, a temperature controlled autosampler and a thermostated column compartment set at 40 ^{o}C. The control software for data acquisition was Analyst version 1.4.2, Dionex Chromatography Mass Spectrometry Link software version 2.0.0.2315 and Chromeleon version 6.80 SP2. The analytical column for the analysis, Merck SeQuant ZIC-HILIC column (5 µm, 2.1 x 100 mm ID), was protected by a guard column (5 µm, 2.1 x 20 mm ID). The mobile phase, 0.1 % FA + 85 % ACN / H_2O, was pumped initially at a flow rate of 300 µL / min. A gradient method was setup for the run as tabulated in Table 3.30.

Table 3.31. LC Gradient Program Gradient Method for the ZIC-HILIC Column.

Time (min)	% B	Flow Rate (µL)
0	84	300
10	84	300
10.5	30	600
13	30	600
13.5	84	600
16	84	600
16.5	84	300
18	84	300

Mobile phase A was 0.1 % FA + 5 % ACN + H_2O and mobile phase B is 0.1 % FA + ACN.

Preparation of Standards. One stock solution, $Stock_{mixed}$, containing Thiamet-G, Thiampro-G, and Thiamme-G (conc = 100000 ng / mL), was prepared by dissolving 10 ± 0.1 mg of each standard in water and making the volume up to 100 mL in a volumetric flask. The stock solution of internal standard, $Stock_{IS}$ (conc = 10000 ng / mL), was prepared by dissolving 1 ± 0.1 mg of Thiambu-G in water and making the volume up to 100 mL in a volumetric flask. The stock solutions were stored at 4 ^{o}C. The actual weights of compounds for preparing the stocks solutions and the procedures for preparing the Calibration Standards (CS) are described in Appendix Section A2.

Preparation of Working Calibration Standard Solutions (WCSS)

11 µL of each calibration standard solution (CS) and 11 µL of a 100 ng / mL internal standard solution were transferred into a centrifuge tube. In addition, two portions of 11 µL of the control rat plasma and 110 µL of water were added into each

tube to give a final total volume of 154 µL. After the tubes were capped and vortexed for 30 sec, they were centrifuged at 10000 rpm for 1 min at room temperature.

Equilibration of the Cartridges

1 mL Hypercarb cartridges were loaded onto the vacuum manifold holder, which was placed on top of a reversible manifold lid. When a vacuum was applied to the assembly, the liquid solutions present inside the cartridges were drawn into the waste container. The steps for equilibration of the cartridges were as follows: a) 1 mL of 0.5 M ammonium hydroxide, b) 2 x 1 mL of HPLC grade water, c) 30% acetic acid, d) 1 mL of HPLC grade water, e) 1 mL of 70% ACN / H_2O (premixed earlier), f) 5 x 1 mL of HPLC grade water

During the equilibration process, the solutions present in the cartridges were kept no lower than the top edge of the manifold holder, which was located immediately above the bed level of the cartridge. Effort was made to avoid trapping air bubbles inside the column bed. The vacuum pressure reading was maintained so that it was no higher than 7 mm Hg. The next equilibration solution was loaded when the level of the previous solution present in the cartridge has just reached the top edge of the holder. Just prior to loading the next solution, the vacuum was released.

Application of the Samples

140 µL of the sample was individually loaded onto the 1 mL Hypercarb SPE cartridge using an adjustable pipette. The vacuum pressure was maintained below mm Hg until the sample had entered into the cartridge bed.

Washes

Five washes each being 720 µL in volume of water were applied into the cartridges. The cartridges were dried completely after both the fourth and fifth wash. When drying the cartridges, a vacuum was drawn through the assembly for 30 sec at 8 mm Hg.

Elution

Two portions of 180 µL of a 70% ACN / H_2O solution (premixed earlier) were applied into the cartridge. The collection tubes were placed underneath the reversible manifold lid, so the eluted fractions were collected. In between the two elution processes, the cartridges were dried completely at 8 mm Hg. When initially passing the eluent into the cartridges, the vacuum reading was kept at 2 mm Hg. The two eluted fractions were pooled into one collection tube. The eluent was dried down completely under vacuum at 55°C.

Preparation of the Test Article

100 µL of a premixed 70% acetonitrile/water solution was transferred into collection tubes to reconstitute the samples. The tubes were capped and vortexed for 30 sec. After 5 min of sonication, the tubes were centrifuged at 10000 rpm for 6 min at room temperature. Hence, the WCSS are five times more dilute than the CS. 7 µL of each sample were transferred into separate HPLC vials containing inserts. All samples were capped. One set of samples were used for LC–MS/MS analysis and other samples were stored either in the 4°C refrigerator or in the -20°C freezer.

Preparation of the QC Samples

Three QC stocks for compounds with high (QC_H = 800 ng / mL), medium (QC_M = 400 ng / mL), and low (QC_L = 1 ng / mL) concentrations of analytes were prepared from the $Stock_{mixed}$. Please see Appendix Section A2 for the procedure used to prepare these QC spiking stocks. These QC stocks were added separately into six aliquots of plasma. Eventually, six replicates of QC samples for three different concentration levels were prepared. 11 µL of a QC stock solution and 11 µL of 100 ng / mL internal standard solution were transferred into a centrifuge tube. In addition, two portions of 11 µL of the control rat plasma and 110 µL of water were added into each tube, total volume of 154 µL. After the tubes were capped and vortexed for 30 sec, they were centrifuged at 10000 rpm for 1 min at room temperature. 140 µL of the QC sample was loaded onto a Hypercarb cartridge for sample cleanup. The procedure for sample cleanup was the same as the sample cleanup for the WCSS samples as described above.

Preparation of the $QC_{stability}$ Samples

Six QC samples containing analytes at the same concentration underwent the sample extraction processes. These samples were pooled together and aliquoted into six portions of $QC_{stability}$ samples. These six stability samples should have identical concentrations because the possible causes of deviation have been eliminated.

Analytical Procedure. 4 µL of sample was injected by the autosampler into the 4000 QTRAP LC-MS/MS system. With the HPLC pump pumping the mobile phase, the 4 µL of the sample was delivered into the turbo ion spray ion source. During acquisition, the MRM transitions were set according to Table 2.2 and the dwell time was set as 200.00 msec. The resolution of Q1 and Q3 was set to be 1 unit mass resolution. With

positive ionisation mode set in the acquisition method, the other parameters were CUR (30.00 psi), ISP (4500.00 V), TEM (200.00 oC), GS1 (20.00 psi), GS2 (20.00 psi), DP (56.00 V), CAD (7.00 psi), EP (8.00 V), CE (31.00 eV), and CXP (10.00 V).

APPENDICES

Appendix A1 PK Parameters

Volume of distribution (V_d): V_d represents the apparent volume of plasma needed to dissolve the compound so that the resulting concentration would give the concentration of compound in plasma[98]. In the equation below, Cp is the drug concentration in plasma, X is the amount of compound and t is the time[98].

$$V_d(t) = X / Cp(t) \quad (15)$$

For a bolus injection, the initial plasma concentration, Cp(0), is equal to the dose divided by the Vd[91].

$$Cp_t = Cp(0) \times \exp(-kt) \quad (16)$$

Equation 14 above describes the plasma concentration when the compound content in the plasma undergoes exponential decay[98]. When the equation is converted into the linear form, the equation becomes

$$\ln Cp_t = \ln Cp(0) - kt, \quad (17)$$

where k is the elimination rate constant and the y intercept is ln Cp(0)[98].

Half-life: Half life is the time needed to reduce the plasma concentration of the compound to half of its original concentration[91]. The equation for defining half-life is

$$t_{1/2} = 0.693 / k \quad (14)$$

Bioavailability (F): Bioavailability refers to the fraction of the dose which gets into the circulatory system[94]. This parameter strongly depends on the rate of absorption at the site of administration[94]. By the intravenous route, 100 % of the dose is considered to be in the bloodstream[94]. A common way to determine the bioavailability of the other routes is by comparing the area under the curve (AUC) obtained from the intravenous route and the other route[91].

$$\text{Bioavailability} = AUC_{\text{other route}} / AUC_{IV} \quad (18)$$

Salt factor (S):

Salt factor, S is the active form of the compound as a salt or an ester. If there is a compound with a salt factor of 0.8, it indicates 1 gram of the salt form of the compound is equal to 800 mg of the active compound[98].

Area under the Curve (AUC): AUC is found by plotting the concentration of plasma against a period of time[91].

Clearance (CL): In general, clearance is a theoretical term, which relates the rates of elimination to the compound concentration in plasma at the site of measurement[91].

CL = Elimination rate of drug from the entire body / concentration

From the physiological perspective, CL is the apparent volume of plasma present in the system, cleared of the compound per unit time by metabolic and elimination processes[91]. In multicompartmental models, the volume of distribution at steady state can be related to clearance by the equation 6[94].

$$CL_{total} = k \times V_d \quad (19)$$

Mathematically, CL is the elimination rate constant in which a portion of drug is constantly lost from the V_d as described in equation 6 above. However, in most cases, the clearance and the volume of distribution are assumed to be independent of each other[94].

Steady State Concentration (Cp^{SS}): A steady state is observed when multiple dosing is applied at a regular dosing interval, T. The condition is reached when the amount of compound applied to a body system is equivalent to the amount of compound that is eliminated from the system within the same time period. By the route of intravenous infusion, steady state is also observable when the compound concentration in the plasma increases with time until it remains constant.

$$\text{Rate of compound administration} = (S \times F \times D) / T \qquad (20)$$

$$\text{Rate of compound elimination} = CL \times Cp^{SS} \qquad (21)$$

When the two rates are equivalent, the following formula is useful for estimating the Cp^{SS}:

$$Cp^{SS} = (S \times F \times D) / (CL \times T) \qquad (22)$$

As a result, one could use equation 9 to calculate Cp^{SS}[98].

Loading Dose (LD): The dose administered at the beginning of a treatment to reach the desired compound concentration in the body system[98].

The LD can be estimated by equation 10 assuming Cp^{SS} is the desired concentration to be reached.

$$LD = V_d \times Cp^{SS} \qquad (23)$$

Since LD is increasing exponentially inside the body system, the above equation is modified into:

$$Cp = LD \times \exp(-kt) / V_d \qquad (24) \quad [98]$$

Maintenance dose: A dose that is used to offset the amount of compound that is being eliminated from the body. The dose is administered by intravenous infusion[98].

Appendix A2 Supplementary Data for the Validated Method

In Table 1A, the weights of the analogues used for making the $Stock_{IS}$, the stock of each compound, and $Stock_{mixed}$ solutions are tabulated. The procedure for preparing these stock solutions is described in the Method of Validation (See Section 3.7). $Stock_{mixed}$ was prepared by mixing samples of Thiamet-G, Thiampro-G, and Thiamme-G in one vial. $Stock_{IS}$ was prepared with Thiambu-G.

Table 1A. Actual Weights of Each Analogue.

	Analogue	Weight (ng)
1	Thiamet-G	1.01220×10^7
2	Thiampro-G	0.99446×10^7
3	Thiamme-G	1.00440×10^7
4	Thiambu-G (IS)	0.10180×10^7

The six calibration standard solutions (CS) ranging from 2.5 to 5000 ng / mL were prepared from the $Stock_{mixed}$ according to Figure 1A. The three different concentration levels of QC stock solutions at different concentrations (QC_L = 62.5 ng / mL, QC_M = 25000 ng / mL, and QC_H = 50000 ng / mL) were also prepared from the stock solution.

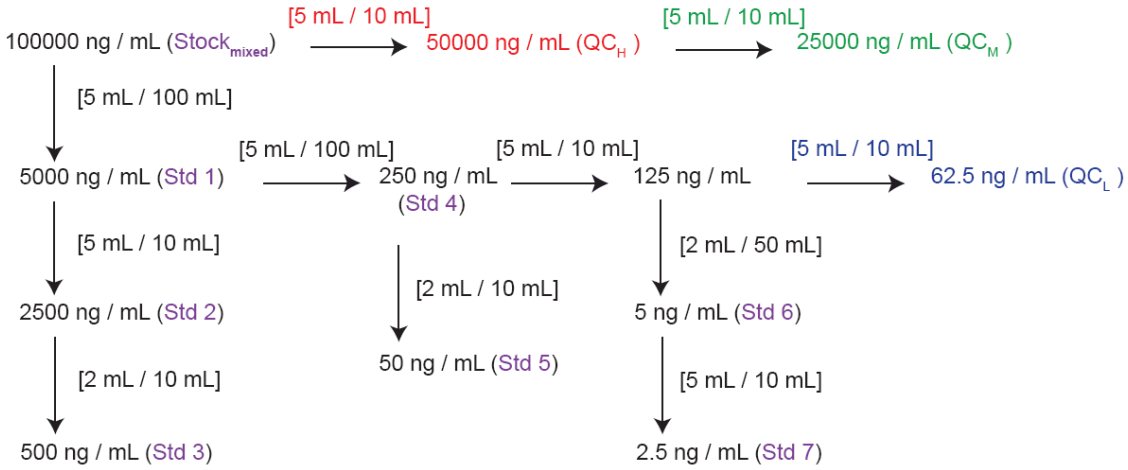

Figure 1A. Dilution Scheme for Calibration standards.
The dilution factors are indicated in the square brackets.

The weights of Thiamet-G, Thiampro-G, and Thiamme-G in the CSSs samples are reported in Table 2A. The weights of these compounds in the QC spiking stocks are reported in Table 3A.

For preparing the internal standard, 5 mL of $stock_{IS}$ was added into a 100 mL volumetric flask. The flask was made up to volume with water. 2 mL of the water mixture was transferred into a 10 mL volumetric flask, and it was made up to the volume with water. The concentration of the prepared internal standard was 102 ng / mL.

Table 2A. Calibration Standard Solutions (CSSs).

No.	[Stock[1]] (ng / mL)	Volume transferred from [stock] (mL)	Final volume (mL)	Final [Thiamet-G] (ng / mL)	Final [Thiampro-G] (ng / mL)	Final [Thiamme-G] (ng / mL)
Std 1	1.000×10^5	5.00	100.0	5.06×10^3	4.97×10^3	5.02×10^3
Std 2	5.00×10^3	5.00	10.0	2.53×10^3	2.49×10^3	2.51×10^3
Std 3	2.50×10^3	2.00	10.0	506	497	502
Std 4	250	2.00	10.0	50.6	49.7	50.2
Std 5	125	2.00	50.00	5.06	4.97	5.02
Std 6	5.00	5.00	10.0	2.53	2.49	2.51

[1]Stock concentration is the approximate concentration of each analogue present with the stock solution. For example, for std 1 it is approximately 1.012×10^5 ng / mL of Thiamet-G, 0.9945×10^5 ng / mL of Thiampro-G, and 1.004×10^5 ng / mL of Thiamme-G.

Table 32A. QC Stocks.

	[Stock[1]] (ng / mL)	Volume transferred from [stock] (mL)	Final volume (mL)	Final [Thiamet-G] (ng / mL)	Final [Thiampro-G] (ng / mL)	Final [Thiamme-G] (ng / mL)
QC_H	1.000×10^5	5.00	10.0	5.06×10^4	4.97×10^4	5.02×10^4
QC_M	5.00×10^4	5.00	10.0	2.53×10^4	2.49×10^4	2.51×10^4
QC_L	125	5.00	10.0	63.3	62.2	62.8

[1]Stock concentration is the approximate concentration of each analogue present in the stock solution. For example, for the stock solution for preparing the QC_H stock it is approximately 1.012×10^5 ng / mL of Thiamet-G, 0.9945×10^5 ng / mL of Thiampro-G, and 1.004×10^5 ng / mL of Thiamme-G.

Appendix A3 Supplementary Experiments on Different Types of Stationary Phases

As discussed in Section 2.3.2 and 2.4.2, the data obtained using other columns are shown in this section.

A3.1 Reverse Phase Columns

A3.11 Phenomenex Synergi 2.5 µm Fusion-RP 100 Å with Guard Column

The Synergi Fusion column uses a polar embedded C_{18} resin with suitable operating pH conditions ranging from 1.5 to 10. The $time_{recommended}$ elution on the Synergi Fusion column was 1.86 min. In chromatogram (A) shown in Figure 2A, none of the analytes were efficiently retained when using water as the mobile phase, and co-elution was observed for Thiampro-G and Thiambu-G. In chromatogram (B), only Thiambu-G was retained efficiently when using 5 % ACN / H_2O as the mobile phase. The ability for the column to retain these polar compounds under these conditions was poor. Other chromatographic conditions have been tested for this column, but none of the conditions demonstrated that the Synergi Fusion column was capable of retaining and separating the analogues (data not shown).

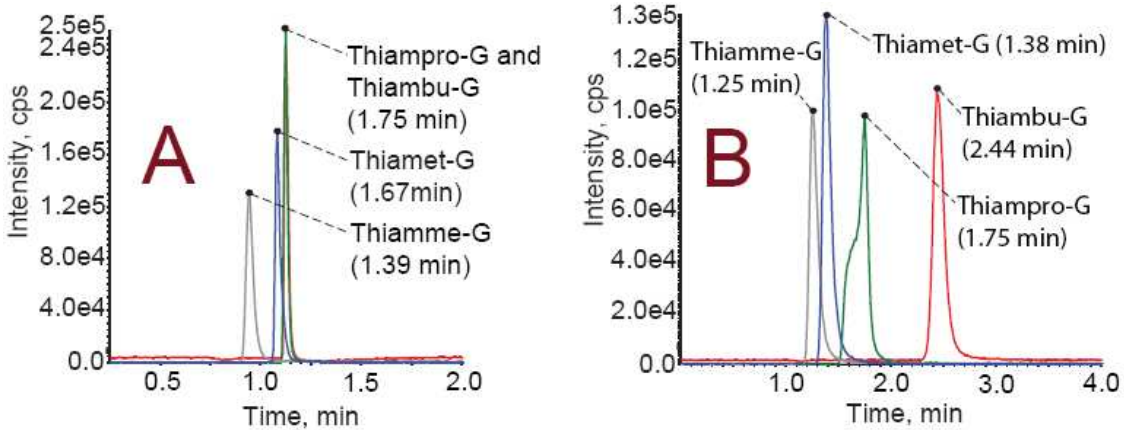

Figure 2A. Attempted Separation and Analysis of the Analogues Using a Synergi Fusion Column.
(Column: 3 x 50 mm; guard: 3 x 4 mm, flow rate: 200 µL / min, CV_{empty}: 382 µL, $Time_{recommended}$: 1.86 min, sample: a mixed compound standard solution dissolved in water, elution with: 100 % H_2O for chromatogram (A) and 5% ACN / H_2O for chromatogram (B)).

The exocyclic nitrogen of the inhibitors have a pKa of 8.0[74]. At physiological pH or under acidic conditions, Thiamet-G and its analogues are in their protonated states. To favour deprotonation of the analytes, the pH of the mobile phase has to be above 8[74]. When compounds are not in their ionised states, they become less polar and are likely to be more easily retained on reverse phase columns. Nevertheless, use of an aqueous solution containing 100 % 10 mM CH_3COONH_4 at pH 8.3 as the mobile phase, illustrated in Figure 3A, did not improve the retention of the compounds and only Thiambu-G was retained on the column. The effect of partially deprotonating the analogues was poor and the separation was even worse than when using the chromatographic conditions outlined for the data described in Figure 3A.

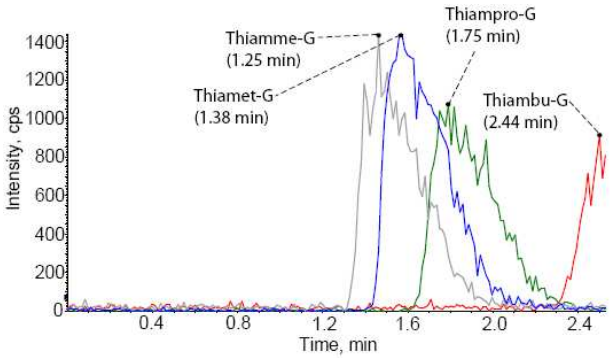

Figure 3A. Attempted Separation of the Analogues on the Synergi Fusion Column Using an Aqueous Mobile Phase, pH 8.3.
The analysis was performed using an API 2000 LC-MS/MS system, and 100 % 10 mM CH_3COONH_4, pH 8.3 was used as the mobile phase. The sample is a mixed compound standard solution dissolved in water. Only Thiambu-G was retained. The resolution of the analogues was poor, and peak tailing was observed.

A3.12 Agilent Zorbax Eclipse XDB

The Zorbax Eclipse column is a normal C_{18} column with operating pH conditions ranging from 2 to 9. In chromatogram (A) shown in Figure A4, all analytes were retained except for Thiamme-G. It took more than 8 min for Thiampro-G and Thiambu-G to elute from the column. In chromatogram (B), only Thiambu-G was fully retained. The separation shown in Figure 4A indicated that this column was not ideal for retaining all these analogues. The column was tested previously with the usual concentration of the analytes used in these studies (1400 ng / mL) but detection of the analogues was very poor when using the API 2000 LC-MS/MS. Hence, the concentration of analytes used in the LC-MS analyses reported in Figure 4A was increased to 2 mg / mL in order to determine the performance of the column. The use of this column was not further pursued.

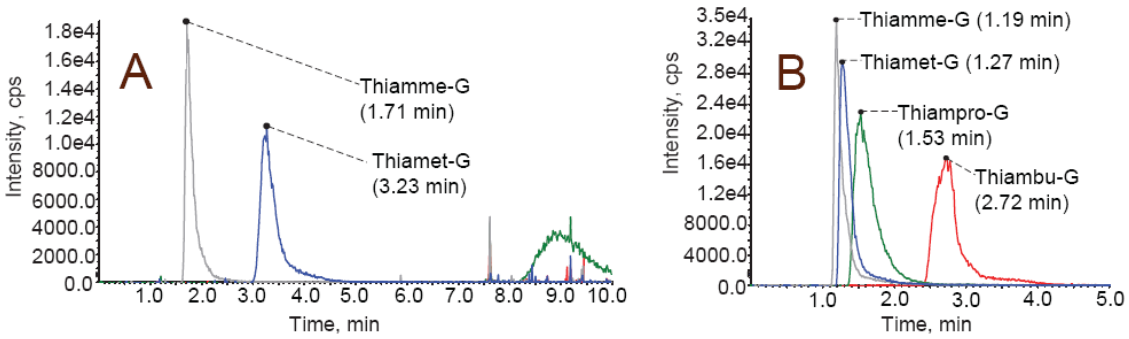

Figure 4A. Attempted Use of Zorbax Eclipse XDB Column for Separation of the Analytes. The analysis was performed using an API 2000 LC-MS/MS system. (Column: 4.6 x 150 mm; flow rate: 1 mL / min, CV_{empty}: 2.49 mL, $Time_{recommended}$: 2.43 min, sample: a mixed compound standard solution dissolved in water, elution with: 100 % 10 mM CH_3COONH_4 at pH 8.3 for chromatogram (A) and 5% ACN / 10 mM CH_3COONH_4 at pH 8.3 for chromatogram (B))

A3.2 PGC Column

A3.2.1 Thermo Scientific Hypercarb Column, 3µm, 200 Å

The Hypercarb column is a porous graphite column (PGC). When the hydrophobicity of the analytes increases, they are retained longer on a reverse phase column. Analytes behave similarly when using a Hypercarb column. As shown in Figure 5A, all four analytes were retained on the column, and they were well separated from each other. Thiamme-G, being the most polar compound, was eluted first while Thiambu-G, being the least polar compound, was retained on the stationary phase for the longest time. All four analogues have tall and narrow peak shapes. The only concern was that background signals matching those for the MRM used for monitoring Thiambu-G continued to increase after the elution of Thiambu-G. The MS parameters were not optimized for this column because of the apparent instability of the column, which is discussed below.

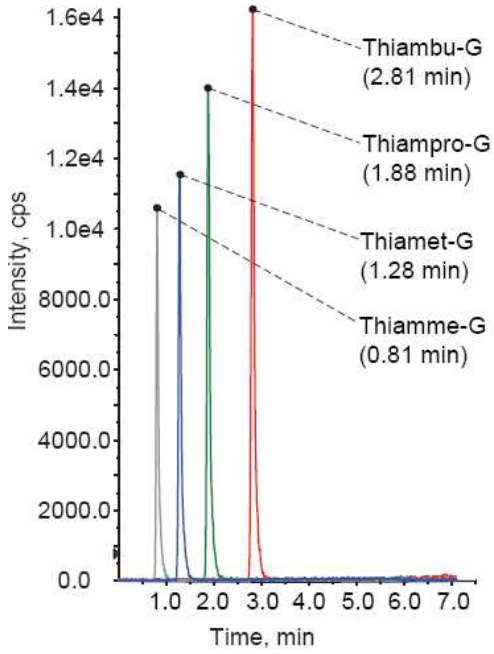

Figure 5A. The PGC Column was able to Retain all Four Analytes.
Analytes were separated with the PGC column. In this figure, only the first seven min of the chromatogram are shown. (Column: 3 x 50 mm; guard: 3 x 4 mm, flow rate: 600 µL / min, CV_{empty}: 353 µL, $Time_{recommended}$: 0.57 min, sample: a mixed compound standard solution dissolved in water, separation conditions: Step 1) 0 min, 600 µL / mL, 0 % B, Step 2) 5 min, 600 µL / mL, 21.1 % B, Step 3) 5.1 – 7.1 min, 600 µL / mL, 94.7 % B, Step 4) 7.2 – 20.1 min, 600 µL / mL, 0 % B (A = 0.5 % FA + 5 % ACN + H_2O, B = 0.1 % FA + ACN))

Stability of the Hypercarb Column

A sample that was treated with plasma was injected into the analytical system connected to the Hypercarb column. The sample cleanup procedure used was ultrafiltration. A control sample, acting as a positive control, was also prepared by replacing the plasma with water. A standard solution was also prepared by dissolving the four analogues into water.

These three samples were injected into the system to measure the repeatability of the retention times of the analytes. Aliquots of each sample were consecutively injected (n = 5) into the autosampler for the LC-MS/MS analysis. Five aliquots of standard were

analysed first, then followed by five aliquots of the control samples. Lastly, five aliquots of plasma samples were analysed. The peak area responses and retention times of the analyses were computed in a statistical manner and are reported in Table 4A and Table 5A.

Before analysing the control and plasma samples, a standard solution was run to determine the stability of the system. Five injections were made with the last four injections showing consistency in peak area responses and retention times. As tabulated in Table 4A, the % RSD of the peak area counts and retention times were in all cases less than 5 % and 2 % respectively.

Table 4A. Analyses of a Standard Solution.

Analyte	Peak Area			RT		
	Average (cps)	SD	% RSD (n = 4)	Average (min)	SD	% RSD (n = 4)
Thiambu-G	8.0×10^4	3×10^3	4	3.02	0.02	1
Thiampro-G	6.9×10^4	2×10^3	2	2.10	0.02	1
Thiamet-G	5.8×10^4	2×10^3	3	1.50	0.03	2
Thiamme-G	4.4×10^4	1×10^3	3	0.98	0.02	2

A total of five injections of the standard solution were made. The data obtained by the first injection of the standard was ignored due to the significant differences in peak area responses and retention times when compared with the other four injections, which suggested the column was likely not appropriately equilibrated.

As mentioned in Section 2.4.1, the desired % RSD for the peak area counts is less than 10 %, and the desired % RSD for the RT is less than 2 %. For the control and plasma samples, the % RSD for both the peak area responses and the retention times are higher than 10 % and 2 % respectively (Table 5A). The data suggest that the retention times became unstable after the introduction of the ultrafiltrated samples. Statistical

analyses confirmed that the retention times of Thiamet-G and its analogues were inconsistent. In summary, the Hypercarb column in combination with ultrafiltration was a poor candidate for column selection and further studies using this column were discontinued. In addition, the time required to equilibrate the column (30 column volumes) was generally unsuitable for further method development.

Table 5A. Analyses of the Ultrafiltrated Samples.

Types of Samples	Peak Area			RT		
	Average (cps)	SD	% RSD (n = 5)	Average (min)	SD	% RSD (n = 5)
Thiambu-G						
Control	8.7×10^4	1×10^4	1×10^1	3.2	0.1	3
Plasma	6.4×10^4	2×10^4	2×10^1	3.20	0.09	3
Thiampro-G						
Control	9×10^4	1×10^4	1×10^1	2.26	0.09	4
Plasma	1.00×10^5	7×10^3	7	2.24	0.08	3
Thiamet-G						
Control	7.8×10^4	8×10^3	1×10^1	1.66	0.10	6
Plasma	8.9×10^4	7×10^3	8	1.63	0.08	5
Thiamme-G						
Control	6.2×10^4	8×10^3	1×10^1	1.11	0.08	7
Plasma	6.8×10^4	5×10^3	8	1.10	0.06	6

Appendix A4 Supplementary Results of using Different Sample Cleanup Procedures

As discussed in Table 2.11, the data obtained with the various clean up methods are reported in this section.

A4.1 Deproteinisation by Protein Precipitation

A4.1.1 Deproteinisation by Protein Precipitation (TSKgel column)

A4.1.1.1 MeOH as the Precipitant

In the chromatograms shown in Figure 6A, MeOH was used to precipitate proteins that were present in the plasma sample. The mobile phase and the test article contained 80 % ACN and 90 % MeOH respectively. Since MeOH and ACN have polarity indexes of 5.1 and 5.8, respectively[156], ACN is slightly more polar than MeOH[156]. Chromatograms (A) and (B) showed a striking difference in the peak shapes for all the analytes. Due to the interaction between the more polar mobile phase and the MeOH in the test article, it was hard to explain the differences observed in the chromatograms. Thus, the organic solvent in the test article should match with the organic solvent in the mobile phase to produce interpretable results, yet this was not the case. It is possible the analytes interact better than intended with MeOH through hydrogen bonding. In any event, MeOH was abandoned as a potential precipitant.

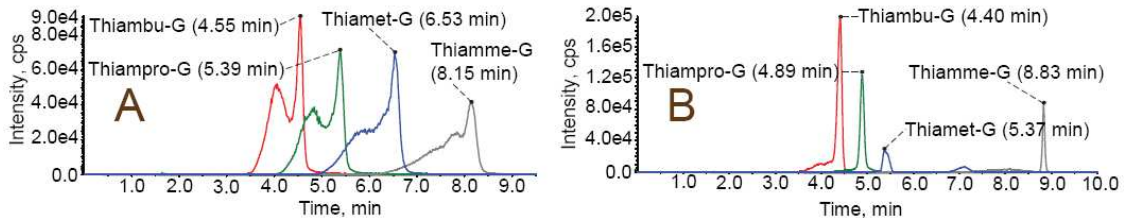

Figure 6A. Attempted Separation of the Analytes Using MeOH as a Precipitant for Sample Clean up.
Supernatants that were collected after protein precipitation were separated with the TSKgel column and analysed using the MS. Analysis of the control and the plasma samples are reported in chromatogram (A) and (B) respectively.

A4.1.1.2 ACN as the Precipitant (TSKgel Column)

In the chromatograms illustrated in Figure 7A, ACN was used to precipitate proteins that were present in the samples. In chromatogram (A), Gaussian peak shapes was observed for the analytes in the control sample. In chromatogram (B), suppression that was caused by matrix ions was seen for the peaks arising from Thiamet-G and Thiamme-G.

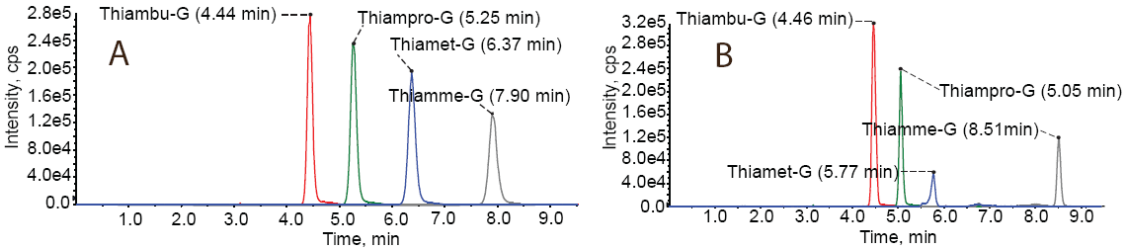

Figure 7A. Attempted Separation of the Analytes using ACN as a Precipitant for Sample Clean up.
Supernatants, collected after precipitation, were analysed using a TSKgel column and analysed with the MS. Analysis of the chromatograms of the control and the plasma samples are shown in (A) and (B) respectively.

By comparing the retention times of the analyte in the two chromatograms, one can see that the retention time of Thiamme-G has shifted by 8 % (Figure 7A). This result suggests that ions present in the plasma might interfere with the analytes and cause deviations in the elution time. Severe suppression was observed for Thiamet-G and Thiamme-G. In Table 6A, the suppression of analogues caused by the matrix ions is

reported in a percent ratio, the % matrix suppression. The deformation of the peak shapes in the plasma sample is also summarised in the last column.

Table 6A. Comparison of the Peak Characteristics from the Chromatograms Shown in Figure 7A.

Analyte	Control Sample (cps)	Plasma Sample (cps)	% Matrix suppression	Peak Shape of the Plasma Sample
Thiamet-G	1.92×10^6	$*4.40 \times 10^5$	22.9 %	Heavily suppressed
Thiambu-G	2.05×10^6	1.99×10^6	97.1 %	N/A
Thiampro-G	2.06×10^6	1.24×10^6	60.2 %	Sharpened
Thiamme-G	1.54×10^6	$*7.24 \times 10^5$	47.0 %	Slight suppression

% Matrix suppression = peak area of (plasma /control) x 100 %.

* = manual integration was used to integrate the peak area counts.

Q1 Scan Analyses

Many peaks were observed in the Q1 chromatogram of the plasma sample, but these ions were not observable during analysis of the control sample. The response for both Thiamet-G and Thiampro-G was impaired by elution along with the species giving rise to this same cluster of peaks, with 430.8 m/z as the representative peak. The cluster as shown in Figure 8A chromatogram (A) extended from 100 m/z all the way to 2400 m/z. Many isotopic peaks were observed as shown in chromatogram (B). Another cluster of peaks, with a representative peak at 431.1 m/z, had a pattern showing a repeating difference of 68 Da (chromatogram not shown). These clusters of ions likely suppressed ionisation of Thiamme-G.

These data support the fact that there were indeed matrix ions causing the suppression observed for all the analytes, except for Thiambu-G. Hence, protein precipitation alone was not capable of efficiently removing interfering matrix ions.

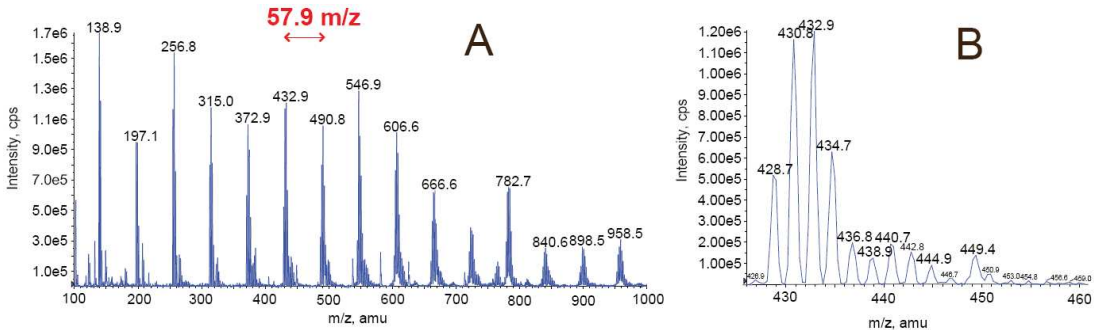

Figure 8A. Ion Clusters that Appear to Interfere with Ionisation of Thiamet-G and Thiampro-G.
Chromatogram (A) shows the pattern of an interfering cluster with 430.8 m/z as the representative peak. Chromatogram (B) was the expanded version of 432.9 m/z. (Sample: plasma sample collected after protein precipitation, Scan type: Q1 scan).

A4.1.2 Deproteinisation by Protein Precipitation (ZIC-HILIC column)

A4.1.2.1 ACN as the Precipitant (Initial Experiment)

The protein precipitated samples, using ACN as the precipitant, were analysed using a ZIC-HILIC column. In Figure 9A chromatogram (A), Gaussian peak shapes were observed for all analytes in the control sample. In chromatogram (B), suppression caused by matrix ions was seen for the peaks corresponding to Thiamet-G and Thiamme-G.

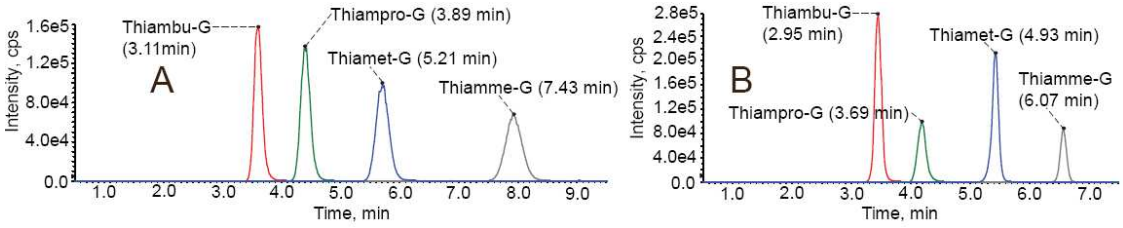

Figure 9A. Attempted Separation of the Analytes using ACN as a Precipitant for Sample Clean up.
Analytes were separated using a ZIC-HILIC column and analysed using the MS. The control and the plasma samples are reported in chromatogram (A) and (B) respectively.

As reported for the % matrix suppression in Table 7A, suppression was found for Thiampro-G and Thiamme-G, with Thiamme-G being suppressed heavily. Enhancement of ionisation was observed for Thiambu-G. The retention times of all analytes were shifted earlier, with Thiamme-G shifted the most.

Table 7A. Peak Characteristics of the Analogues from the Chromatograms Shown in Figure 9A.

Analyte	Peak Area		% Matrix suppression	Peak Shape of the Plasma Sample
	Control Sample (cps)	Plasma Sample (cps)		
Thiamet-G	1.55×10^6	1.70×10^6	110 %	Sharpened
Thiambu-G	1.59×10^6	2.28×10^6	143 %	Sharpened
Thiampro-G	1.62×10^6	1.03×10^6	63.6%	Suppressed
Thiamme-G	1.36×10^6	6.63×10^5	48.8%	Sharpened

% Matrix suppression = peak area of (plasma /control) x 100 %.
The analysis was carried out when the column was used for a brief period of time.

Q1 Scan Analysis

The same matrix ions as reported in Section A4.1.2, were observed in the plasma sample when the sample was analysed using a ZIC-HILIC column. Thiamme-G was

found to co-elute with the clusters of ions having a representative 430.8 m/z. Some new matrix ions were detected when the analysis was performed on the TSKgel column due to the different elution time of these matrix ions and the compounds. The matrix ions, such as those having 524.4 and 496.5 m/z, were found to co-elute with Thiambu-G and Thiamme-G. Based on a literature search, these ions could be phospholipids[157]. The protein precipitation experiment was repeated in Section A 4.1.2.2

A 4.1.2.2 ACN as the Precipitant (Repeated Experiment)

Samples prepared using the same procedure as used for the samples analysed in Figure 9A were injected into the autosampler for LC-MS/MS analysis equipped with a ZIC-HILIC column. In the experiment the column had been conditioned and this enabled a comparison of the effect of this conditioning on performance of this clean up method. In chromatogram (A) of Figure 10A, Gaussian peak shape was observed for the analytes in the control sample. Based on the % matrix suppression reported in Table 8A, Thiambu-G and Thiamme-G were found to be suppressed, with minor suppression observed for Thiamme-G.

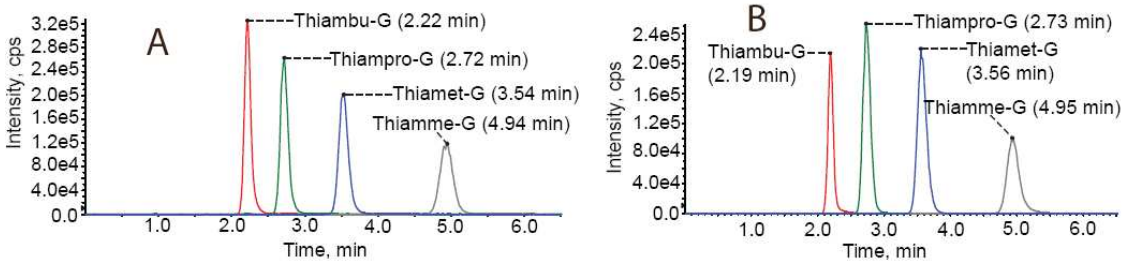

Figure 10A. Another Attempt of Separating the Analytes using ACN as a Precipitant for Sample Clean up, Using a Conditioned ZIC-HILIC Column
The control and the plasma samples are reported in chromatogram (A) and (B) respectively.

Table 8A. Peak Characteristics of the Analogues in the Chromatograms Shown in Figure 10A (after Partial Conditioning of a ZIC-HILIC Column).

Analyte	Control Sample (cps)	Plasma Sample (cps)	% Matrix suppression	Peak Shape of the Plasma Sample
Thiamet-G	1.91×10^6	2.15×10^6	113 %	Sharpened
Thiambu-G	2.08×10^6	1.26×10^6	60.6 %	Sharpened
Thiampro-G	2.03×10^6	2.09×10^6	103 %	Suppressed
Thiamme-G	1.53×10^6	1.35×10^5	88.2 %	Sharpened

% Matrix suppression = peak area of (plasma / control) x 100 %
The analysis was carried out with the column in use for awhile.

Behaviour of the ZIC-HILIC Column

There were some noticeable differences in the behaviour of the ZIC-HILIC column prior to conditioning (as illustrated in Figure 9A) and when it had been conditioned by extended use (as illustrated in Figure 10A). In Figure 9A, the control sample was analysed, followed by analysis of nine samples before analysis of the plasma sample. The nine samples analysed were the SS and plasma samples. All the analytes in chromatogram (B) of Figure 9A eluted earlier than in chromatogram (A). In the case of the chromatograms reported in Figure 10A, the control and plasma samples were analysed almost one after the other and after extensive conditioning of the column. The

retention times of the same analytes in both chromatograms were similar. It seems that when using the ZIC-column, the retention time of the analytes would shift depending on whether the column was conditioned. Suppression observed in the plasma sample, reported in chromatogram (B) of Figure 10A, was not as severe as in the case of the corresponding sample reported in Figure 9A. Severe suppression was only observable when the column was first being used, further suggesting that conditioning of the column was important.

A4.2 Altering the Mobile Phase

Changing the mobile phase is a possible way to alter the elution times of the matrix ions and the analytes and therefore to perhaps eliminate matrix suppression. In this experiment, the samples for the analysis were the protein precipitated samples using methanol as the precipitant. These samples were separated using a TSKgel column and analysed using the MS. The mobile phase was changed from 80 % ACN to 100 % MeOH. This could also be beneficial for samples obtained using MeOH as a precipitant because the mobile phase and solvent containing the analyte would be similar.

A4.2.1 MeOH as the Mobile Phase

The MRM chromatogram (A) of Figure 11A suggests that there was no interaction between the analytes and the stationary phase. With final composition of the sample being less polar than the mobile phase, the analytes eluted out without being retained on the column. The possible reason was that MeOH in the mobile phase interacted with the hydroxyl groups of the ions to obstruct with the binding of the analytes to the stationary phase.

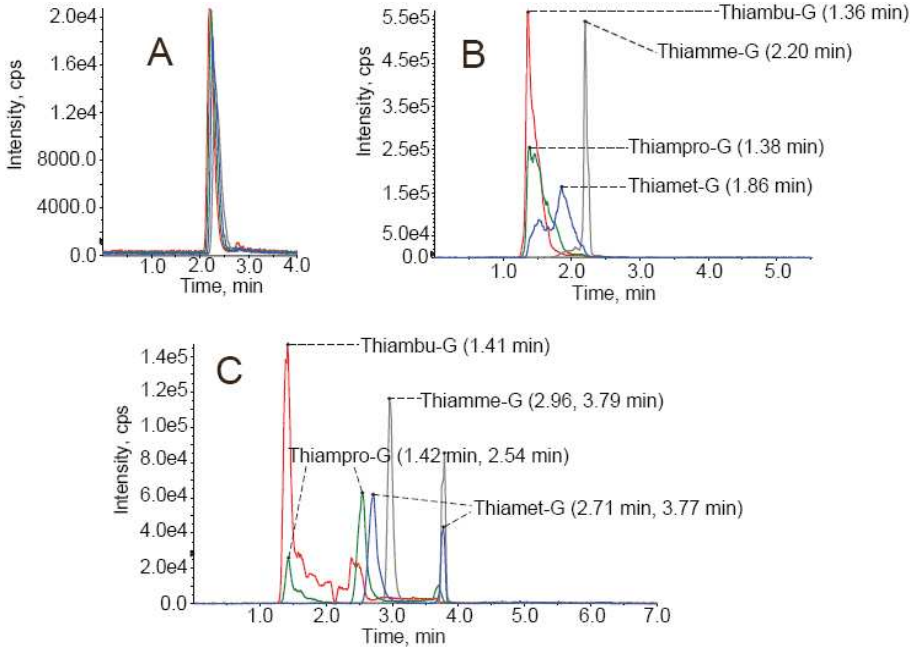

Figure 11A. Attempted Separation of the Analytes using the TSKgel column with MeOH as the Mobile Phase.
In chromatogram (A) of Figure 11A, a standard solution that was dissolved in 90 % MeOH / H_2O was injected into the system with 0.1% FA + 80% MeOH / H_2O as the mobile phase. In chromatograms (B) and (C), the control (B) and the plasma (B) samples were prepared with 90 % MeOH / H_2O, and the mobile phase was 0.1% FA + MeOH.

As discussed in Section 2.3.3.1, the $T_{recommended}$ for the TSKgel column is 2.45 min. In chromatogram (A), none of the analytes was retained. In chromatogram (B), two of the analytes, Thiamet-G and Thiamme-G were retained while Thiampro-G was partially retained. This chromatogram shows that the matrix alters the retention time of the analytes. Presumably by altering the interaction between the eluent and the analytes or by affecting the stationary phase. This data also indicate that the eluent might interact with the matrix ions, or the matrix ions might have formed a complex with the ions. For either reason, the separation of the analytes has changed making this an inappropriate approach. A similar observation was made when the precipitant of the samples was changed to ACN (data were not shown).

Summary of the Q1 Scan Analysis

With the mobile phase composed of MeOH, the elution of the matrix ions in the plasma sample changed in comparison to using ACN in the mobile phase. The 430.8 m/z cluster, which happened to interfere with Thiamet-G and Thiampro-G, was found to elute at the beginning of the run. The other cluster, with 431.1 m/z as the representative peak, eluted at 2.154 min. This set of ions have mass differences of 68 Da cluster was suppressed by the 430.8 m/z cluster, and its elution was also hastened when MeOH was present in the eluent. Another matrix ion having 132.3 m/z was also apparent at the beginning of the run. These matrix ions tended to elute at the middle or at the end of the run when ACN was used in the mobile phase. A similar observation was made for the matrix ions when the precipitated samples were analysed using a ZIC-HILIC column (data not shown). Since some matrix ions co-eluted with the analytes, it was crucial to try other sample preparation procedures before doing any further analysis on the MS.

A4.2.2 ACN as the Mobile Phase

In Figure 12A, 99.9 % of ACN was used as the mobile phase. No analyte eluted during the run due to the absence of water in the mobile phase. None of the analytes eluted in both the MRM chromatograms of the control and plasma samples (only the plasma sample was shown in Figure 12A.) In the Q1 scan analysis, no other matrix ions were found, except for 118.2 m/z (data not shown). This finding suggests that most of the matrix ions are polar. The elution of the unretained analytes with 99.9 % MeOH as the mobile phase (A 4.3.1) supported the fact that MeOH interacts with the analogues.

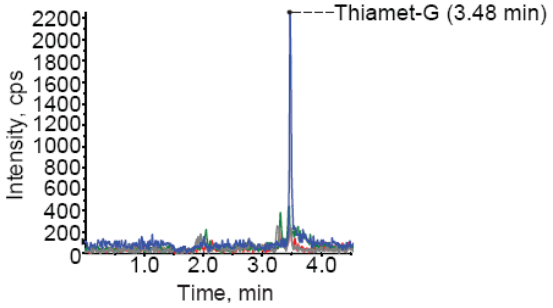

Figure 12A. Attempted Separation of the Analytes using the TSKgel column with ACN as the Mobile Phase.
Plasma sample with final composition of 90 % ACN / H_2O was injected into TSKgel column and analysed in MS. The mobile phase was 0.1 % FA + ACN. A minimal amount of Thiamet-G eluted during the run.

A4.3 Deproteinisation by Ultrafiltration

A4.3.1 Deproteinisation by Ultrafiltration (TSKgel column)

Since protein precipitation as the sample preparation procedure resulted in test article that still had high levels of interference, it was important to try other deproteinisation processes. Removal of protein by using a size exclusion filter is a common process which traps proteins in the filter while obtaining the small compounds in the filtrate.

Samples were analysed using ultrafiltration. In chromatogram (A) of Figure 13A, Gaussian peak shapes were observed for the analytes. For the plasma sample, as illustrated in chromatogram (B), severe suppression was observed for both Thiamet-G and Thiamme-G. Differences in retention times between the control and plasma samples were noted for Thiamet-G and Thiamme-G.

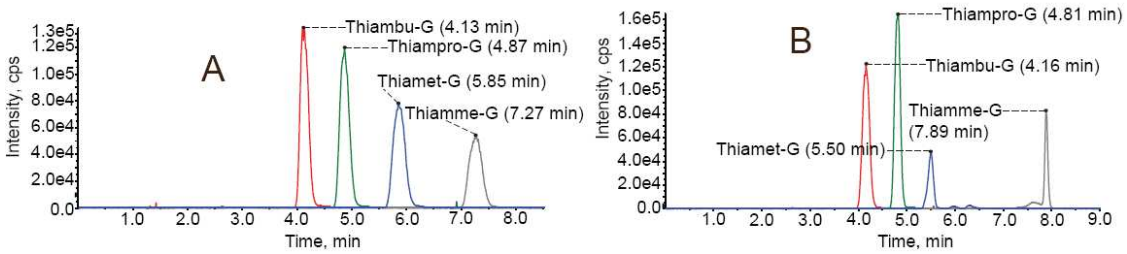

Figure 13A. Attempted Separation of the Ultrafiltrated Analytes.
Samples were cleaned up using ultrafiltration and the final solvent composition was 90 % ACN / H_2O. Analytes were separated using a TSKgel column and analysed by LC-MS/MS. The mobile phase was 0.1 % FA + 80 % ACN / H_2O. Data for the control and the plasma samples are reported in chromatogram (A) and (B) respectively.

As indicated by the % matrix suppression shown in Table 9A, the ionisation of all the compounds was affected by the matrix of the plasma sample, except for Thiampro-G.

Table 9A. Peak Characteristics of the Analogues of the Chromatograms in Figure 13A.

Analyte	Peak Area		% Matrix suppression	Peak Shape of the Plasma Sample
	Control Sample (cps)	Plasma Sample (cps)		
Thiamet-G	1.20 x 10^6	*4.19 x 10^5	34.9 %	Suppressed Severely
Thiambu-G	1.46 x 10^6	1.25 x 10^6	85.6 %	Lower Intensity than Thiampro-G
Thiampro-G	1.45 x 10^6	1.42E x 10^6	97.9 %	Slightly Sharpened
Thiamme-G	8.93 x 10^5	*4.75 x 10^5	53.2 %	Severely Suppressed

% Matrix suppression = peak area of (plasma /control) x 100 %

* = manual integration was used to integrate the peak area counts

Summary of the Q1 Scan Analysis

Based on the analysis on the Q1 mass spectra, the major matrix ions likely contributing to suppression of Thiamet-G and Thiamme-G were the 430.8 m/z cluster and

431.1 m/z cluster respectively. Other major matrix ions had 118.2, 132.3, and 162.3 m/z. Thus, the matrix affected the ionisation of some analytes, and the process of ultrafiltration alone was not capable of removing these matrix ions. The use of ultrafiltration for clean and TSKgel column for analysis was therefore inappropriate.

A4.3.2 Deproteinisation by Ultrafiltration (ZIC-HILIC column)

As shown in Figure 14A, samples were cleaned up by passing through ultrafilters before analysis using the LC-MS/MS. The chromatographic conditions were modified to include a wash cycle to remove matrix ions that were possibly present in the column after eluting the targeted analytes. Earlier data in Section A4.2.1, confirmed that samples did not have stable retention times when separated using a ZIC-HILIC column. Removal of the matrix ions that were left behind in the column could prevent the interference of these matrix ions with analytes present in the next injected sample. An online wash cycle was therefore incorporated into the LC program.

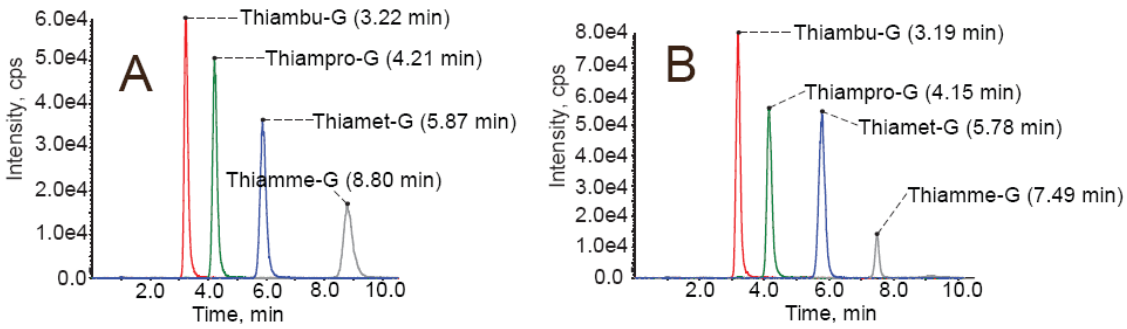

Figure 14A. Attempted Separation of the Ultrafiltrated Analytes Using an Online Wash Cycle.
Samples analysed in chromatogram (A) and (B) were cleaned up with ultrafilters and analysed by LC-MS/MS. The final sample composition was 90 % ACN / H_2O and analytes were separated using a ZIC-HILIC column. The mobile phase was 0.1 % FA + 85 % ACN / H_2O. Data for the control and the plasma samples are reported in chromatogram (A) and (B) respectively.

In chromatogram (A) of Figure 14A, Gaussian peak shapes were observed for all the analytes. In chromatogram (B), suppression caused by matrix ions was seen for Thiamme-G. The % matrix suppression of Thiamme-G (in Table 10A) was calculated to be less than 40 %. This suggests that some substance co-eluted with this analyte and caused serious ion suppression despite the online wash cycle. The difference in the retention times of Thiamme-G between control and plasma samples indicated that there was need for further sample cleanup. It was not known why the percent peak area for Thiambu-G and Thiamet-G were so high, but the % matrix suppression for Thiampro-G was reasonable.

Table 10A. Peak Characteristics of the Analogues in the Chromatograms of Figure 14A.

Analyte	Peak Area		% Matrix suppression	Deformation in Peak Shape of the Plasma Sample
	Control Sample (cps)	Plasma Sample (cps)		
Thiamet-G	5.32×10^5	$7.32E \times 10^5$	138 %	Enhanced
Thiambu-G	5.82×10^5	7.42×10^5	127 %	Enhanced
Thiampro-G	5.72×10^5	6.23×10^5	109 %	N / A
Thiamme-G	3.79×10^5	$*1.30 \times 10^5$	34.3 %	Severe Suppression

% Matrix suppression = peak area of (plasma /control) x 100 %

* = manual integration was used to integrate the peak area counts

Q1 Scan Analysis

Interestingly, in the Q1 scan analysis, ion clusters having representative ions with 430.8 m/z and 431.1 m/z were not detected during the elution time frame of all the analytes (data not shown). The substance that co-eluted with Thiamme-G cannot be detected using the Q1 scan analysis. The results demonstrate that under these chromatographic conditions involving a wash cycle, some of the matrix ions were removed from the column prior to the injection of the next sample. Overall, however, this sample clean up method still was inappropriate for further development.

Stability of Retention Times when Using a ZIC-HILIC Column

As shown in Table 11A, the % RSD of the retention times of standard, control, and plasma samples are summarised. With the incorporation of a wash cycle in the run, the shifting of the retention times of the analytes was reduced. The % RSD of the retention times was generally lower than 2 %. The low % RSD of the retention times for the standard solution indicated that the column was stable. Because Thiamet-G eluted earlier in the plasma sample than in the control sample, it is likely that some matrix ions co-elute with it. Nevertheless, as mentioned above, a better sample preparation process is necessary to improve the sample analyses.

Table 11A. The % RSD of the RT of SS, the Control, and Plasma Samples.

Thiambu-G	Average RT (min)	% RSD		Thiamet-G	Average RT (min)	% RSD
Control Sample	3.22	0.63		Control Sample	5.84	1.01
Plasma Sample	3.23	0.99		Plasma Sample	5.85	0.96
*SS	3.21	0.80		*SS	5.83	0.98
^Sum	3.23	0.83		^Sum	5.85	0.94
Thiampro-G	**Average RT (min)**	**% RSD**		**Thiamme-G**	**Average RT (min)**	**% RSD**
Control Sample	4.20	0.73		Control Sample	8.72	1.35
Plasma Sample	4.20	0.93		Plasma Sample	7.58	1.21
*SS	4.19	0.96		*SS	8.71	1.01
^Sum	4.20	0.80		^Sum	8.15	7.37

Two sets of control and plasma samples were prepared, and they were injected into the MS twice.

*SS = during the run, SS was run after the analyses of every three samples. The % RSD of the standard was also calculated.

^Sum = the sum of the % RSD of the RT of the control samples and the plasma samples was also calculated.

A4.4 Protein Precipitation + LLE

A4.4.1 Ultrafiltration + LLE (TSKgel column)

A different approach was attempted using ultrafiltration and liquid-liquid extraction. After the samples were cleaned up by ultrafiltration, the collected filtrates were extracted with DCM and the aqueous phase was analysed. In chromatogram (A) of Figure 15A, Gaussian shapes were observed for the analytes present in a control sample of analogues lacking plasma. In chromatogram (B), when matrix ions were present,

distortion in peak shape was observed for Thiamet-G and Thiamme-G. In Table 12A, missing peak area counts are observable for Thiamet-G and Thiamme-G. This sample cleanup process did not improve the ionisation of the compound ions.

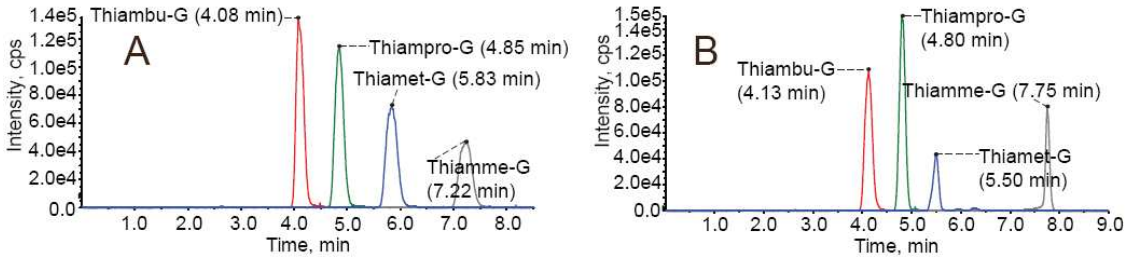

Figure 15A. Analysis of Samples of Analytes that were Cleaned up by Ultrafiltration and LLE Using the TSKgel column.
Samples were passed through ultrafilters and the collected filtrates were extracted with DCM. The final solvent composition was 90 % ACN / H_2O**.** The mobile phase was 0.1 % FA + 80 % ACN / H_2O. Upon centrifugation, the supernatants were injected into the autosampler for MS analysis. Chromatogram (A) and (B) of the above figure are the control and the plasma samples respectively.

Table 12A. Peak Characteristics of the Analogues of the Chromatograms in Figure 15A.

Analyte	Peak Area		% Matrix suppression	Peak Shape of the Plasma Sample
	Control Sample (cps)	Plasma Sample (cps)		
Thiamet-G	1.07×10^6	*3.78×10^5	35.3 %	Suppressed Severely
Thiambu-G	1.37×10^6	1.15×10^6	83.9 %	Lower Intensity than Thiampro-G
Thiampro-G	1.34×10^6	1.29×10^6	96.3 %	N / A
Thiamme-G	7.83×10^5	4.79×10^5	61.2 %	Sharpened

% Matrix suppression = peak area of (plasma /control) x 100 %

* = manual integration was used to integrate the peak area counts

A4.4.2 Ultrafiltration + LLE (ZIC-HILIC)

In this experiment, samples were cleaned up by ultrafiltration. Half of the filtrate of each sample was saved for analysis, and half of the filtrate was extracted with DCM.

In chromatogram (A) of Figure 16A, Gaussian peak shapes are observed for the analytes. In chromatogram (B), when matrix ions were present, no distortion in peak shape was observed.

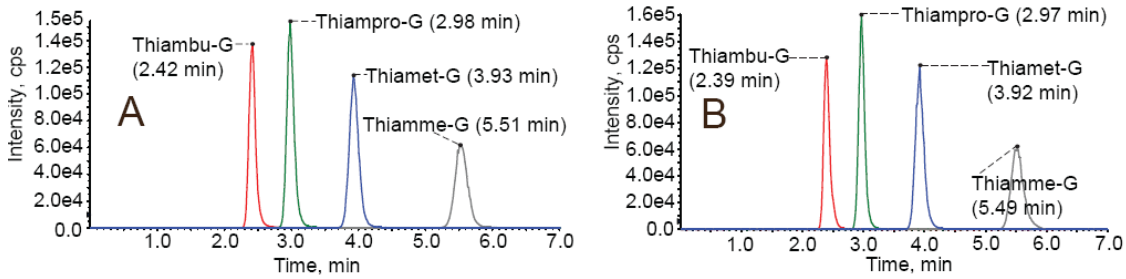

Figure 16A. Attempted Separation of the Analytes that were Cleaned up by Ultrafiltration and LLE Using the ZIC-HILIC Column.
Samples were passed through ultrafilters and the collected filtrates were extracted with DCM. The final solvent composition was 90 % ACN / H_2O. The mobile phase was 0.1 % FA + 85 % ACN / H_2O. Upon centrifugation, the collected water portions were separated with the ZIC-HILIC column and were analysed in the MS.

However, the peak area counts for Thiamet-G and Thiamme-G were higher when compared to the corresponding peaks observed during analysis of the control sample. The comparison is reported in Table 13A. A stable retention time was observed for all the analytes.

Table 13A. Peak Characteristics of the Analogues of the Chromatograms in Figure 16A.

Analyte	Peak Area		% Matrix suppression	Peak Shape of the Plasma Sample
	Control Sample (cps)	Plasma Sample (cps)		
Thiamet-G	3.96×10^5	5.06×10^5	128 %	Higher in Intensity
Thiambu-G	4.16×10^5	4.18×10^5	101 %	N/A
Thiampro-G	4.05×10^5	4.70×10^5	116 %	Higher in Intensity
Thiamme-G	3.54×10^5	5.65×10^5	160 %	Higher in Intensity

In Table 14A, the % recovery data are reported for both for the samples that have passed through the ultrafilters followed by extraction with DCM (Table a) and the samples that have just passed through the ultrafilters (Table b). By using the same standard solution for comparison, one can observe that the peak area counts obtained for the control and plasma samples were lower when the extraction process was carried out using DCM. Compounds are likely lost during the extraction process making this process inappropriate for further development.

Table 14A. Comparison of Response for the Analogues in the Standard Solution, the Control, and the Plasma Samples.

a) % Recovery for Samples (Ultrafiltration + LLE)					
Analyte	**Peak Area (cps)**			**% Recovery$_{control}$**	**% Recovery$_{plasma}$**
	Standard	**Control Sample**	**Plasma Sample**	**Control Sample / standard**	**Plasma Sample / standard**
Thiambu-G	6.04 x 10^5	4.16 x 10^5	4.18 x 10^5	68.9 %	69.2 %
Thiampro-G	6.20 x 10^5	4.05 x 10^5	4.70 x 10^5	64.8 %	75.8 %
Thiamet-G	6.58 x 10^5	3.96 x 10^5	5.06 x 10^5	60.2 %	76.9 %
Thiamme-G	6.56 x 10^5	3.54 x 10^5	5.65 x 10^5	54.0 %	86.1 %
b) % Recovery for Samples (Ultrafiltration)					
Analyte	**Peak Area (cps)**			**% Recovery$_{control}$**	**% Recovery$_{plasma}$**
	Standard	Control Sample	Plasma Sample	Control Sample / Standard	Plasma Sample / Standard
Thiambu-G	5.59E+05	5.28 x 10^5	5.27 x 10^5	94.5 %	94.3 %
Thiampro-G	5.68E+05	5.19 x 10^5	6.00 x 10^5	91.4 %	106 %
Thiamet-G	5.75E+05	4.99 x 10^5	6.27 x 10^5	86.8 %	109 %
Thiamme-G	5.48E+05	4.46 x 10^5	7.19 x 10^5	81.4 %	131 %

Appendix A5 Supplementary Results of using Further Sample Preparation Procedures in Conjunction with Different Columns

A5.1 Ultrafiltration + Zip tip$_{C18}$

From a plasma sample that was cleaned up by ultrafiltration the collected filtrate was divided into two portions. One portion was directly injected onto the analytical system for the LC-MS/MS analysis, and the other portion was further cleaned up using the C_{18} ziptip. Chromatogram (A) in Figure 17A was produced by analysing the filtrate that was obtained by using only ultrafiltration. For chromatogram (B), the samples were analysed using the portion of the filtrate that was further cleaned up using a ziptip.

The two resulting samples have the same final solvent composition, and the analogues have the same final concentrations. Comparing the two chromatograms side by side, one can easily observe that the less polar compounds, Thiambu-G, Thiampro-G, and Thiampro-G, are much less intense in chromatogram (B). The purpose of cleaning the filtrate with ziptip was to remove the possible hydrophobic interferences present in the samples. The results have demonstrated there was a poor recovery of the analytes after this treatment and this approach was not pursued further.

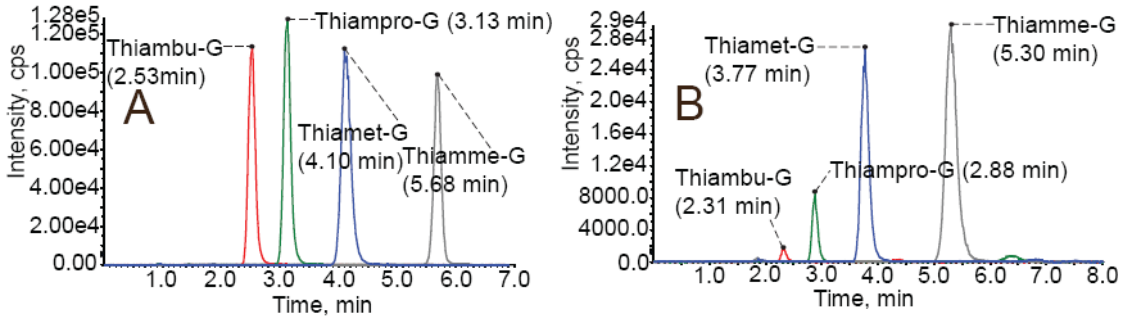

Figure 17A. Analysis of Zip tip Cartridge Clean up of Analyte Samples.
The final sample composition was 90 % ACN / H_2O and analytes were separated using a ZIC-HILIC column. The mobile phase was 0.1 % FA + 85 % ACN / H_2O**.** In chromatogram (A), the plasma sample was cleaned up by passing it through an ultrafilter. In chromatogram (B), the filtrate obtained from the ultrafilter was further cleaned up by ziptip.

A5.2 Protein Precipitation Followed by the Sigma Hybrid SPE

A set of control and plasma samples underwent protein precipitation using ACN and half of the supernatants from both the control and plasma samples were analysed by LC-MS/MS analyses using a ZIC-HILIC column. The supernatant of the control sample was labeled as B1 in Table 15A whereas the supernatant of the plasma sample was labeled as B3. The remainder of each supernatant was passed through Sigma Hybrid SPE cartridges. This SPE cartridge is reported to be able to remove phospholipids from plasma samples[157]. The supernatant from the control and the plasma samples that were cleaned up by the SPE cartridges were labeled as B1 (II) and B3 (II), respectively.

The peak area responses observed for the protein precipitated samples, and the samples that were cleaned up with the SPE Hybrid SPE cartridges, are reported in Table 15A. In Table 16A, a comparison of these peak area responses are made.

Table 15A. Analyte Response of Protein Precipitated Samples versus the SPE Hybrid SPE Cartridges.

Analyte	Peak Area (cps)			
	Control Sample (B1)	Plasma Sample (B3)	Control Sample (B1 II)	Plasma Sample (B3 II)
Thiambu-G	5.26×10^5	6.62×10^5	6.06×10^5	4.44×10^5
Thiampro-G	5.06×10^5	7.58×10^5	4.99×10^5	4.34×10^5
Thiamet-G	4.87×10^5	7.54×10^5	4.66×10^5	3.99×10^5
Thiamme-G	4.50×10^5	6.89×10^5	6.42×10^5	7.02×10^5

In the first column of Table 16A, B1 was compared with B3 by dividing the peak area counts of B3 by B1. The reported percentages provide insight into the % matrix effect. These percentages, which were far from 100 %, suggest that ionisation enhancement is occurring as a result of the clean up procedure or, alternatively the high viscosity of the plasma sample caused some sampling variation in this experiment. Comparison between B1 (II) and B1 yields % recovery, which is a calculation of the efficiency of the sample extraction process. These samples were not treated with plasma before the sample extraction process. The % recovery for all the compounds were nearly 100 %, except for Thiamme-G. The high % recovery for Thiamme-G suggests that there might some leaching materials from the cartridge, which shares the same MRM transition as Thiamme-G. It is possible the high % matrix effects are caused by leaching of materials when matrix is present and these might have similar MRM transitions. Another way to calculate % recovery is to compare B3 (II) with B3. The recoveries of the analogues were low. In the last column, B3 (II) was compared with B1 (II). By dividing the peak area responses of B3 (II) with the peak area responses of B1 (II) the % matrix effect was evaluated. The reported percentages suggest that the ionisation of the

analogues was poor. In summary, the concentrations of the analogues were high when using Hybrid SPE cartridges as a sample clean up tool. This effect discouraged us from pursuing this approach further.

Table 16A. The % Matrix Effect and % Recovery.

Analyte	B3 vs B1	B1 (II) vs B1	B3 (II) vs B3	B3 (II) vs B1 (II)
Thiambu-G	126%	115%	67.1%	73.3%
Thiampro-G	150%	98.6%	57.3%	87.0%
Thiamet-G	155%	95.7%	52.9%	85.6%
Thiamme-G	153%	143%	102%	109%

A5.3 Protein Precipitation Followed by Captiva Cartridge Clean up

A different SPE method was attempted in combination with protein precipitation. A set of control and plasma samples was cleaned up using Captiva Cartridge after going through the process of protein precipitation. A standard solution composed of 10.5 ng / mL was also prepared to act as a reference standard for analysing the extraction efficiency and the matrix suppression effect for the plasma sample. In Table 17A, the peak area responses of the analogues for all three samples are tabulated.

Table 17A. Peak Area Responses for the Analytes.

Analyte	Peak Area		
	Control Sample (cps)	Plasma Sample (cps)	Standard (cps)
Thiambu-G	1.52×10^5	1.48×10^5	1.71×10^5
Thiampro-G	1.62×10^5	1.60×10^5	1.81×10^5
Thiamet-G	1.53×10^5	1.55×10^5	1.78×10^5
Thiamme-G	1.20×10^5	5.85×10^4	1.59×10^5

The % recovery and % matrix suppression are calculated and reported in Table 18A. The recoveries of the analytes in the control sample are higher than 80 % with Thiamme-G being the exception. For the case of the plasma sample, the recoveries of the analogues are similar to the control samples except with Thiamme-G which is only 37 %. The % matrix suppression is close to 100 % for Thiamet-G, Thiampro-G, and Thiambu-G. For the case of Thiamet-G, the % matrix suppression is reported to be 48.8 %. The result suggests that either the ionisation of Thiamet-G was poor or the cartridge retained some of this compound.

Table 18A. The % Recovery and the % Matrix Suppression of the Captiva Treated Samples.

Analyte	% Recovery		% Matrix Suppression
	Control Sample (cps)	Plasma Sample (cps)	
Thiambu-G	88.9%	86.5%	97.4%
Thiampro-G	89.5%	88.4%	98.8%
Thiamet-G	86.0%	87.1%	101%
Thiamme-G	75.5%	36.8%	48.8%

When analysing the samples using the Q1 scan, more problems were observed when using the captive cartridge as the clean up device. Phospholipids were observed in the plasma sample. Many other ions of unknown origin and identity were observed to elute prior to the analogues. These observations suggest that the captive cartridge might not be compatible with the organic mixture, resulting in the leaching of bulk material from the cartridge. This approach was ultimately abandoned in preference to the optimized method that was ultimately established.

Appendix A6 Method Section

A6.1 Method A1: Synergi Fusion Column – 4000 QTRAP (Figure 2A)

The method was similar to the generic method for the 4000 QTRAP LC/MS system (See Section 2.5.2) with the following changes:

Instrumentation. The analytical column for the analysis, Phenomenex Synergi Fusion-RP (2.5 µm, 50 x 3 mm ID), was protected by a guard column (Phenomenex Security Guard cartridge, 4 x 3 mm ID). The mobile phase, 0.1% FA + H_2O, was pumped at a flow rate of 200 µL / min for chromatogram (A) illustrated in Figure 1A. The mobile phase for generating chromatogram (B) was 0.1% FA + 5% ACN + H_2O.

Preparation of Standards. Stock solutions for Thiamet-G, Thiambu-G, Thiampro-G, and Thiamme-G (conc. = 70000 ng / mL)* were prepared separately in water, 30 µL from each stock solution was added to water to yield mixed compound standard solution D (210 ng / mL), which was stored in an HPLC vial at 4 ^{o}C until required.

Analytical Procedure. 3 µL of standard solution D was injected by the autosampler of the LC–MS/MS system. With the HPLC pump pumping the mobile phase, the sample was delivered into the turbo ion spray ion source. In the acquisition method, the MRM transitions were set according to Table 2.2, and the dwell time was set as 200.00 µsec. The resolution for Q1 was set at 1 unit mass resolution and Q3 was set to be low mass resolution. A positive ionisation mode was set in the acquisition method, the other parameters were CUR (30.00 psi), ISP (4500.00 V), TEM (150.00 ^{o}C), GS1

(20.00 psi), GS2 (20.00 psi), DP (50.00 eV), CAD (7.00 psi), EP (6.00 V), CE (32.00 V), and CXP (10.00 V).

*The stock concentration is approximately (70000 ng / mL of each analogue). Throughout the methods, the stock concentration is given as approximate for the ease of discussion.

A6.2 Method A2: Synergi Fusion Column – API 2000 (Figure 3A)

The method was similar to the generic method for the API 2000 LC-MS/MS system (See Section 2.5.2) with the following changes:

Chemicals and reagents. Reagent grade glacial acetic acid was purchased from Anachemia.

Instrumentation. The analytical column was same as the one used in Method A 1 (See Section A6.1). The mobile phase, 10 mM CH_3COONH_4 adjusted to pH 8.3 with concentrated acetic acid, was pumped at a flow rate of 200 µL / min for analysis of the samples; the MRM chromatogram is shown in Figure 3A.

Preparation of Standards. 20 µL of standard solution D, prepared as described in Method A1 (See Section A6.1), was injected by the autosampler of the LC-MS/MS system. With the HPLC pump pumping the mobile phase, the sample was delivered into the turbo ion spray ion source. The software initiated acquisition prior to the injection of solution D. For the acquisition method, the MRM transitions were set according to Table 2.2 and the dwell time was set as 200.00 µsec. The resolution of Q1 and Q3 was set to be 1 unit mass resolution. A positive ionisation mode was set in the acquisition method, the other parameters were CUR (25.00 psi), ISP (5000.00 V), TEM (100.00 ^oC), GS1 (20.00

psi), GS2 (40.00 psi), CAD (7.00 psi), DP (31.09 V), FP (200.00 V), EP (9.00 V), CE (30.00 eV), and CXP (25.00 V).

A6.3 Method A3: Zorbax Eclipse XDB Column – API 2000 (Figure 4A)

The method was similar to Method A 2 (Section A6.2) with the following changes:

Instrumentation. The analytical column used for the analysis was an Agilent Zorbax Eclipse XDB (5 µm, 4.6 x 150 mm). The mobile phase, 10 mM CH_3COONH_4, pH 8.3, was pumped at a flow rate of 1 mL / min to obtain the data shown in the MRM chromatogram in Figure 4A (A). For the data shown in the MRM chromatogram illustrated in Figure 4A (B), the same flow rate was used, but the mobile phase was 5 % ACN / 95 % 10 mM CH_3COONH_4, pH 8.3.

Preparation of Standards. 2.0 mg of each analogue was weighed out separately using a 4 decimal place analytical balance (Mettler-Toledo International Inc.) and transferred into a 2 mL HPLC vial. 1 mL of water was pipetted into the vial. The vial was vortexed until the sample dissolved. This sample, standard solution E, was roughly 2 mg/mL, and it was not used for exact quantitative purposes. The vial was stored at 4 ^{o}C until required.

Analytical Procedure. 1 µL of solution E was injected by the autosampler of the API 2000 LC-MS/MS system.

A6.4 Method A4: Hypercarb column – 4000 QTRAP (Figure 5A)

The method was similar to the generic method used when using a ZIC-HILIC column for LC-MS/MS analysis (See Section 2.5.4) with the following changes:

Instrumentation. The analytical column for the analysis was a Thermo Scientific Hypercarb Column (3µm, 3 x 50 mm). The LC gradient program is reported in Table 19A.

Table 19A. LC Gradient Program for Hypercarb Column.

RT (min)	Flow (µL / min)	%B
0	600	0
0	600	0
5	600	21.1
5.1	600	94.7
7.1	600	94.7
7.2	600	0
20.1	600	0

Solvent A: 0.1% FA + 5% ACN + H_2O, Solvent B: 0.1% FA + ACN

Preparation of Standards. Stock solutions for Thiamet-G, Thiambu-G, Thiampro-G, and Thiamme-G (conc. = 70000 ng / mL) were prepared separately in water. 200 µL from each stock solution were added to a 10 mL volumetric flask and made to 10 µL by adding water to yield mixed compound standard solution H (200 mM NH_4HCO_2, pH 4, conc. = 1400 ng / mL), which was stored at 4 ^oC. Mixed compound standard solution I (final conc. = 10 ng / mL) was prepared by adding 10 µL from standard solution H into a 2 mL standard HPLC vial containing 1390 µL of water and was stored at 4 ^oC until required.

Analytical Procedure. 10 µL of standard solution I was injected by the autosampler of the LC-MS/MS system.

A6.5 Method A5: MeOH as the Protein Precipitant Using the TSKgel Column (Figure 6A)

The method was similar to the generic method for TSKgel-MS-analysis (See Section 2.5.3) with the following changes:

Chemicals and reagents. HPLC grade MeOH was purchased from Caledon Laboratories Ltd. Control rat plasma was obtained from the animal facility of Simon Fraser University (Burnaby, BC, Canada).

Preparation of Samples. The plasma sample was prepared by transferring 10 µL of solution A (conc. = 1400 ng / mL), as prepared according to Method 1 (See Section 2.5.1), into a centrifuge tube. 20 µL of the rat plasma and 10 µL of water were added to the tube. After vortexing the tube for 30 sec, the tube was centrifuged at 5000 rpm for 1 min at room temperature. 360 µL of MeOH was added as a precipitant, and the tube was vortexed for 10 to 30 sec. The tube was centrifuged at 10000 rpm for 5 min at room temperature. 160 µL of the supernatant was transferred into a HPLC vial with insert and the HPLC vial was capped prior to LC-MS/MS analysis. An extra sample was prepared by pipetting the remaining supernatant into a HPLC vial and this was stored at -20°C. The control sample was prepared the same way, except that the rat plasma was replaced with water. A blank sample was also prepared using the same sample preparation procedure as the plasma sample, except that solution A was replaced with water.

Duplicate sets of samples were prepared for both the control, blank, and plasma samples. The final sample composition of the control and plasma samples was 90 % MeOH in H_2O, and the final concentration of the samples was 35 ng / mL.

Analytical Procedure. 10 µL of the plasma sample was injected by the autosampler for the LC-MS/MS system after the analysis of the control sample has finished. The 10 µL control sample was analysed first, followed by seven samples, the SS and plasma samples, and only then the plasma sample.

A6.6 Method A6: ACN as the Protein Precipitant Using the TSKgel Column (Figure 7A)

The method was similar to Method A5 (See Section A6.5) with the following changes:

Preparation of Samples. Instead of MeOH, ACN was used as the precipitant. As a result, the final sample composition of the control and plasma samples was 90 % ACN in H_2O, and the final concentration of the samples was 35 ng / mL.

Analytical Procedure. The control sample was analysed first, followed by three samples, SS and blank samples, and only then the plasma sample. Only one set of the duplicate samples were analysed.

A6.7 Method A7: Q1 Scan Analyses using the TSKgel Column (Figure 8A)

The method was similar to Method A6 (See Section A6.6) with the following changes:

Analytical Procedure. Instead of using the MRM scan mode, Q1 scan analysis was used. The scanning range used was from 100.00 amu to 1000.00 amu. The dwell time was 3.00 sec. The resolution of Q1 was one mass unit, and the step size was 0.3 amu. The set parameters were the same, except that setting of the CUR, CAD, and CXP

were not required for this scan mode. The control sample was analysed first, followed by two samples, SS and plasma blank, and only then the plasma sample.

A6.8 Method A8: ACN as the Protein Precipitant Using the ZIC-HILIC Column (Figure 9A)

The method was similar to the generic method for ZIC-HILIC-MS-analysis (see Section 2.5.4) with the following changes:

Preparation of Samples. The samples were the same samples that were prepared as described in Method A6 (See Section A6.6).

Analytical Procedure. The control sample was analysed first, followed by nine samples, SS and blank samples, and only then the plasma sample. Only one set of the duplicate samples was analysed. 10 µL of samples were injected by the autosampler.

A6.9 Method A8b: Q1 Scan Analyses using the ZIC-HILIC Column

The method was similar to Method A7 (See Section A6.7) with the following changes:

Preparation of Samples. The samples were the same samples prepared as described in Method A6 (See Section A6.6).

Analytical Procedure. The control sample was analysed first, followed by six samples, SS and blank samples, and only then the plasma sample.

A6.10 Method A9: ACN as the Protein Precipitant with the ZIC-HILIC Column (Figure 10A)

The method was similar to Method A8 (See Section A6.8) with the following changes:

Analytical Procedure. The control sample was analysed first, followed by a plasma blank, and then the plasma sample.

A6.11 Method A10: MeOH as Part of the Mobile Phase (Figure 11A)

The method was similar to Method A5 (See Section A6.5) with the following changes:

Preparation of Samples. Mixed standard solution K (conc. = 10 ng / mL) was prepared by transferring 10 µL from mixed standard solution J (conc. = 1400 ng / mL, water) into a standard 2 mL HPLC vial. To this vial, 1260 µL of MeOH and 130 µL of H_2O were added to yield solution X with a final solvent composition of 90 % MeOH / H_2O. Standard solution X was stored at 4 ^oC prior until required. Samples used to obtain chromatograms (B) and (C) of Figure 10 A were the same samples as chromatograms (A) and (B) in Figure 6A, respectively.

Analytical Procedure. 4 µL of the solution X was injected by the autosampler for analysis while 10 µL was injected for both the control and the plasma samples. The control sample was analysed first, followed by six samples, SS and blank samples, and only then the plasma sample. Solution X was analysed in a different batch as the control and the plasma samples. A duplicate set of samples were also analysed.

A6.12 Method A10b: Q1 Scan Analyses using MeOH as Part of the Mobile Phase

The method was the same as described in Method A7 (See Section A6.7).

A6.13 Method A11: 99.9 % ACN as the Mobile Phase (Figure 12A)

The method was similar to the generic method for TSKgel-MS-analysis column (See Section 2.5.3) with the following changes:

Instrumentation. The mobile phase was 0.1 % FA + 99.9 % ACN.

Preparation of Samples. The plasma sample was the same sample that was prepared as described in Method A6 (See Section A6.6). 10 µL of the sample was injected by the autosampler.

A6.14 Method A12: Ultrafiltration Using the TSKgel Column (Figure 13A)

The method was similar to the generic method for TSKgel-MS-analysis column (See Section 2.5.3) with the following changes:

Chemicals and reagents. Control rat plasma was obtained from the animal facility of Simon Fraser University (Burnaby, BC, Canada).

Preparation of Samples. The plasma sample was prepared by transferring 20 µL of solution A (conc. = 1400 ng / mL), as prepared according to Method 1 (See Section 2.5.1), into a centrifuge tube. 20 µL of the rat plasma and 40 µL of water were added to the tube. After vortexing the tube for 30 sec, the tube was centrifuged at 5000 rpm for 1 min at room temperature. The mixture was transferred into an Ultrafree-MC 5000NMWL (Sigma-Aldrich, USA), which is an ultrafiltration device having a 5000 Da cut off size. The ultrafilter was centrifuged at 12000 x g until a minimal amount of residue was left (45 minutes). 28 µL of the filtrate was taken from the tube and spiked into 252 µL of ACN. The final sample composition of the control and plasma samples

was 90 % ACN / H_2O, and the final concentration of the samples was estimated to be 20 ng / mL.

140 µL supernatant was transferred into a HPLC vial with an insert. The HPLC vial was capped and then used for the LC-MS/MS analysis. An extra sample was prepared by pipetting the rest of the diluted filtrate into a HPLC vial and this was stored at -20 °C. The control sample was prepared the same way, except that the rat plasma was replaced with water. A blank sample was also prepared using the same sample preparation procedure of the plasma sample, except that solution A was replaced with water.

Analytical Procedure. 10 µL of the plasma sample was injected by the autosampler into the LC-MS/MS system after analysis of the 10 µL of the control sample had finished. A plasma blank was analysed in between the control and the plasma analyte samples in order to minimize RT deviations.

A6.15 Method A12b: Q1 Scan Analysis (TSKgel Column)

The method was similar to Method A7 (See Section A6.7) with the following changes:

Preparation of Samples. The samples were the same samples that were prepared in Method A12 (See Section A6.14).

A6.16 Method A13: Ultrafiltration Using the ZIC-HILIC Column (Figure 14A)

The method was similar to Method A8 (See Section A6.8) with the following changes:

Instrumentation. A gradient method was established for the run as tabulated in Table 20A.

Table 20A. LC Gradient Program Gradient Method for the ZIC-HILIC Column.

Time (min)	% B	Flow Rate (µL / min)
0	84	300
10.5	84	300
10.8	50	800
12.8	84	800
16.8	84	800
17.1	84	400
18.1	84	400

Mobile phase A was 0.1 % FA + 5 % ACN + H_2O and mobile phase B is 0.1 % FA + ACN.

Preparation of Samples. The procedure for the preparation was similar to method A11 (See Section A6.13), except that the ultrafilter was replaced with Microcon Ym-3 (Sigma-Aldrich, USA), which has a cutoff size of 3000 Da. The speed for centrifugation was 12000 x g. Instead of using water, 200 mM NH_4HCO_2, pH 4 (buffer A) was used to prepare the samples. A 10 ng / mL standard, solution M, was also prepared by spiking 10 µL of standard solution L (conc. = 1400 ng / mL, 92 % buffer A / H_2O) into a mixture of solvent comprised of 1260 µL of ACN and 130 µL of buffer A.

Analytical Procedure. Two sets of samples were prepared separately and analysed using the LC-MS/MS. The control sample was analysed first, followed by a blank sample, and then the plasma sample. Solution M was run after every three samples.

A6.17 Method A13b: Q1 Scan Analysis

The method was similar to Method A8b (See Section A6.9) with the following changes:

Instrumentation. The setup of the system was same as Method A 13 (See Section A6.16).

Preparation of Samples. The samples were the same samples that were prepared as described in Method A13 (See Section A6.16).

A6.18 Method A14: Ultrafiltration + LLE Using the TSKgel Column (Figure 15A)

The method was similar to Method A12 (See Section A6.14) with the following changes:

Preparation of Samples. The plasma sample was prepared as described in Method A12 (See Section A6.14). The mixture was transferred into the Ultrafree-MC 5000NMWL. The ultrafilter was centrifuged at 12000 x g until a minimal amount of residue was left. 30 µL of water was added into the ultrafilter and centrifugation was continued until a minimal amount of residue was left. This process of recentrifugation was repeated one more time by adding a further 30 µL of water into the ultrafilter. 14 µL of the filtrate was taken from the tube and spiked into 126 µL of ACN. The prepared solution was the plasma sample that was cleaned up by ultrafiltration (process # 1). 70 µL was added to 400 µL of DCM to perform LLE. The mixture was vortexed for 5 min. The tube was centrifuged at 10000 x g. 14 µL of the supernatant was spiked into 126 µL of ACN. The resulting solution was the plasma sample that had been cleaned up using a combination of ultrafiltration and LLE (process # 2)

The control and a blank sample for both process # 1 and # 2 were also prepared, except that the rat plasma was replaced with water and solution A was replaced with water. The final sample composition of the control and plasma samples was 90 % ACN in H_2O, and the final concentration of the analogues was 20 ng / mL each.

A6.19 Method A15: Ultrafiltration + LLE Using the ZIC-HILIC Column (Figure 16A)

The method was similar to Method A13 (See Section A6.16) with the following changes:

Preparation of Samples. The samples were the same samples that were prepared in Method A14 (See Section A6.18).

A6.20 Method A16: Ultrafiltration + Ziptip Using the ZIC-HILIC Column (Figure 17A)

The method was similar to Method A15 (See Section A6.19) with the following changes:

Preparation of Samples. 30 µL of the filtrate that were obtained after ultrafiltration as described in Method A 14 (See Section A6.18) was transferred into a centrifuge tube. A $ziptip_{c18}$ was equilibrated with 50 % ACN / H_2O three times. The ziptip was then equilibrated with 0.1 % FA + H_2O. The filtrate was pipetted up and down slowly ten times through the ziptip. The ziptip was then cleaned three times with a solution of 0.1 % FA + H_2O. The compounds that were bound onto the ziptip were eluted by the eluting solution composed of 30 µL of 0.1 % FA + 80 % ACN. The elution was performed by pipetting the eluting solution up and down through the ziptip. The eluant was dried down completely under vacuum at 35 °C. 30 µL of H_2O was transferred

into the collection tube to reconstitute the sample. The tube was capped and vortexed for 30 sec. Followed by 5 min of sonication, the tube was centrifuged at 10000 rpm for 5 min at room temperature. 14 µL of the water mixture was spiked into 126 µL of ACN. The resulting solution was the plasma sample that had been cleaned up using a combination of ultrafiltration and ziptip.

The control and a blank sample were also prepared the same way except that the rat plasma was replaced with water and solution A was replaced with water. The final sample composition of the control and plasma samples was 90 % ACN into H_2O, and the final concentration of the analogues was 20 ng / mL each.

A6.21 Method A17: Hybrid SPE Cartridge Using the ZIC-HILIC Column (Table 15A and 16A)

The method was similar to Method A9 (See Section A6.10) with the following changes:

Preparation of Samples. 6 µL of mixed standard solution J (water as solvent, conc. = 1400 ng / mL) was added into a centrifuge tube. 12 µL of plasma and 182 µL of water were also added into the tube. The tube was centrifuged at 5000 rpm for 1 min at room temperature. 600 µL of ACN that had been acidified by addition of 10 µL of FA was added into the tube. After vortexing the tube for 2 min, it was centrifuged at 14000 x g for 20 min at room temperature. Half of the supernatant was saved for LC-MS/MS analyses. The other half of the supernatant was added onto a Hybrid SPE cartridge. Vacuum was applied to the cartridge (10 to 15 mm Hg). The liquid that was collected from the outlet of the cartridge was used for analysis. A standard solution was also prepared by spiking 3 µL of solution J into a mixture composed of 97 µL of water and

300 µL of ACN. A control and a blank sample were also prepared the same way except that the rat plasma was replaced with water and solution J was replaced with water respectively. The final sample composition of the control and plasma samples was 75 % ACN in H_2O, and the final concentration of the analogues was 10.5 ng / mL each.

A6.22 Method A18: Captiva Cartridge Using the ZIC-HILIC Column (Table 17A and 18A)

The method was similar to Method A9 (See Section A6.10) with the following changes:

Instrumentation. The run time was extended from 10 min to 20 min.

Preparation of Samples. 600 µL of ACN was added into a centrifuge tube, Tube A. 1 µL of FA was spiked into ACN. 6 µL of mixed standard solution H (200 mM NH_4HCO_2, pH 4, conc. = 1400 ng / mL), 12 µL of plasma, and 182 µL of water were premixed together in another centrifuge tube, Tube B. The resulting plasma mixture was vortexed for 30 sec and then centrifuged at 5000 rpm for 1 min at room temperature. The plasma mixture supernatant was spiked into the mixture in Tube A. Upon vortexing the tube for 2 min, the tube was centrifuged at 14000 x g for 20 min at room temperature. Half of the supernatant was dried down under vacuum at room temperature and it was redissolved in 10 % 200 mM NH_4HCO_2, pH 4 in 90 % ACN.

The other half of the supernatant was added to the Captiva cartridge. Vacuum was applied to the cartridge (5 mm Hg). The liquid that was collected from the outlet of the cartridge was used for analysis. A standard solution was also prepared by spiking 3 µL of solution J into a mixture composed of 97 µL of water and 300 µL of ACN. The control and a blank sample were also prepared the same way, except that the rat plasma

was replaced with water and solution J was replaced with water, respectively. The final sample composition of the control and plasma samples was 75 % ACN in H_2O, and the final concentration of the analogues was 10.5 ng / mL each.

Analytical Procedure. 4 µL of the plasma sample was injected by the autosampler into the LC-MS/MS system after the analysis of the control sample (injection volume = 4 µL) has finished. The plasma blank was analysed in between the control and the plasma samples. The standard solution, 4 µL injection volume, was analysed before the control sample and after the plasma sample.

REFERENCE LIST

1. *Essentials of Glycobiology*, ed. A. Varki, et al. 1999, New York: Cold Spring Harbor Laboratory Press.
2. Lis, H. and N. Sharon, *Protein glycosylation. Structural and functional aspects.* Eur J Biochem, 1993. **218**(1): p. 1-27.
3. Walsh, M.T., et al., *Effect of the carbohydrate moiety on the secondary structure of beta 2-glycoprotein. I. Implications for the biosynthesis and folding of glycoproteins.* Biochemistry, 1990. **29**(26): p. 6250-7.
4. Kobata, A., *Structures and functions of the sugar chains of glycoproteins.* Eur J Biochem, 1992. **209**(2): p. 483-501.
5. Garrett, R., and Grisham, C.M., *Biochemistry*. 4th ed, ed. L. Lockwood. 2010, Boston, USA: Brooks/Cole.
6. Hart, G.W., et al., *Glycosylation in the nucleus and cytoplasm.* Annu Rev Biochem, 1989. **58**: p. 841-74.
7. Torres, C.R. and G.W. Hart, *Topography and polypeptide distribution of terminal N-acetylglucosamine residues on the surfaces of intact lymphocytes. Evidence for O-linked GlcNAc.* J Biol Chem, 1984. **259**(5): p. 3308-17.
8. Holt, G.D. and G.W. Hart, *The subcellular distribution of terminal N-acetylglucosamine moieties. Localization of a novel protein-saccharide linkage, O-linked GlcNAc.* J Biol Chem, 1986. **261**(17): p. 8049-57.
9. Hart, G.W., *Dynamic O-linked glycosylation of nuclear and cytoskeletal proteins.* Annu Rev Biochem, 1997. **66**: p. 315-35.
10. Wells, L., K. Vosseller, and G.W. Hart, *Glycosylation of nucleocytoplasmic proteins: signal transduction and O-GlcNAc.* Science, 2001. **291**(5512): p. 2376-8.
11. Vosseller, K., et al., *Diverse regulation of protein function by O-GlcNAc: a nuclear and cytoplasmic carbohydrate post-translational modification.* Curr Opin Chem Biol, 2002. **6**(6): p. 851-7.
12. Zachara, N.E. and G.W. Hart, *Cell signaling, the essential role of O-GlcNAc!* Biochim Biophys Acta, 2006. **1761**(5-6): p. 599-617.
13. Zachara, N.E., et al., *Dynamic O-GlcNAc modification of nucleocytoplasmic proteins in response to stress. A survival response of mammalian cells.* J Biol Chem, 2004. **279**(29): p. 30133-42.

14. Sohn, K.C., et al., *OGT functions as a catalytic chaperone under heat stress response: a unique defense role of OGT in hyperthermia.* Biochem Biophys Res Commun, 2004. **322**(3): p. 1045-51.

15. Han, I. and J.E. Kudlow, *Reduced O glycosylation of Sp1 is associated with increased proteasome susceptibility.* Mol Cell Biol, 1997. **17**(5): p. 2550-8.

16. Gao, Y., J. Miyazaki, and G.W. Hart, *The transcription factor PDX-1 is post-translationally modified by O-linked N-acetylglucosamine and this modification is correlated with its DNA binding activity and insulin secretion in min6 beta-cells.* Arch Biochem Biophys, 2003. **415**(2): p. 155-63.

17. Chou, T.Y. and G.W. Hart, *O-linked N-acetylglucosamine and cancer: messages from the glycosylation of c-Myc.* Adv Exp Med Biol, 2001. **491**: p. 413-8.

18. Housley, M.P., et al., *A PGC-1alpha-O-GlcNAc transferase complex regulates FoxO transcription factor activity in response to glucose.* J Biol Chem, 2009. **284**(8): p. 5148-57.

19. Zeidan, Q., et al., *O-GlcNAc cycling enzymes associate with the translational machinery and modify core ribosomal proteins.* Mol Biol Cell. **21**(12): p. 1922-36.

20. Vosseller, K., et al., *Elevated nucleocytoplasmic glycosylation by O-GlcNAc results in insulin resistance associated with defects in Akt activation in 3T3-L1 adipocytes.* Proc Natl Acad Sci U S A, 2002. **99**(8): p. 5313-8.

21. Arnold, C.S., et al., *The microtubule-associated protein tau is extensively modified with O-linked N-acetylglucosamine.* J Biol Chem, 1996. **271**(46): p. 28741-4.

22. Dong, D.L., et al., *Glycosylation of mammalian neurofilaments. Localization of multiple O-linked N-acetylglucosamine moieties on neurofilament polypeptides L and M.* J Biol Chem, 1993. **268**(22): p. 16679-87.

23. Luthi, T., et al., *Synapsins contain O-linked N-acetylglucosamine.* J Neurochem, 1991. **56**(5): p. 1493-8.

24. Chou, C.F., A.J. Smith, and M.B. Omary, *Characterization and dynamics of O-linked glycosylation of human cytokeratin 8 and 18.* J Biol Chem, 1992. **267**(6): p. 3901-6.

25. Hart, G.W., Housley, M.P. and Slawson C., *Cycling of O-linked beta-N-acetylglucosamine on nucleocytoplasmic proteins.* Nature, 2007. **446**(7139): p. 6.

26. Butkinaree, C., Park, K., and Hart G.W., *O-linked beta-N-acetylglucosamine (O-GlcNAc): Extensive crosstalk with phosphorylation*

to regulate signaling and transcription in response to nutrients and stress. Biochimic et Biophysica Acta, 2010. **1800**(2): p. 10.

27. Macauley, M.S., et al., *Elevation of global O-GlcNAc levels in 3T3-L1 adipocytes by selective inhibition of O-GlcNAcase does not induce insulin resistance.* J Biol Chem, 2008. **283**(50): p. 34687-95.
28. Macauley, M.S., et al., *Elevation of Global O-GlcNAc in rodents using a selective O-GlcNAcase inhibitor does not cause insulin resistance or perturb glucohomeostasis.* Chem Biol. **17**(9): p. 949-58.
29. Haltiwanger, R.S., M.A. Blomberg, and G.W. Hart, *Glycosylation of nuclear and cytoplasmic proteins. Purification and characterization of a uridine diphospho-N-acetylglucosamine:polypeptide beta-N-acetylglucosaminyltransferase.* J Biol Chem, 1992. **267**(13): p. 9005-13.
30. Kreppel, L.K., M.A. Blomberg, and G.W. Hart, *Dynamic glycosylation of nuclear and cytosolic proteins. Cloning and characterization of a unique O-GlcNAc transferase with multiple tetratricopeptide repeats.* J Biol Chem, 1997. **272**(14): p. 9308-15.
31. Gao, Y., et al., *Dynamic O-glycosylation of nuclear and cytosolic proteins: cloning and characterization of a neutral, cytosolic beta-N-acetylglucosaminidase from human brain.* J Biol Chem, 2001. **276**(13): p. 9838-45.
32. Shafi, R., et al., *The O-GlcNAc transferase gene resides on the X chromosome and is essential for embryonic stem cell viability and mouse ontogeny.* Proc Natl Acad Sci U S A, 2000. **97**(11): p. 5735-9.
33. Hanover, J.A., et al., *A Caenorhabditis elegans model of insulin resistance: altered macronutrient storage and dauer formation in an OGT-1 knockout.* Proc Natl Acad Sci U S A, 2005. **102**(32): p. 11266-71.
34. Forsythe, M.E., et al., *Caenorhabditis elegans ortholog of a diabetes susceptibility locus: oga-1 (O-GlcNAcase) knockout impacts O-GlcNAc cycling, metabolism, and dauer.* Proc Natl Acad Sci U S A, 2006. **103**(32): p. 11952-7.
35. Yang, W.H., et al., *Modification of p53 with O-linked N-acetylglucosamine regulates p53 activity and stability.* Nat Cell Biol, 2006. **8**(10): p. 1074-83.
36. Hanks, S.K. and T. Hunter, *Protein kinases 6. The eukaryotic protein kinase superfamily: kinase (catalytic) domain structure and classification.* Faseb J, 1995. **9**(8): p. 576-96.
37. Barford, D., *Molecular mechanisms of the protein serine/threonine phosphatases.* Trends Biochem Sci, 1996. **21**(11): p. 407-12.
38. Kamemura, K., et al., *Dynamic interplay between O-glycosylation and O-phosphorylation of nucleocytoplasmic proteins: alternative glycosylation/phosphorylation of THR-58, a known mutational hot spot of*

c-Myc in lymphomas, is regulated by mitogens. J Biol Chem, 2002. **277**(21): p. 19229-35.

39. Hart, G.W., et al., *O-linked N-acetylglucosamine: the "yin-yang" of Ser/Thr phosphorylation? Nuclear and cytoplasmic glycosylation.* Adv Exp Med Biol, 1995. **376**: p. 115-23.
40. Comer, F.I. and G.W. Hart, *Reciprocity between O-GlcNAc and O-phosphate on the carboxyl terminal domain of RNA polymerase II.* Biochemistry, 2001. **40**(26): p. 7845-52.
41. Cheng, X. and G.W. Hart, *Alternative O-glycosylation/O-phosphorylation of serine-16 in murine estrogen receptor beta: post-translational regulation of turnover and transactivation activity.* J Biol Chem, 2001. **276**(13): p. 10570-5.
42. Cole, R.N. and G.W. Hart, *Glycosylation sites flank phosphorylation sites on synapsin I: O-linked N-acetylglucosamine residues are localized within domains mediating synapsin I interactions.* J Neurochem, 1999. **73**(1): p. 418-28.
43. O'Donnell, N., et al., *Ogt-dependent X-chromosome-linked protein glycosylation is a requisite modification in somatic cell function and embryo viability.* Mol Cell Biol, 2004. **24**(4): p. 1680-90.
44. Yki-Jarvinen, H., et al., *Insulin and glucosamine infusions increase O-linked N-acetyl-glucosamine in skeletal muscle proteins in vivo.* Metabolism, 1998. **47**(4): p. 449-55.
45. Hazel, M., et al., *Activation of the hexosamine signaling pathway in adipose tissue results in decreased serum adiponectin and skeletal muscle insulin resistance.* Endocrinology, 2004. **145**(5): p. 2118-28.
46. Clark, R.J., et al., *Diabetes and the accompanying hyperglycemia impairs cardiomyocyte calcium cycling through increased nuclear O-GlcNAcylation.* J Biol Chem, 2003. **278**(45): p. 44230-7.
47. Marshall, S., O. Nadeau, and K. Yamasaki, *Dynamic actions of glucose and glucosamine on hexosamine biosynthesis in isolated adipocytes: differential effects on glucosamine 6-phosphate, UDP-N-acetylglucosamine, and ATP levels.* J Biol Chem, 2004. **279**(34): p. 35313-9.
48. Hresko, R.C., et al., *Glucosamine-induced insulin resistance in 3T3-L1 adipocytes is caused by depletion of intracellular ATP.* J Biol Chem, 1998. **273**(32): p. 20658-68.
49. Marshall, S., K. Yamasaki, and R. Okuyama, *Glucosamine induces rapid desensitization of glucose transport in isolated adipocytes by increasing GlcN-6-P levels.* Biochem Biophys Res Commun, 2005. **329**(3): p. 1155-61.

50. Matthews, J.A., et al., *Glucosamine-induced increase in Akt phosphorylation corresponds to increased endoplasmic reticulum stress in astroglial cells.* Mol Cell Biochem, 2007. **298**(1-2): p. 109-23.

51. Ohtsubo, K., et al., *Dietary and genetic control of glucose transporter 2 glycosylation promotes insulin secretion in suppressing diabetes.* Cell, 2005. **123**(7): p. 1307-21.

52. Lau, K.S., et al., *Complex N-glycan number and degree of branching cooperate to regulate cell proliferation and differentiation.* Cell, 2007. **129**(1): p. 123-34.

53. Ohtsubo, K. and J.D. Marth, *Glycosylation in cellular mechanisms of health and disease.* Cell, 2006. **126**(5): p. 855-67.

54. McClain, D.A., et al., *Altered glycan-dependent signaling induces insulin resistance and hyperleptinemia.* Proc Natl Acad Sci U S A, 2002. **99**(16): p. 10695-9.

55. Slawson, C., et al., *Perturbations in O-linked beta-N-acetylglucosamine protein modification cause severe defects in mitotic progression and cytokinesis.* J Biol Chem, 2005. **280**(38): p. 32944-56.

56. Knight, Z.A. and K.M. Shokat, *Chemical genetics: where genetics and pharmacology meet.* Cell, 2007. **128**(3): p. 425-30.

57. Kanin, E.I., et al., *Chemical inhibition of the TFIIH-associated kinase Cdk7/Kin28 does not impair global mRNA synthesis.* Proc Natl Acad Sci U S A, 2007. **104**(14): p. 5812-7.

58. Sakabe, K. and G.W. Hart, *O-GlcNAc transferase regulates mitotic chromatin dynamics.* J Biol Chem.

59. Haltiwanger, R.S., K. Grove, and G.A. Philipsberg, *Modulation of O-linked N-acetylglucosamine levels on nuclear and cytoplasmic proteins in vivo using the peptide O-GlcNAc-beta-N-acetylglucosaminidase inhibitor O-(2-acetamido-2-deoxy-D-glucopyranosylidene)amino-N-phenylcarbamate.* J Biol Chem, 1998. **273**(6): p. 3611-7.

60. *Carbohydrate-Active Enzymes Database*. September 7th, 2010 [cited 2010 September 17th]; Available from: http://www.cazy.org/Home.html.

61. Vocadlo, D.J. and G.J. Davies, *Mechanistic insights into glycosidase chemistry.* Curr Opin Chem Biol, 2008. **12**(5): p. 539-55.

62. Macauley, M.S., et al., *O-GlcNAcase uses substrate-assisted catalysis: kinetic analysis and development of highly selective mechanism-inspired inhibitors.* J Biol Chem, 2005. **280**(27): p. 25313-22.

63. Triggs-Raine, B., D.J. Mahuran, and R.A. Gravel, *Naturally occurring mutations in GM2 gangliosidosis: a compendium.* Adv Genet, 2001. **44**: p. 199-224.

64. Toleman, C., et al., *Characterization of the histone acetyltransferase (HAT) domain of a bifunctional protein with activable O-GlcNAcase and HAT activities.* J Biol Chem, 2004. **279**(51): p. 53665-73.

65. Ueno, R. and C.S. Yuan, *Purification and properties of neutral beta-N-acetylglucosaminidase from carp blood.* Biochim Biophys Acta, 1991. **1074**(1): p. 79-84.

66. Dennis, R.J., et al., *Structure and mechanism of a bacterial beta-glucosaminidase having O-GlcNAcase activity.* Nat Struct Mol Biol, 2006. **13**(4): p. 365-71.

67. Ficko-Blean, E. and A.B. Boraston, *Cloning, recombinant production, crystallization and preliminary X-ray diffraction studies of a family 84 glycoside hydrolase from Clostridium perfringens.* Acta Crystallogr Sect F Struct Biol Cryst Commun, 2005. **61**(Pt 9): p. 834-6.

68. Schimpl, M., et al., *Human O-GlcNAcase binds substrates in a conserved peptide recognition groove.* Biochem J, 2010.

69. Whitworth, G.E., et al., *Analysis of PUGNAc and NAG-thiazoline as transition state analogues for human O-GlcNAcase: mechanistic and structural insights into inhibitor selectivity and transition state poise.* J Am Chem Soc, 2007. **129**(3): p. 635-44.

70. Mayer, T.U., *Chemical genetics: tailoring tools for cell biology.* Trends Cell Biol, 2003. **13**(5): p. 270-7.

71. Macauley, M.S., Vocadlo, D.J., *Increasing O-GlcNAc levels: An overview of small-molecule inhibitors of O-GlcNAcase.* Biochimica et Biophysica Acta, 2010. **1800**(2): p. 14.

72. Arias, E.B., J. Kim, and G.D. Cartee, *Prolonged incubation in PUGNAc results in increased protein O-Linked glycosylation and insulin resistance in rat skeletal muscle.* Diabetes, 2004. **53**(4): p. 921-30.

73. Akimoto, Y., et al., *Elevation of the post-translational modification of proteins by O-linked N-acetylglucosamine leads to deterioration of the glucose-stimulated insulin secretion in the pancreas of diabetic Goto-Kakizaki rats.* Glycobiology, 2007. **17**(2): p. 127-40.

74. Yuzwa, S.A., et al., *A potent mechanism-inspired O-GlcNAcase inhibitor that blocks phosphorylation of tau in vivo.* Nat Chem Biol, 2008. **4**(8): p. 483-90.

75. Zou, L., et al., *The protective effects of PUGNAc on cardiac function after trauma-hemorrhage are mediated via increased protein O-GlcNAc levels.* Shock, 2007. **27**(4): p. 402-8.

76. Dong, D.L. and G.W. Hart, *Purification and characterization of an O-GlcNAc selective N-acetyl-beta-D-glucosaminidase from rat spleen cytosol.* J Biol Chem, 1994. **269**(30): p. 19321-30.

77. Stubbs, K.A., M.S. Macauley, and D.J. Vocadlo, *A selective inhibitor Gal-PUGNAc of human lysosomal beta-hexosaminidases modulates levels of the ganglioside GM2 in neuroblastoma cells.* Angew Chem Int Ed Engl, 2009. **48**(7): p. 1300-3.

78. Macauley, M.S., et al., *Inhibition of O-GlcNAcase using a potent and cell-permeable inhibitor does not induce insulin resistance in 3T3-L1 adipocytes.* Chem Biol, 2010. **17**(9): p. 937-48.

79. Konrad, R.J., et al., *The potential mechanism of the diabetogenic action of streptozotocin: inhibition of pancreatic beta-cell O-GlcNAc-selective N-acetyl-beta-D-glucosaminidase.* Biochem J, 2001. **356**(Pt 1): p. 31-41.

80. Roos, M.D., et al., *Streptozotocin, an analog of N-acetylglucosamine, blocks the removal of O-GlcNAc from intracellular proteins.* Proc Assoc Am Physicians, 1998. **110**(5): p. 422-32.

81. Bennett, R.A. and A.E. Pegg, *Alkylation of DNA in rat tissues following administration of streptozotocin.* Cancer Res, 1981. **41**(7): p. 2786-90.

82. Kroncke, K.D., et al., *Nitric oxide generation during cellular metabolization of the diabetogenic N-methyl-N-nitroso-urea streptozotozin contributes to islet cell DNA damage.* Biol Chem Hoppe Seyler, 1995. **376**(3): p. 179-85.

83. Yamamoto, H., Y. Uchigata, and H. Okamoto, *Streptozotocin and alloxan induce DNA strand breaks and poly(ADP-ribose) synthetase in pancreatic islets.* Nature, 1981. **294**(5838): p. 284-6.

84. Gao, Y., G.J. Parker, and G.W. Hart, *Streptozotocin-induced beta-cell death is independent of its inhibition of O-GlcNAcase in pancreatic Min6 cells.* Arch Biochem Biophys, 2000. **383**(2): p. 296-302.

85. Okuyama, R. and M. Yachi, *Cytosolic O-GlcNAc accumulation is not involved in beta-cell death in HIT-T15 or Min6.* Biochem Biophys Res Commun, 2001. **287**(2): p. 366-71.

86. Knapp, S., Vocadlo, D., Gao, Z., Kirk, B., Lou, J., Withers, S.G., *NAG-thiazoline, An N-Acetyl-β-hexosaminidase Inhibitor That Implicates Acetamido Participation.* J. Am. Chem. Soc., 1996. **118**(28): p. 2.

87. Mark, B.L., et al., *Crystal structure of human beta-hexosaminidase B: understanding the molecular basis of Sandhoff and Tay-Sachs disease.* J Mol Biol, 2003. **327**(5): p. 1093-109.

88. Cetinbas, N., et al., *Identification of Asp174 and Asp175 as the key catalytic residues of human O-GlcNAcase by functional analysis of site-directed mutants.* Biochemistry, 2006. **45**(11): p. 3835-44.

89. Macauley, M.S., K.A. Stubbs, and D.J. Vocadlo, *O-GlcNAcase catalyzes cleavage of thioglycosides without general acid catalysis.* J Am Chem Soc, 2005. **127**(49): p. 17202-3.

90. Derendorf, H., *Handbook of Pharmocokinetics/Pharmacodynamic Correlation.*, ed. G. Hochhaus. 1995, Boca Raton, USA: CRC Press.

91. Kwon, Y., *Handbook of Essential Pharmacokinetics, Pharmacodynamics, and Drug Metabolism for Industrial Scientist.* 2001, New York, USA: Kluwer Academic/Plenum Publishers.

92. Ritschel, W.A., *Handbook of Basic Pharmcokinetics*. 6th ed, ed. J.I. Graubart, Corrigan, L.L. 2004, Washington, DC, USA: American Pharmacists Association.

93. *Pharmacokinetics tutorial and competency assessment*. 1984-2010 [cited 2010 June 29th]; Available from: http://www.rxkinetics.com.

94. *Pharmacokinetics and Pharmacodynamics of Abused Drugs*, ed. S.B. Karch. 2008, Boca Raton, USA: CRC Press.

95. Amdur, M.O., Doull, J., *Casarett and Doull's Toxicology: The Basic Science*, ed. C.D. Klaassen. 1991, New York, USA: Pergamon Press.

96. Benz, R., Janko, K., and Langer, P., *Pore formation by the matrix protein (porin) to Escherichia coli in planar bilayer membranes.* Annu. N.Y. Acad Sci., 1980. **358**: p. 11.

97. Lullmann, H., Mohr, K., Hein, L., Bieger, D., *Color Atlas of Pharmacology*. 3rd ed, ed. H. Lullmann. 2005, Stuttgart, Germany: Thieme Publishing Group.

98. Dhillon, S., Gill, K., *Clinical Pharmacokinetics.*, ed. S. Dhillon, Kostrzewski, A. 2006, London, UK: Pharmaceutical Press.

99. Bio-medicine. 2003-present [cited 2009 Feb. 25th]; Available from: <http://www.bio-medicine.org/Biology-Definition/Blood_plasma>.

100. *Handbook of analytical separations*. Biological Separations, ed. I.D. Wilson. Vol. 4. 2004, Alderley Park, U.K.: Elsevier. 1-39.

101. Wang, Y., et al., *Rapid and sensitive liquid chromatography-tandem mass spectrometric method for the quantitation of metformin in human plasma.* J Chromatogr B Analyt Technol Biomed Life Sci, 2004. **808**(2): p. 215-9.

102. Cai, F., et al., *A rapid and sensitive liquid chromatography-tandem mass spectrometric method for the determination of timosaponin B-II in blood plasma and a study of the pharmacokinetics of saponin in the rat.* J Pharm Biomed Anal, 2008. **48**(5): p. 1411-6.

103. Vesterqvist, O., F. Nabbie, and B. Swanson, *Determination of metformin in plasma by high-performance liquid chromatography after ultrafiltration.* J Chromatogr B Biomed Sci Appl, 1998. **716**(1-2): p. 299-304.

104. Cheng, C.L. and C.H. Chou, *Determination of metformin in human plasma by high-performance liquid chromatography with spectrophotometric detection.* J Chromatogr B Biomed Sci Appl, 2001. **762**(1): p. 51-8.

105. Varian. *Captiva™ ND^lipid* 2000-present [cited 2009 Feb. 25th]; Available from:

<http://www.varianinc.com/image/vimage/docs/products/consum/samprep/filtration/shared/captiva_lipids_brochure.pdf>.

106. Lindegardh, N., et al., *Development and validation of a liquid chromatographic-tandem mass spectrometric method for determination of oseltamivir and its metabolite oseltamivir carboxylate in plasma, saliva and urine.* J Chromatogr B Analyt Technol Biomed Life Sci, 2007. **859**(1): p. 74-83.

107. Kopp, E.K., et al., *Rapid and sensitive HILIC-ESI-MS/MS quantitation of polar metabolites of acrylamide in human urine using column switching with an online trap column.* J Agric Food Chem, 2008. **56**(21): p. 9828-34.

108. Li, X., et al., *Determination of miglitol in human plasma by liquid chromatography/tandem mass spectrometry.* Rapid Commun Mass Spectrom, 2007. **21**(2): p. 247-51.

109. Hanai, T., *Separation of polar compounds using carbon columns.* J Chromatogr A, 2003. **989**(2): p. 183-96.

110. Antonio, C., et al., *Hydrophilic interaction chromatography/electrospray mass spectrometry analysis of carbohydrate-related metabolites from Arabidopsis thaliana leaf tissue.* Rapid Commun Mass Spectrom, 2008. **22**(9): p. 1399-407.

111. Thompson, R., LoBrutto, R., *HPLC for Pharmaceutical Scientists*, ed. Y. Kazakevich, LoBrutto, R. 2007, New Jersey: Wiley-interscience 129, 303, 644.

112. Alpert, A.J., *Hydrophilic-interaction chromatography for the separation of peptides, nucleic acids and other polar compounds.* J. Chromatogr., 1990. **499**: p. 177-196.

113. Tosoh. *Amide-80 Columns for Hydrophilic Interaction Liquid Chromatography*. 2009 [cited 2009 Feb. 25th]; Available from: <http://www.separations.eu.tosohbioscience.com/NR/rdonlyres/2FABDA77-D538-4AA4-AD22-451871C64870/0/B07L03A_TSKgelAmide80_HILIC_brochure.pdf>.

114. *Method Development Guide for Hypercarb Columns*. 2007 [cited 2009 Feb. 21st]; Available from: <http://www.thermo.com/eThermo/CMA/PDFs/Product/productPDF_28871.pdf>.

115. Jackson, P.T. and P.W. Carr, *Study of polar and nonpolar substituted benzenes and aromatic isomers on carbon-coated zirconia and alkyl bonded phases.* J Chromatogr A, 2002. **958**(1-2): p. 121-9.

116. Pereira, L., *Porous graphitic carbon as a stationary phase in HPLC: theory and applications.* J Liq Chromatogr R T, 2008. **31**: p. 1689-1731.

117. Mckela, H.J., et al., *A Comparison of the Retention of Homologous Series and Other Test Solutes on an Ods Column and a Hypercarb Carbon Column* J. Liq. Chromatogr., 1991. **14**: p. 21.

118. Tanaka, N., et al., *Selectivity of carbon packing materials in comparison with octadecylsilyl- and pyrenylethylsilylsilica gels in reversed- phase liquid chromatography.* J. Chromatogr., 1991. **549**: p. 12.

119. LCresources.com. *Advanced HPLC Method Development-section 8 Normal-phase & Ion-exchange*. 2007 [cited 2009 Feb. 25th].

120. Strege, M.A., *Hydrophilic interaction chromatography-electrospray mass spectrometry analysis of polar compounds for natural product drug discovery.* ANAL CHEM, 1998. **70**: p. 2439-2445.

121. Downard, K., *Mass spectromety: a foundation course*. 2004, Cambridge, UK: Royal Society of Chemistry.

122. Gaskell, S.J., *Electrospray: Principles and Practice.* J. Mass Spectrom., 1997. **32**: p. 11.

123. Dass, C., *Fundamentals of Contemporary Mass Spectrometry* Wiley-Interscience Series on Mass Spectrometry, ed. D.M. Desiderio, Nibbering, N.M. 2007, New Jersey, USA: John Wiley & Sons, Inc.

124. Gross, J.H., *Mass Spectrometry: A Textbook*. 2004, Heidelberg, Germany: Springer-Verlag

125. de Hoffmann, E., Stroobant, V. , *Mass Spectrometry: Principles and Applications*. 2nd ed. 2001, Chichester: John Wiley and Sons, LTD.

126. Taylor, G., *Disintegration of Water Drops in an Electric Field.* Proc. R. Soc. Lond. A, 1964. **280**: p. 383-397.

127. Kebarle, P. and Y. Ho, *Electrospray Ionization Mass Spectrometry*, ed. R.B. Cole. 1997, New Orleans, U.S.A.: John Wiley and Sons, Inc. p. 6-31.

128. Wilm, M.S. and M. Mann, *Electrospray and Taylor-Cone Theory, Dole's Beam of Macromolecules at Last?* Int. J. Mass Spectrom. Ion Proc., 1994. **136**: p. 167-180.

129. Rayleigh, L., *On the Equilibrium of Liquid Conducting Masses charged with Electricity.* Philos. Mag., 1882. **14**: p. 184-186.

130. Kebarle, P. and L. Tang, *From ions in solution to ions in the gas phase - the mechanism of electrospray mass spectrometry.* Anal. Chem., 1993. **65**: p. 972A-986A.

131. Dunnivant, F.M. and J. Ginsbach. *Quadrupole Mass Filter*. 2009 [cited 2010 November 18th]; Available from: http://people.whitman.edu/~dunnivfm/FAASICPMS_Ebook/CH4/4_2_6_2.html.

132. *Basic QTRAP for Biomolecules Training Manual*. 2007, Foster city, California, USA: Applied Biosystems, MDS Sciex.

133. Kwon, Y., *Handbook of Essential Pharmacokinetics, Pharmacodynamics, and Drug Metabolism for Industrial Scientist*. 2001: Kluwer Academic/Plenum Publishers. 1-27.

134. Nuengchamnong, N., et al., *Quantitative determination of 1-deoxynojirimycin in mulberry leaves using liquid chromatography-tandem mass spectrometry.* J Pharm Biomed Anal, 2007. **44**(4): p. 853-8.

135. Mao, Y., Dube, D., Duggan, Q.J. *Quantitative Determination of Benzenesulfonic Acid, a Highly Polar Compound, in Rat Plasma by 96-well Solid-phase Extraction and Negative Ion Electrospray LC/MS/MS*. [Poster] 2006 [cited; Available from: <http://www.aapsj.org/abstracts/AM_2006/AAPS2006-000695.pdf>.

136. Phenomenex. *Synergi Fusion-RP*. 2009 [cited 2009 Mar. 5th]; Available from: <http://www.phenomenex.com/products/brands/view2.aspx?id=8953>.

137. *Agilent ZORBAX Eclipse XDB-C18 Rapid Resolution Threaded Column - Datasheet*. 2007 July 13th, 2007 [cited 2009 April]; Available from: https://www.chem.agilent.com/Library/specifications/Public/820116-002.pdf.

138. Heller, D.N., and Nochetto, C.B. *Simultaneous Determination of Melamine and Cyanuric Acid in Animal Feed via ZIC®-HILIC Chromatography - Mass Spectrometry*. 2008 [cited 2009 Mar. 5th]; Available from: <http://www.sequant.com/files/documents/technicalnotes/sequant_technicalnote_tn-015.pdf>.

139. Appelblad, P. *Mass Spectrometric Detection of Homocysteine, Methylmalonic Acid and Succinic Acid using HILIC on a Zwitterionic Stationary Phase*. 2005 [cited 2009 Mar. 5th]; Available from: <http://www.sequant.com/sn/ufiles/SeQuant_ApplicationNote_LCGC-Europe_March_2005.pdf>.

140. Lindegardh, N., et al. *Increasing the Sensitivity for Oseltamivir using ZIC-HILIC Chromatography*. 2008 [cited 2009 Mar. 5th]; Available from: <http://www.sequant.com/files/documents/technicalnotes/SeQuant_TechnicalNote_TN-003.pdf>.

141. *TSK-GEL Amide-80 HILIC Columns for the Analysis of Melamine and Cyanuric Acid in Milk by LC-MS/MS*. [cited 2009 Mar. 5th]; Available from: <http://www.separations.us.tosohbioscience.com/NR/rdonlyres/AN197f7cemkrugxnpbivierlqytpfkbxtqrykar.pdf>.

142. Qin, F., et al., *Hydrophilic interaction liquid chromatography-tandem mass spectrometry determination of estrogen conjugates in human urine.* Anal Chem, 2008. **80**(9): p. 3404-11.

143. Shabir, G.A. *HPLC Method Development and Validation for Pharmaceutical Analysis*. 2004 [cited 2009 Mar. 5th]; Available from:

http://pharmtech.findpharma.com/pharmtech/article/articleDetail.jsp?id=89002.

144. Ornaf, R.M., and Dong, M.W., *Handbook of Pharmaceutical Analysis by HPLC*. Separation Science and Technology, ed. S. Ahuja, and Dong, M.W. Vol. 6. 2005: Elsevier Academic Press. 25.

145. Ardrey, R.E., *Liquid chromatography-mass spectrometry: an introduction*. 2003, Chichester, UK: John Wiley and Sons Ltd.

146. Skoog, D.A., Holler, F.J., and Crouch, S.R., *Principles of Instrumental Analysis*. 6th ed, ed. S. Kiselica. 2007, Belmont, USA: Thomson Brooks/Cole.

147. Viswanathan, C.T., et al., *Quantitative bioanalytical methods validation and implementation: best practices for chromatographic and ligand binding assays.* Pharm Res, 2007. **24**(10): p. 1962-73.

148. *Guidance for industry: bioanalytical method validation.* 2001, U.S. Department of Health and Human Services, Food and Drug Administration, Center for Drug Evaluation and Research (CDER): Rockville, USA.

149. Vogt, W.P., *Dictonary of statistics and methodology: a nontechnical guide for the social sciences*. 3rd ed, ed. L.C. Shaw. 2005, Thousand Oaks, USA: Sage Publications, Inc.

150. Dolan, J.W., *Calibration curves, part 2: what are the limits?*, in *LCGC Europe*. 2009.

151. Huber, L. *Validation of analytical methods and procedures*. [cited 2010 September 1st]; Available from: http://www.labcompliance.com/tutorial/methods/default.aspx.

152. Bansal, S. and A. DeStefano, *Key elements of bioanalytical method validation for small molecules.* Aaps J, 2007. **9**(1): p. E109-14.

153. Chambers, E., et al., *Systematic and comprehensive strategy for reducing matrix effects in LC/MS/MS analyses.* J Chromatogr B Analyt Technol Biomed Life Sci, 2007. **852**(1-2): p. 22-34.

154. *Guidance for Industry: Q2B Validation of Analytical Procedures: Methodology*. 1996, ICH.

155. Nowatzke, W. and E. Woolf, *Best practices during bioanalytical method validation for the characterization of assay reagents and the evaluation of analyte stability in assay standards, quality controls, and study samples.* Aaps J, 2007. **9**(2): p. E117-22.

156. *Polarity Index*. August 3rd, 2010 [cited 2010 September 6th]; Available from: http://macro.lsu.edu/howto/solvents/Polarity%20index.htm.

157. Aurand, C.R., Bell, D.S., and Brandes, H.K., *Selective Depletion of Phospholipids Interference Utilizing HybridSPE-PPT Technology*. 2007, Supelco, Sigma-Aldrich Co.: Bellefonte, USA.